Doctoral Programme in Neuroscience
Instituto de Neurociencias

Functional analysis of the tumor suppressor gene *p53* in the process of asymmetric cell division

Sandra Manzanero Ortiz

Thesis director

Dr. Ana Carmena de la Cruz

Universidad Miguel Hernández de Elche

- 2023 -

The Doctoral Thesis entitled “Functional analysis of the tumor suppressor gene *p53* in the process of asymmetric cell division” is presented as a compendium of the following publications:

- **Manzanero-Ortiz S**, de Torres-Jurado A, Hernández-Rojas R, Carmena A. Pilot RNAi Screen in Drosophila Neural Stem Cell Lineages to Identify Novel Tumor Suppressor Genes Involved in Asymmetric Cell Division. Int J Mol Sci. 2021, 22(21), 11332. DOI: 10.3390/ijms222111332

  International Journal of Molecular Sciencies, IF 2020: 5.923 (Q1, Biochemistry & Molecular Biology).

Sant Joan d'Alacant, 27 of September 2023

Dr. Ana Carmena de la Cruz, Director of the doctoral thesis entitled "Functional analysis of the tumor suppressor gene *p53* in the process of asymmetric cell division",

INFORM

That Mrs. Sandra Manzanero Ortiz has carried out under my supervision the work entitled **"**Functional analysis of the tumor suppressor gene *p53* in the process of asymmetric cell division**"** in accordance with the terms and conditions defined in her Research Plan and in accordance with the Code of Good Practice of the University Miguel Hernández of Elche, satisfactorily fulfilling the objectives foreseen for its public defense as a doctoral thesis.

I sign for appropriate purposes, in Sant Joan d'Alacant, on September of 2023.

Thesis director

Dr. Ana Carmena de la Cruz

Dr. Elvira Mª de la Peña García, Coordinator of the Neurosciences PhD programme at the Institute of Neurosciences in Alicante, a joint centre of the Miguel Hernández University (UMH) and the Spanish National Research Council (CSIC),

INFORMS:

That Mrs. Sandra Manzanero Ortiz has carried out under the supervision of our PhD Program the work entitled "Functional analysis of the tumor suppressor gene *p53* in the process of asymmetric cell division" in accordance with the terms and conditions defined in its Research Plan and in accordance with the Code of Good Practice of the University Miguel Hernández de Elche, fulfilling the objectives satisfactorily for its public defense as a doctoral thesis.

Which I sign for the appropriate purposes, in Sant Joan d'Alacant on September, 2023

Dr. Elvira de la Peña García

Coordinator of the PhD Programme in Neurosciences

Av Ramón y Cajal s/n
SANT JOAN CAMPUS
03550 SANT JOAN D'ALACANT-SPAIN

E-mail: elvirap@umh.es
www.in.umh.es

Tel: +34 965 919533
Fax: +34 965 919549

The doctoral thesis entitled “Functional analysis of the tumor suppressor gene *p53* in the process of asymmetric cell division” has been developed by myself, Sandra Manzanero Ortiz (53258491J). This work has been financially supported by the competitive predoctoral FPI fellowship BFU2015-64251, granted by the Ministry of Economy and Competitiveness, “Agencia Estatal Consejo Superior de Investigaciones Científicas (CSIC)”, Spain.

AGRADECIMIENTOS

Han pasado ya muchos años desde que decidí embarcarme en esta aventura y no me creo que haya llegado el final. Hay tantas personas a las que me gustaría agradecer el haberme acompañado durante todo este tiempo que, dado que no me gustaría extenderme demasiado (y que no soy muy buena expresándome por escrito), intentaré hacerlo brevemente.

En primer lugar, a mi directora de tesis, Ana. Muchísimas gracias por ofrecerme esta increíble oportunidad y depositar en mi la confianza que necesitaba, al principio en el máster, y posteriormente durante el Doctorado. También a todas las personas que han pasado por el laboratorio durante todos estos años, especialmente a mi "melli", compañera de alegrías, lloros y desesperaciones, bailes y "liadas" tanto dentro como fuera del laboratorio. A mi otro pilar en el laboratorio, Maribel, gracias infinitas por ser mi faro, incluso en los momentos más oscuros y desalentadores. Si algo he aprendido contigo es a luchar contra la frustración (tan presente en nuestras vidas). Nunca podré agradecerte lo suficiente todo lo que he aprendido (tanto a nivel laboral como personal), eres una persona maravillosa y con uno de los fondos más bonitos que he conocido.

A todas las personas que he conocido por el paso del instituto (y aquellas que han vuelto a mi vida), sobre todo a las que ya se han convertido en una parte más de mi vida.

A mis amigos, a todos con los que empecé, a los que me he ido encontrado por el camino y a los que han "reaparecido", por aguantarme, acompañarme y guiarme cuando la situación lo ha necesitado. ¡Cuánto bien me hacéis! A mis dos pilares fundamentales que, aunque aparecieron al principio de diferentes etapas, a día de hoy no imagino una vida sin ellas, no sois conscientes de la suerte que tengo.

A mi amenizador de fiestas particular, por ayudarme, animarme, aguantar el chaparrón (aunque a veces ha sido bastante difícil) y valorarme incluso cuando yo he flaqueado. Gracias.

A mi familia por el apoyo incondicional, por quererme y animarme. Soy muy afortunada de teneros. En especial a mi madre, por tu fortaleza y perseverancia. Siempre has sido y serás un referente y, en cierto modo, lo que soy es gracias a ti.

INDEX

LIST OF ABBREVIATIONS

Ab	Antibody
Ac	Achaete
ACD	Asymmetric cell division
AEL	After egg laying
Ago	Archipelago
ALH	After larval hatching
aPKC	Atypical protein kinase C
AS-C	Achaete-scute complex
AurA	Aurora A
Baz	Bazooka
bHLH	Basic helix-loop-helix
Brat	Brain tumor
BSA	Bovine serum albumin
CB	Central brain
Cdc42	Cell division cycle 42
Cdk	Cyclin-dependet kinase
CNS	Central nervous system
Cno	Canoe
CycE	Cyclin E
DAB	Diaminobenzidine
Dilp	*Drosophila* insulin-like protein
Dl	Delta
DL	Dorsal-lateral
Dlg1	Discs large 1
DM	Dorsal-medial
Dmp53	*Drosophila* p53
DNF	Aspartatic acid-proline-phenylalanine
Dpn	Deadpan
E(spl)	Enhancer of Split
Egr	Eiger

E_{EPC}	Founder of the Eve pericardial cells
Eve	Even-skipped
FA	Fortaldehyde
F_{DO2}	Founder cell of the dorsal oblique muscle 2
FLP	Flippase
FRT	FLP recombination target
Gαi	G protein α-i subunit
GOF	Gain of function
GMC	Ganglion mother cell
If	Irregular facets
immINP	Immature intermediate progenitor
INP	Intermediate neural progenitor
Insc	Inscuteable
JNK	Jun N-terminal kinase
Khc-73	Kinesin heavy chain 73
L'sc	Lethal of scute
L(2)gl	Lethal (2) giant larvae
MARCM	Mosaic analysis with a repressible cell marker
MB	Mushroom body
Mdm2	Murine doble minute 2
Mira	Miranda
mNumb	Mammalian Numb
Mud	Mushroom body defect
N	Notch
NB	Neuroblast
NE	Neuroepithelium
NF-κB	Nuclear factor kappa B
NHL	NCL1, HT2A and LIN-41
NPF	Asparagine-proline-phenylalanine
OL	Optic lobe
ON	Over-night
OSVZ	Outer subventricular zone
p53RE	p53 response element

PBS	Phosphate-buffered saline
PBT	PBS with Triton X-100
PFA	Paraformaldehyde
PH3	Phospho-histone H3
Pins	Partner of Inscuteable
Pon	Partner of Numb
PP2A	Protein phosphatase 2A
Pros	Prospero
PTB	Phosphotyrosine-binding
Robo	Roundabout
RT	Room temperature
Sc	Scute
Scrib	Scribble
SOP	Sensory organ precursor
Sp	Sternopleural
Stau	Staufen
Tb	Tubby
TF	Transcription factor
TNF	Tumor necrosis factor
Traf4	TNF receptor-associated factor 4
TRIM	Tripartite motif
TS	Tumor suppressor
UAS	Upstream activating sequence
VNC	Ventral nerve cord
w	White
Wg	Wingless
WT	Wild-type

LIST OF FIGURES

ABSTRACT

The process of asymmetric cell division (ACD) is a key and highly conserved mechanism to balance the expansion of stem/progenitor cells and the generation of cell diversity during development. Alterations in the ACD process can disrupt this delicate balance, triggering failures in cell identity and cell overgrowth, even tumor formation. *Drosophila melanogaster* neural stem cells, known as neuroblasts (NBs), divide asymmetrically giving rise to two different daughter cells: one of them retains the self-renewal capacity of the stem cell (the NB), while the other daughter cell is committed to neural differentiation. These NBs have been employed for decades as an excellent model system to study the ACD process. Remarkably, over the past years, it has been determined that genes that regulate ACD can behave as tumor suppressors. Likewise, genes initially discovered as tumor suppressors have been shown a posteriori to modulate ACD. Thus, the main objective of this PhD thesis was to get deep insight into the potential function of known tumor suppressors as novel ACD regulators. Specifically, we aimed to analyze the function of the tumor suppressor gene *p53* in ACD, as p53 is a crucial tumor suppressor mutated in most human cancers. Intriguingly, in addition to the classical functions of p53 as inductor of cell cycle arrest and apoptosis in cells under stress conditions, novel functions for p53 in unstressed cells have been more recently unveiled, such as the regulation of the mode of stem cell division. In this work, we have found that *Drosophila* p53 does have an impact on ACD. The absence of *p53* affected the correct asymmetric division of embryonic neural progenitor lineages. Additionally, p53 was required for the correct localization in mitotic NBs of the ACD regulators Numb, Pins and Brat, critical in the ACD process for the correct identity of the daughter cells. Moreover, we observed that p53 transcriptionally activates the ACD regulators Numb, Brat and Traf4. Recent work in the lab has shown that p53, in fact, directly binds the regulatory regions of all these three genes. Interestingly, human and mouse homologs of *Drosophila brat* and *Traf4* (*TRIM32* and *TRAF4*, respectively) were recently identified in a meta-analysis of transcriptomic and ChIP-seq datasets as conserved targets of p53. Lastly, we found that the lack of *p53* did not cause tumor-like overgrowth in larval brain NB lineages, result that can be explained by the high redundancy in ACD regulation.

RESUMEN

El proceso de división celular asimétrica (DCA) es un mecanismo clave y muy conservado para equilibrar la expansión de células madre/progenitoras y la generación de diversidad celular durante el desarrollo. Las alteraciones en el proceso de DCA pueden alterar este delicado equilibrio, desencadenando fallos en la identidad celular y sobrecrecimiento celular, incluso la formación de tumores. Las células madre neurales de *Drosophila melanogaster*, conocidas como neuroblastos (NBs), se dividen asimétricamente dando lugar a dos células hijas diferentes: una de ellas conserva la capacidad de autorrenovación de la célula madre (el NB), mientras que la otra célula hija seguirá un proceso de diferenciación neural. Estos NBs se han empleado durante décadas como un excelente sistema modelo para estudiar el proceso de DCA. Sorprendentemente, en los últimos años se ha determinado que los genes que regulan la DCA pueden comportarse como supresores tumorales. Asimismo, genes inicialmente descubiertos como supresores tumorales se ha demostrado a posteriori que modulan la DCA. Así pues, el objetivo principal de esta tesis doctoral fue profundizar en la potencial función de conocidos supresores tumorales como nuevos reguladores de la DCA. En concreto, nos propusimos analizar la función del gen supresor de tumores *p53* en la DCA, ya que p53 es un supresor tumoral crucial que se encuentra mutado en la mayoría de los cánceres humanos. Curiosamente, además de las funciones clásicas de p53 como inductor de la detención del ciclo celular y de la apoptosis en células sometidas a estrés, recientemente se han desvelado nuevas funciones de p53 en células no sometidas a estrés, como la de regulador del modo de división de las células madre. En este trabajo, hemos descubierto que p53 de *Drosophila* regula la DCA. La ausencia de *p53* afecta a la correcta división asimétrica de los linajes progenitores embrionarios neurales. Además, p53 es necesario para la correcta localización de los reguladores de ACD Numb, Pins y Brat en los NBs mitóticos, críticos en el proceso de DCA para la correcta identidad de las células hijas. Además, observamos que p53 activa transcripcionalmente los reguladores de DCA Numb, Brat y Traf4. Trabajos recientes en el laboratorio han demostrado que p53, de hecho, se une directamente a las regiones reguladoras de estos tres genes. Curiosamente, los homólogos humanos y de ratón de *Drosophila brat* y *Traf4* (*TRIM32* y *TRAF4*, respectivamente) fueron identificados recientemente en un meta-análisis de conjuntos de

datos transcriptómicos y ChIP-seq como dianas conservadas de p53. Por último, hemos determinado que la falta de *p53* no provoca un sobrecremiento tumoral en los linajes de NBs del cerebro larvario, resultado que puede explicarse por la elevada redundancia en la regulación de la DCA.

I. INTRODUCTION

1. *Drosophila melanogaster* as an animal model system

The fruit fly *Drosophila melanogaster* has been widely used for more than a century as a model animal to study a great variety of biological processes such as the organization of the nervous system, the regulation of gene expression, development and cell biology processes, behavior, age and the pathophysiology of human diseases, among others. This is because, despite its simplicity, *Drosophila* has notorious advantages. For example, *Drosophila* contains only four chromosomes, its genome is fully sequenced (Adams et al., 2000) and it has low redundancy with just one or very few genes encoding the different members of the same protein class. In addition, the fruit fly life cycle takes only about 10 days **(Figure 1)** at 25ºC, and it has different very well-defined stages: 1) embryo development, which occurs during 22h after egg laying (AEL), 2) larval period that lasts approximately 4 days, in which larvae start feeding and growing from first larval instar until third larval instar, 3) pupa stage, during which mature larvae gets encapsulated and metamorphosis takes place along other 5 days and, at the end, 4) adult fly, which will emerge from the pupal case.

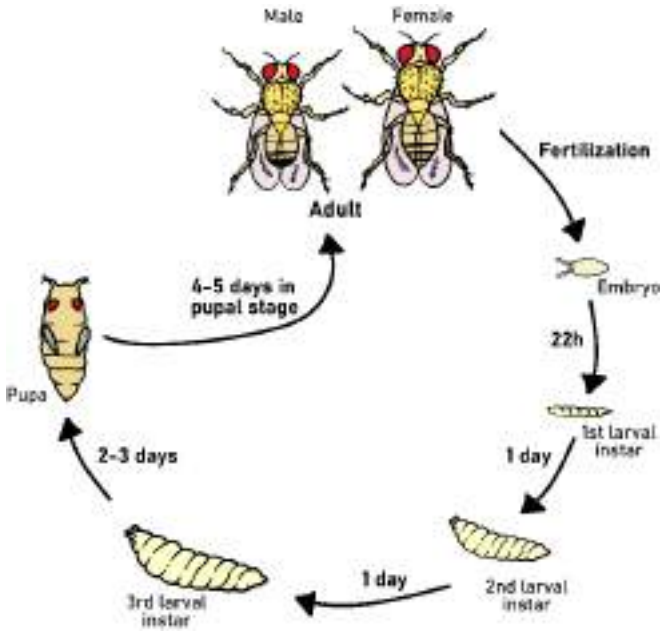

Figure 1. The *Drosophila melanogaster* life cycle. After fertilization, it takes about 10 days for the egg to develop into the new adult through a process that includes 3 larval stages and the pupal stage in which the metamorphosis takes place.

Due to the small number of chromosomes and their rapid life cycle, with well-differentiated developmental stages and a large number of progeny, *Drosophila* is relatively easy to manipulate for genetic, biochemical and molecular analyses. In addition, an increasing number of techniques and tools to manipulate gene expression have been developed over the years, improving enormously the versatility of experimentation and rendering excellent characterization of anatomy and phenotypes. Many of the genetic pathways that drive basic developmental processes in both invertebrates and vertebrates have remained almost unaltered throughout evolution. Thus, in many cases, genes from one organism can be functionally replaced by their equivalents in another organism. The case of flies and humans is not an exception. In fact, it has been found that 75% of the genes involved in human diseases have related sequences in the *Drosophila* genome that, when altered, can give rise to similar diseases, such as cancer, neurological or metabolic disorders, among others (Fortini & Bonini, 2000; Bier, 2005). With all this in mind, it is not surprising that many studies carried out in *Drosophila* have contributed to uncovering key cellular and signaling processes in development that are conserved from flies to mammals (Bilen & Bonini, 2005; Fernández-Moreno et al., 2007; Bellen et al., 2010).

2. *Drosophila* central nervous system and its stem cells: the neuroblasts

The simplicity of *Drosophila* development, as well as the large number of advanced genetic tools initially created to study it, allowed us to obtain a deep insight into multiple tissues at the cellular level. One historical example is the *Drosophila* central nervous system (CNS). *Drosophila* CNS can be divided into the brain, formed by the optic lobes (OLs) and the central brain (CB) in the head, and the ventral nerve cord (VNC) in the trunk region (Skeath & Thor, 2003; Kang & Reichert, 2015). Although it is a rather simple organism, the adult central brain of *Drosophila* is a very complex neural structure consisting of approximately 25,000 neurons that are interconnected in intricate neural

circuits (Scheffer et al., 2020). All these neurons are originated during development from a small subset of neural stem-like cells called neuroblasts (NBs). These stem cells have been used extensively over the past decades to understand the mechanisms of cell fate specification, asymmetric cell division (see below), as well as other key processes such as cytokinesis (Cabernard, 2012), cell polarity, mitotic spindle orientation (Lu & Johnston, 2013) and in vivo tumor formation (Caussinus & González, 2005; Knoblich, 2010; González, 2013).

The development of the CNS in *Drosophila* takes place in two waves of neurogenesis **(Figure 2A)**. The first wave occurs in the embryonic phase during stages 9-11, when CNS embryonic NBs delaminate from the neuroectoderm, which is located in the ventrolateral part of the embryo, in a very dynamic process associated with morphological modifications (Hartenstein & Campos-Ortega, 1984). A combination of three proneural genes belonging to the Achaete-scute complex (AS-C): *achaete* (*ac*), *scute* (*sc*) and *lethal of scute* (*l'sc*) (García-Bellido & Santamaría, 1978; Cabrera et al., 1987; Romani et al., 1987; Martín-Bermudo et al., 1991) are expressed in the neuroectoderm, just before the delamination process occurs, in 10 groups of 6-8 cells per hemisegment, the so-called "proneural clusters". The proneural genes encode proteins that possess a basic helix-loop-helix (bHLH) motif and confer NB identity (Skeath & Carroll, 1992). Hence, only one cell of the proneural cluster that maintains the expression of *AS-C* proteins becomes the NB, while in the rest of the cells, proneural gene expression gradually disappears. This neural fate restriction is mediated by the neurogenic genes *Delta* (*Dl*) and *Notch* (*N*) through the lateral inhibition process, which involves intercellular communication (Martín-Bermudo et al., 1995; Urbach & Technau, 2004). Both *Dl* and *N* encode large transmembrane proteins that are very well conserved throughout evolution. The activation of both proteins triggers another type of bHLH transcription factors (TFs) encoded by the *Enhancer of Split* (*E(spl)*) gene complex. These factors directly repress proneural gene expression and initiate the epidermal fate in the cells of the proneural cluster that have not delaminated as NB (Knust et al., 1987; Heitzler et al., 1995). Each of the NBs delaminated will generate a single lineage, which progresses through multiple rounds of asymmetric cell divisions, renewing itself and generating daughter cells called ganglion mother cells (GMCs), which will stop

proliferating. Each GMC undergoes a final terminal asymmetric division to generate a pair of post-mitotic neurons and/or glial cells **(Figure 2B)** (Doe, 1992).

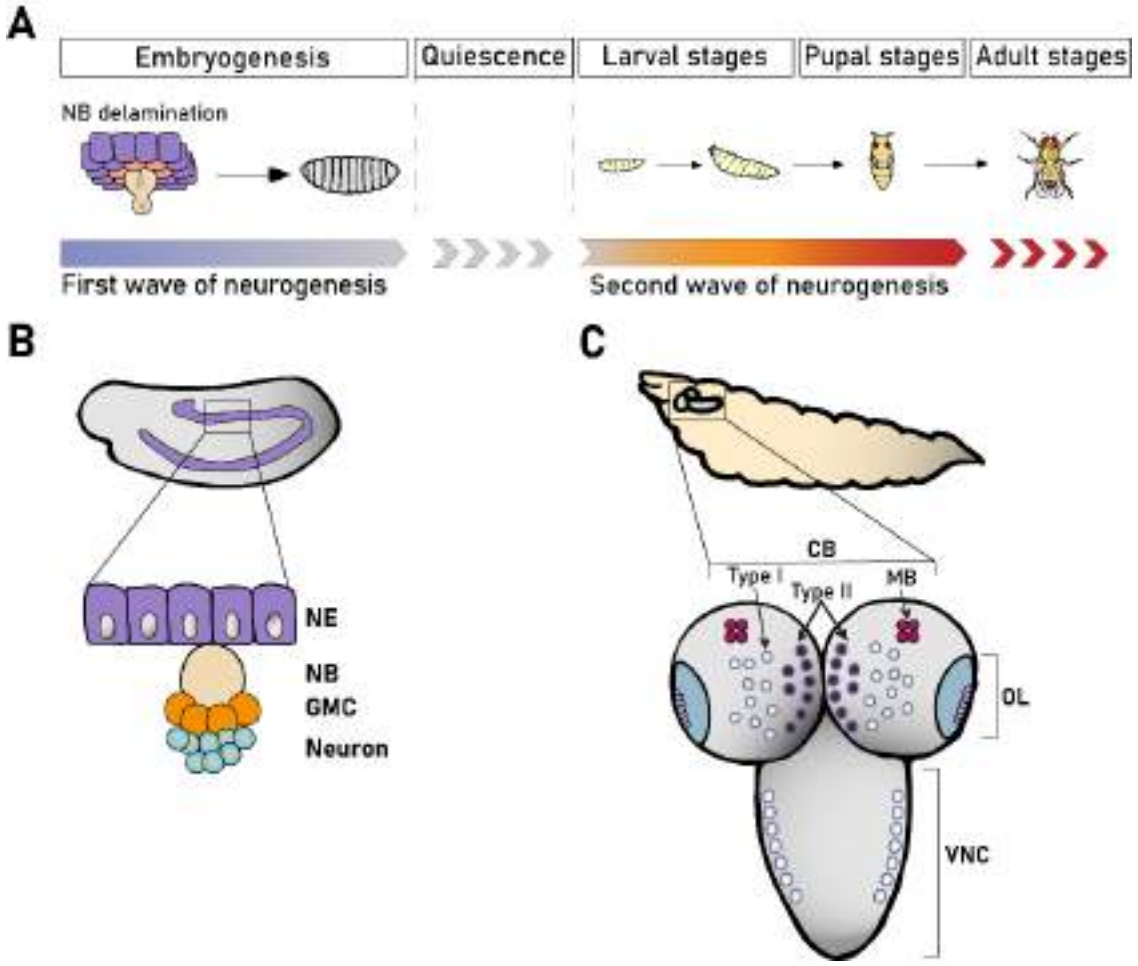

Figure 2. Waves of neurogenesis in the *Drosophila* CNS. (A) The *Drosophila* CNS is produced from two distinct waves of neurogenesis separated by a period of quiescence. The delaminated NBs pause their division at the end of the embryonic stage to reactivate in proliferative mode at the end of the first instar larval instar extending to the pupal stages. **(B)** NBs first delaminate and divide from the ventral neurogenic region of the *Drosophila* embryo during stages 9 to 11. **(C)** *Drosophila* larval CNS is divided into the CB, the OLs and the VNC, where can be distinguished abdominal and thoracic NBs in VNC. Type I, type II NBs, MBs and optic lobe NBs can be clearly differentiated in the brain lobes.

2.1. Waves of neurogenesis

Although the divisions of embryonic NBs produce all the neurons that will give rise to the larval CNS, only 10% of these neurons will remain in the *Drosophila* adult CNS. Once embryogenesis is completed, most abdominal NBs are eliminated by apoptosis; however, NBs from the cephalic and thoracic regions stop their cycle in G1 and enter into a mitotic dormancy period, termed quiescence (G0) (Egger et al., 2008; Hartenstein & Campos-Ortega, 1984). This process of quiescence is mainly regulated by intrinsic cell factors, Hox genes and temporal identity factors (Tsuji et al., 2008). There is another group of four NBs that have a different behavior and do not enter quiescence neither they are eliminated, they continue their divisions giving rise to the so-called mushroom bodies (MBs), a pair of structures in the brain involved in olfactory learning and memory **(Figure 2C)**.

The second wave of neurogenesis starts at the end of the first larval instar/early second larval instar, around 8-10 hours after larval hatching (ALH), when silent NBs exit the quiescent stage and reinitiate proliferation. This second wave will give rise to 90% of the neurons in the adult CNS (Egger et al., 2008; Homem & Knoblich, 2012). Re-entry of NBs into the cell cycle is mediated by extrinsic signals related to larval growth and development via nutritional stimulus through the fat body, which induces the release of the *Drosophila* insulin-like protein (Dilp) from glial cells. Then, activation of the PI3K/Akt signaling pathway induces NBs to exit quiescence, to promote cell growth and finally reactivate the cell cycle (Britton & Edgar, 1998; Chell & Brand, 2010; Sousa-Nunes et al., 2011).

In addition to the embryonic and larval NBs previously described, there is a third source of neurogenesis that will generate NBs from the optic lobe neuroepithelia, also in the larval brain. Symmetrically dividing neuroepithelial cells of the optic lobe will eventually change to an asymmetric mode of cell division generating NBs. This switch from a neuroepithelial to a NB fate involves a series of changes such as down-regulation of adherens junctions, reorientation of the mitotic spindle and, finally, up-regulation of

genes regulating asymmetric cell division, among other signaling events (Yasugi et al., 2008; Egger et al., 2010; Morante & Desplan, 2011; Slováková et al., 2012).

2.2. Types of Neuroblasts

Based on their lineage characteristics, different NBs can be distinguished in the CNS of *Drosophila melanogaster*.

2.2.1. Type I NBs

Type I NBs are the most abundant in the embryonic CNS (where they were initially described) and in the larval CNS. In fact, they constitute the majority of NBs in the central brain and are located both in the forebrain and in the hindbrain (Doe, 1992; Homem & Knoblich, 2012). These NBs have a relatively simple cell lineage: they divide asymmetrically giving rise to another NB with self-renewal capacity and a GMC that divides once again to generate two differentiated cells (neurons or glial cells) **(Figure 3B)**. At the end of embryogenesis, many type I NBs switch their mode of division to a "type 0" lineage, which directly generates a NB and a daughter cell that will differentiate directly into a neuron **(Figure 3A)**. This switch from type I to type 0 NB lineage is driven by a temporal cascade of TFs. They have been described in basically all NB lineages including late-embryonic ventral nerve cord NBs, all larval central brain NB lineages, as well as larval optic lobe NB lineages (Baumgardt et al., 2014; Bertet et al., 2014; Walsh & Doe, 2017).

2.2.2. Type II NBs

Type II NBs are the most recently discovered type of NB in the larval brain. Unlike type I NBs that are numerous and evenly distributed throughout the CNS, type II NB lineages are only eight per hemisphere in the central brain, and are specifically located at the dorsal part: six at the dorsal-medial location (DM1-6) and the other two at a dorsal-lateral position (DL1 and DL2) (B. C. Bello et al., 2008; Boone & Doe, 2008). Although type II NBs were firstly described in the larval brain, they have subsequently been shown to be originated in the embryo, to undergo a period of quiescence and to reactivate during larval stage to generate the CNS of the adult flies. Type II NB lineages are more complex: they divide asymmetrically to bud off smaller intermediate neural progenitors (INPs) which, after undergoing a maturation process, divide asymmetrically giving rise to a series of 4 to 6 GMCs that divide just once more originating a pair of neurons or glial cells **(Figure 3C)**. INPs are a transit amplifying population that confers to the lineage the ability to generate a much larger number of cells than type I NBs, thus giving rise to most of the intrinsic neurons of the adult CNS (Homem & Knoblich, 2012; Walsh & Doe, 2017). In fact, neurons derived from type II NB lineages constitute approximately one-fourth of the adult brain. The division of this type of NBs is similar to that shown by the radial glial cells in the outer subventricular zone (OSVZ) during the development of the mammalian cerebral cortex (Brand & Livesey, 2011; Holguera & Desplan, 2018).

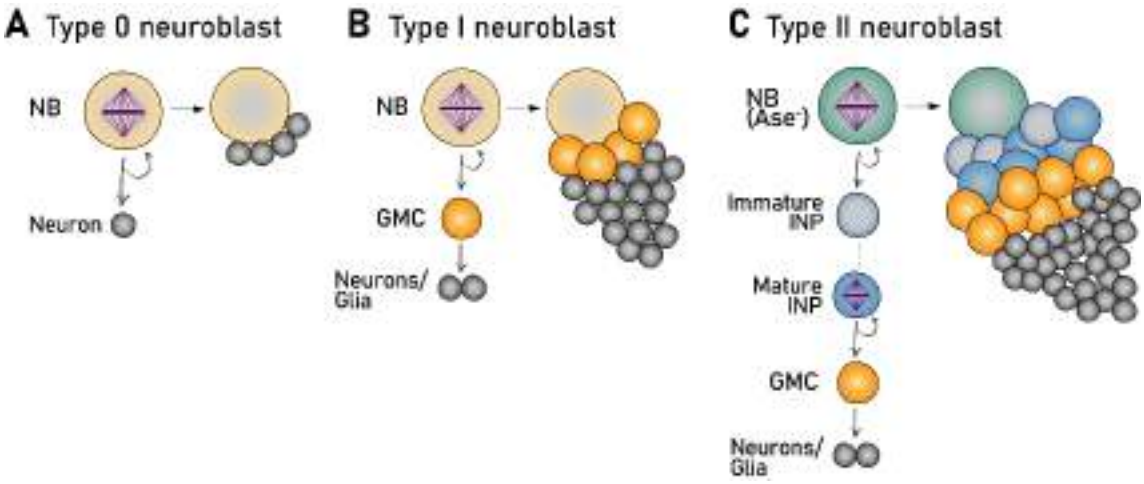

Figure 3. Types of *Drosophila* NBs in the CNS and their progeny. (A) Type 0 NBs divide asymmetrically, generating directly a NB and a differentiated neuron (in dark grey). **(B)** Type I NBs divide unequally originating a self-renewing NB and a GMC (in orange) that terminally divides giving rise to two neurons or glial cells. **(C)** A Type II NB divide asymmetrically to self-renew and produce an immature intermediate neural progenitor (immINP, in light blue) that, after a process of maturation divides giving rise an INP and a GMC that terminally divides originating two neurons or glial cells.

3. Asymmetric Cell Division

Asymmetric cell division (ACD) is a very well conserved mechanism from prokaryotes to eukaryotes to generate cell diversity, a key process in evolution and developmental biology. Most of the different cell types that form tissues originate in the early stages of embryonic development, and ACD is going to balance stem/progenitor cell expansion and cell diversity generation, giving rise to differentiated progeny (Knoblich, 2008; Sunchu & Cabernard, 2020). In an ACD, the mother cell divides to give rise to two daughter cells with different fates: one of the daughter cells retains the self-renewal and proliferative capacity of the mother cell while the other daughter cell is committed to start a differentiation program. The two daughter cells differ in size, morphology, shape and gene expression pattern (Horvitz & Herskowitzt, 1992). Most of our knowledge about the machinery that regulates ACD comes originally from the study of simple organisms, such as the bacteria *Caulobacter crescentus* or the yeast *Saccharomyces cerevisiae*, and specially from invertebrates, such as the nematode *Caenorhabditis elegans* and the fruit fly *Drosophila melanogaster* (Betschinger & Knoblich, 2004).

An essential pre-requisite for an ACD is the establishment of an axis of polarity in the mother cell. Once this axis of polarity is established, and to ensure the proper identity of the daughter cells, it is fundamental: first, the proper orientation of the mitotic spindle along the established axis of cell polarity and second, either the asymmetric orientation of the so-called cell-fate determinants in the mother cell, or the asymmetric orientation of the mother cell respect to a source of external signals called a niche (Knoblich, 2001; Yamashita et al., 2010). Based on that, there are two main mechanisms to generate two

different daughter cells in an ACD: (1) intrinsic or autonomous mechanisms, based on the asymmetric location of cell-fate determinants in the mother cell and (2) extrinsic or non-autonomous mechanisms, based mainly on niche-secreted signals **(Figure 4)**. In the first case, the cell-fate determinants are going to provide a differentiation identity to the daughter cell in which they are segregated, while the other daughter cell, which does not receive those determinants, keeps on self-renewing. In the second mode, through extrinsic mechanisms, the mitotic spindle orientated perpendicularly to the stem cell niche ensures that only the daughter cell that is in contact with the niche receives its signals, retaining the self-renewal ability, while the other daughter cell is committed to differentiate. This latter mode of division offers more flexibility, allowing in certain circumstances, the generation of two stem cells and thus expanding the stem-cell pool. Because of this, niche-based mechanisms are more common in adult stem cells, whereas intrinsic asymmetric divisions predominate during development (Knoblich, 2008; Kelsom & Lu, 2012).

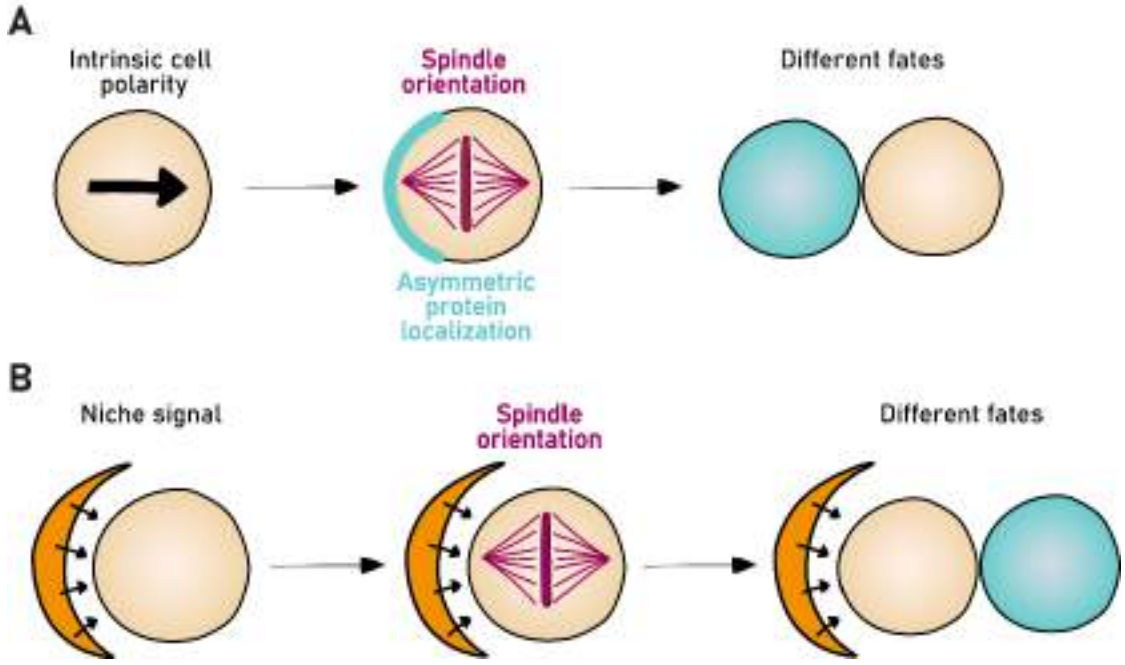

Figure 4. Asymmetric stem cell division is regulated by intrinsic and extrinsic factors. (A) Intrinsic mechanisms. Stem cells orientate the mitotic spindle respect to an axis of cell polarity previously established during interphase. Then, cell fate determinants can asymmetrically localize during mitosis coupled to the spindle orientation to only segregate into one of the two daughter cells. **(B)** Extrinsic mechanisms. Stem cells depend on an external signal source. Through the orientation of the mitotic spindle perpendicular to the surface of the niche, it is ensured that only the daughter cell closer to the niche maintains the capacity for self-renewal.

Drosophila melanogaster NBs, especially embryonic NBs, have been used for a long time as an excellent paradigm to study ACD intrinsic mechanisms. These embryonic NBs are highly polarized along an apico-basal axis of cell polarity that inherits from the epithelial cells of the neurogenic ectoderm. Although NB polarity is established in interphase, most of the machinery required for the division process is only asymmetrically localized during the mitosis phase (Knoblich, 2008; Sousa-Nunes & Somers, 2013). The maintenance of NB polarization is regulated by that machinery, organized in different apical and basal protein complexes, that eventually confer to the daughter cells their cellular identity (see below).

3.1. ACD Mechanisms

3.1.1. The Apical Complex

The establishment and maintenance of NB polarity is controlled by a group of highly conserved proteins located at the apical part of the cell cortex during mitosis (Knoblich, 2008). These apical proteins regulate both the basal localization and correct segregation of cell-fate determinants, as well as the proper orientation of the mitotic spindle and the size of the generated daughter cells **(Figure 5)** (Wodarz & Huttner, 2003; Homem & Knoblich, 2012; Sousa-Nunes & Somers, 2013). There are two main apical protein complexes: the Par/aPKC Complex and the Gαi/Pins/Cno/Mud Complex. The Par/aPKC complex will provide the first polarity signal to the cell; it is essential for the recruitment of other apical proteins and the consequent asymmetric localization of cell-fate determinants. The Gαi/Pins/Cno/Mud complex will be responsible for establishing the correct orientation of the mitotic spindle along the apico-basal polarity axis (Betschinger & Knoblich, 2004; Knoblich, 2008). Although the two events are independent, both complexes are linked by a protein called Inscuteable (Insc) which starts to be expressed in NBs (i.e., it is not detected in epithelial cells) (Kraut & Campos-Ortega, 1996; Knoblich, 2001; Wodarz & Huttner, 2003).

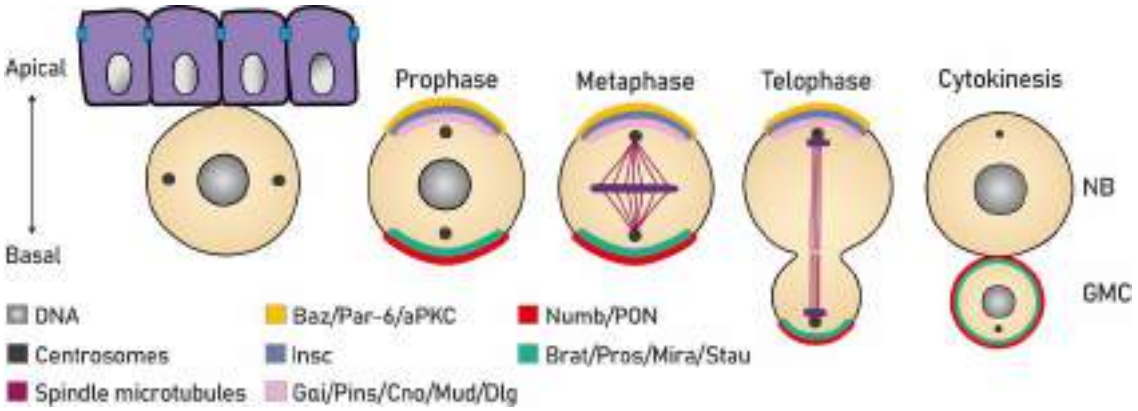

Figure 5. Asymmetric orientation of ACD regulators in *Drosophila* mitotic NBs. After delamination from a polarized epithelium, the NB divides asymmetrically along the apical-basal axis to self-renew and to give rise to a GMC. At mitosis, the Par Complex (Baz, Par-6 and aPKC, yellow line) together with Insc (blue line) and the Gαi/Pins/Cno/Mud Complex (pink line) localize into an apical crescent in the cell. The apical Par complex directs the cell-fate determinants Numb/PON (red line) and Brat/Pros/Mira (green line) to the basal pole of the cell cortex. These cell-fate determinants are going to segregate into the GMC where they promote differentiation.

The Par/aPKC Complex is formed by the proteins Par-3 (Bazooka, Baz in *Drosophila*), Par-6 and atypical Protein Kinase C (aPKC) (Kuchinke et al., 1998; Schober et al., 1999; Wodarz et al., 2000a; Petronczki & Knoblich, 2001). The formation and localization of this complex is regulated by a phosphorylation cascade triggered by the activation of the mitotic kinase Aurora A (AurA) **(Figure 6)**, event that leads to Par-6 phosphorylation and a consequent aPKC activation (Lee et al., 2006a; Wirtz-Peitz et al., 2008). Other proteins involved in these first steps are the Cell division cycle 42 Rho GTPase (Cdc42) (Atwood et al., 2007) and the protein phosphatase 2A (PP2A). Cdc42 binds directly to Par-6 and recruits it to the apical cell cortex by inducing in Par-6 a conformational change. PP2A regulates the suppression of aPKC activation by promoting Par-6 dephosphorylation (Krahn et al., 2009; Ogawa et al., 2009). aPKC plays a key role in the regulation of the ACD process, being itself a determinant of NB self-renewal (Lee, Robinson, et al., 2006b). A key substrate for aPKC is Lethal (2) giant larvae (L(2)gl), a cytoskeleton-binding protein mediator (Betschinger et al., 2003; Plant et al., 2003). When L(2)gl is active it is localized throughout the cell cortex, but when it is phosphorylated and inactivated by aPKC, it is restricted to the basal cell cortex; here, L(2)gl, in turn, excludes aPKC from the basal part, restricting it apically to form the complex with Par-6

(Ohshiro et al., 2000; Peng et al., 2000). In addition, aPKC phosphorylates Numb and Mira (cell-fate determinants, see below) restricting their localization to the basal pole during mitosis (Smith et al., 2007; Haenfler et al., 2012).

Once the apico-basal axis of cell polarity has been established in the cell, the localization of the mitotic spindle along this axis of cell polarity is essential to ensure a correct ACD process, including the localization of the cell fate determinants (Cabernard & Doe, 2009). This step is mainly driven by the Gαi/Pins/Cno/Mud apical complex. The PDZ-domain-containing protein Baz (from the Par/aPKC Complex) links the apical polarity and spindle orientation processes by recruiting Partner of Inscuteable (Pins) through Insc (Wodarz et al., 1999; Yu et al., 2000). Pins, in turn, binds the heterotrimeric G protein α i subunit (Gαi), attached to the membrane (Schaefer et al., 2000; Yu et al., 2005; Nipper et al., 2007). Next, the PDZ protein Canoe (Cno) displaces Insc and binds to Pins at the same site. Cno contributes to spindle alignment by recruiting apically the Mushroom body defect protein (Mud), which then binds Pins displacing Cno (Bowman et al., 2006; Izumi et al., 2006; Speicher et al., 2008; Keder et al., 2015). Mud, in a complex with Pins, interacts with Dynein-Dynactin forcing the movement of the mitotic spindle through the microtubules to the apical side (Mauser & Prehoda, 2012; Carter et al., 2018). In addition, Pins binds Discs Large 1 (Dlg1) (Bellaïche et al., 2001), which in turn recruits the aster microtubule-bound kinesin heavy chain 73 adaptor (Khc-73) forming the complex Pins-Dlg1-Khc-73 and thus bundling the polarity complex in the direction of the mitotic spindle (Siegrist & Doe, 2005; Siller et al., 2006; Mauser & Prehoda, 2012).

The correct action of all these proteins controls the proper orientation of the spindle and the exclusion of the cell-fate determinants from the apical part of the NB, localizing them at the basal pole **(Figure 6)**. Failures in the localization and function of the apical proteins can lead to mis-segregation of the cell-fate determinants in the cell during metaphase. To correct these failures, additional mechanisms of regulation operate during anaphase/telophase, such is the case of the process called "telophase rescue". Although it is not fully understood, two main mechanisms (Insc-dependent or Insc-independent) have been shown to operate in this regulatory process. Both mechanisms act downstream of the *snail* gene family and Baz (Cai et al., 2001). The Insc-dependent pathway is the

dominant one and involves the Baz/Insc/Pins complex. The Insc-independent pathway only acts when Insc fails. In this case, the tumor necrosis factor (TNF) receptor-associated factor 4 (TRAF4) (Bradley & Pober, 2001) along with Eiger (Egr, the fly homolog of TNF) (Igaki et al., 2002) regulate the basal localization of the cell-fate determinants Mira and Pros in the presence of Baz (Preiss et al., 2001).

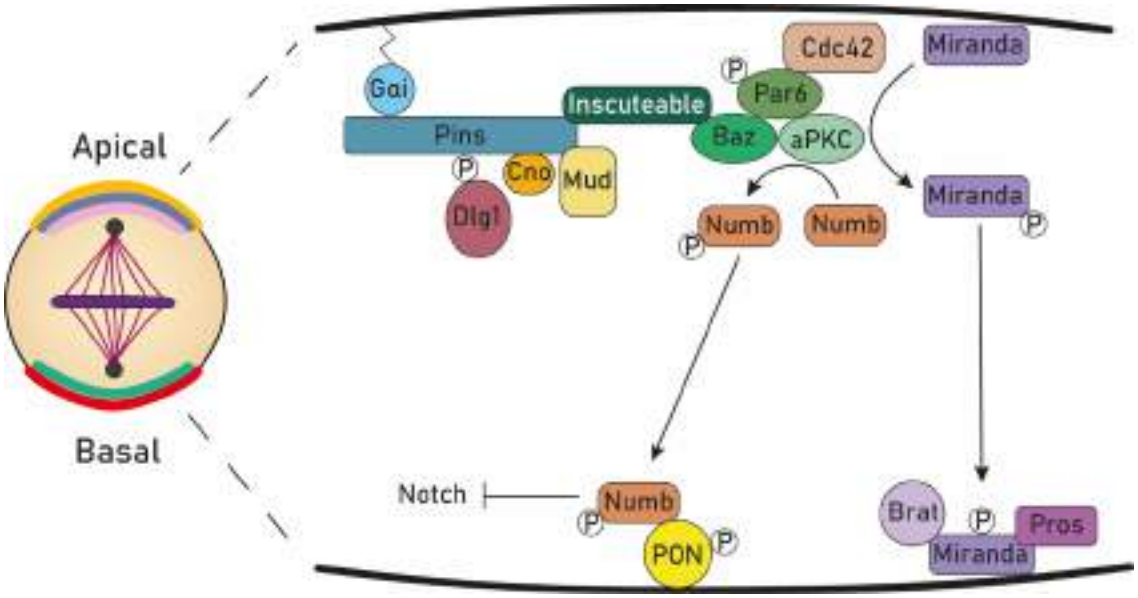

Figure 6. Apico-basal polarity in mitotic NBs. The localization and segregation of determinants is the result of phosphorylation and dephosphorylation. aPKC phosphorylates Mira and Numb leading to their exclusion from the apical cortex, restricting it to the basal cortex. Numb will segregate into the GMC where it will inhibit Notch signaling and thereby imitate the differentiation. The Mira cargo proteins Brat and Pros also segregate into the GMC to induce the differentiation program.

Finally, another aspect to take into account in a NB ACD is the difference in size of the generated daughter cells. In metaphase, the mitotic spindle is evenly distributed along the cell; however, in anaphase, the spindle microtubules move closer to the basal cortex becoming asymmetric. This process is regulated in parallel by the apical Par/aPKC and Pins/Gαi complexes (Cai et al., 2003), along with other ACD regulators, such as Dlg1 and L(2)gl (Albertson & Doe, 2003). The Cno protein together with the GTPase Rap1 also participate in the generation of this asymmetry between cells (Speicher et al., 2008; Carmena et al., 2011). The result is a larger cell that maintains NB identity with

proliferative and self-renewal capacity, and a smaller GMC cell destined to stop proliferation and to initiate cell differentiation (Kaltschmidt et al., 2000).

3.1.2. The Cell-fate determinants

As mentioned above, during mitosis cell-fate determinants accumulate asymmetrically at the basal cell cortex and they segregate exclusively to the basal GMC, promoting in this daughter cell a differentiation program (Sousa-Nunes & Somers, 2013). There are two main and independent cell-fate determinant complexes that colocalize at the basal cortex: (1) the Prospero (Pros)-Brain Tumor (Brat) complex and (2) the Numb-Partner of Numb (Pon) complex. Both complexes are independent, i.e., the failure or disruption of one of these complexes does not affect the other.

3.1.2.1. The Pros-Brat complex

This complex contains the homeodomain transcription factor Pros, which can act both as an activator and as a repressor (Doe et al., 1991; Knoblich et al., 1995; Spana & Doe, 1995), and the post-transcriptional repressor Brat, a member of the conserved family of tripartite motif (TRIM)-NHL (NCL-1, HT2A, and LIN-41) (Slack & Ruvkun, 1998; Arama et al., 2000; Frank et al., 2002). Both Pros and Brat can complex with their adaptor protein called Miranda (Mira), a coiled-coil protein (Schuldt et al., 1998).

Pros is synthesized in the NB but it is only active in the GMC. At prophase, Pros has a cytoplasmic location; however, at metaphase, Pros translocates to the basal membrane (Vaessin et al., 1991; Matsuzaki et al., 1992; Fuerstenberg et al., 1998). When Pros adaptor protein Mira is phosphorylated by aPKC, it is also excluded to the basal cell cortex, where Mira recruits Pros preventing it from entering the NB nucleus to regulate

transcription **(Figure 6)**. In addition, the RNA-binding protein Staufen (Stau) also interacts with Mira. Stau acts downstream of Insc and binds Pros mRNA participating in its localization to the basal membrane (Li et al., 1997; Shen et al., 1998). Once Mira and Pros have been secreted to the GMC, Mira is rapidly degraded releasing Pros, which will then enter the cell nucleus activating the differentiation gene transcription program (Choksi et al., 2006; Atwood & Prehoda, 2009). In contrast to Brat, Pros is not expressed in type II NBs and this may be one of the reasons why these NBs are more sensitive to the loss of some of the determinants and are more susceptible to neoplastic overgrowth and tumor formation in the larval brain (Lee, Wilkinson, et al., 2006; Neumüller & Knoblich, 2009).

The other cell-fate determinant, Brat, contains two B-boxes, a coiled-coil domain at the N-terminal end that mediates protein-protein interactions, and an NHL domain at the C-terminal end. Many of *brat* mutant alleles have the NHL domain mutated, which indicates the functional relevance of it. In fact, in the context of ACD this NHL domain binds its adaptor protein Mira, as well as other Brat mRNA targets, promoting their degradation (Reichardt et al., 2018). Brat also acts as a translational repressor in ACD by negatively regulating ribosomal RNA synthesis of the transcription and proliferative factor dMyc, thereby suppressing self-renewal programs and cell growth in one of the daughter cells (Sonoda & Wharton, 2001; Frank et al., 2002; Bello et al., 2006). During mitosis, Brat, like Pros, is localized basally by its adaptor protein Mira, and, at the end of division, Brat becomes cytoplasmic in interphase after Mira is degraded (Betschinger et al., 2006; Zhong & Chia, 2008; Kelsom & Lu, 2012). In *brat* mutants, Pros also fails in segregating to the GMC (Lee, Wilkinson, et al., 2006c). With all, in normal conditions, Brat promotes differentiation and inhibits self-renewal in the GMC acting as a tumor suppressor (TS). Furthermore, Brat inhibits the proliferation process even in symmetrically dividing cells, such as epithelial cells, since overexpression of *brat* is able to reduce the nucleolus size and inhibits mitotic proliferation (Frank et al., 2002).

There are several homologs of Brat in humans, TRIM2, TRIM3 and TRIM32. They are highly expressed in the brain and equally distant from Brat (Schwamborn et al., 2009). However, *Drosophila* Brat is an atypical TRIM-NHL protein as it lacks the characteristic RING domain of these proteins (Arama et al., 2000; Loedige & Filipowicz, 2009).

TRIM32 is also polarized during mitosis and is secreted to only one of the daughter cells, where it regulates protein degradation and microRNA activity to inhibit cell proliferation and to induce neuronal differentiation (Schwamborn et al., 2009; Vessey et al., 2012; Gómez-López et al., 2014). TRIM3 has been shown to regulate cell proliferation and cancer stem cell suppression, having therefore the potential of acting as a TS gene (see below) in the human brain (Boulay et al., 2009; Liu et al., 2014). TRIM2 on the other hand regulates different aspects in tumor occurrence and development such as tumor proliferation, migration, invasion and apoptosis. In addition, it regulates ubiquitination and degradation of the proapoptotic protein Bim, which confers a neuroprotective function (Thompson et al., 2011; Sarute et al., 2019). On the other hand, TRIM2 is highly expressed in tumor cells, aggravating cell proliferation, invasion and migration through regulation of Snail1 ubiquitination degradation, thus having an oncogenic function (Qin et al., 2018; Lin et al., 2020).

3.1.2.2. The Numb-Pon complex

The second complex is formed by the phosphotyrosine-binding (PTB) domain-containing protein Numb, firstly identified in *Drosophila* sensory organ precursor (SOP) cells (Uemura et al., 1989; Rhyu et al., 1994; Knoblich et al., 1995), and by its adaptor protein known as Partner of Numb (Pon) (Lu et al., 1998).

As previously stated, phosphorylation of Numb by aPKC causes its dissociation from the apical cortex, thus inducing its localization in the basal cortex of the cell. Numb partner Pon is normally phosphorylated by the Polo kinase cell cycle regulator excluding it from the apical side (Wang et al., 2007). Then, Pon binds Numb contributing to its basal asymmetric localization. In situations where Pon fails, Numb is unable to localize properly, leading to neural progenitor hyperproliferation (Lu et al., 1999; Shan et al., 2018). Numb contains a PTB domain at the N-terminal end, through which Numb interacts with Pon, two Aspartic Acid-Proline-Phenylalanine (DNF) motifs and an Asparagine-Proline-Phenylalanine (NPF) motif at the C-terminal part of the protein, that

binds components of the endocytic machinery (Neumüller & Knoblich, 2009; Krieger et al., 2013). Numb negatively regulates Notch signaling (an inductor of proliferation) **(Figure 6)** by binding α-adaptin, which promotes intracellular transport of Notch and its subsequent degradation. Thus, the GMC, in which Numb is segregated, is directed towards a differentiation process (Frise et al., 1996; Guo et al., 1996; Berdnik et al., 2002; Couturier et al., 2012).

Vertebrate homologues of *Drosophila* Numb have been identified in chicken, mouse, rat and human. Studies have shown a highly conserved role for the Numb protein (Verdi et al., 1996). *Drosophila* and mammalian Numb (mNumb) are evolutionarily conserved functional homologues. Both, *Drosophila* and mNumb, are asymmetrically localized in dividing neural precursors and can physically interact with mouse Notch-1 leading to a process of differentiation (Zhong et al., 1996; McGill & McGlade, 2003). Later, another homologue with a similar sequence to *Drosophila* Numb was discovered, named as mouse Numblike (also known as Numbl). Although both, Numb and Numblike, present a conserved structure and play redundant but critical roles in maintaining neural progenitor cells, they show different functions. Numblike seems to be a cytoplasmic protein distributed symmetrically throughout the cell in non-dividing NBs of the mice CNS and segregated symmetrically to daughter cells, although there are many aspects of this protein that are still unknown (García-Heredia & Carnero, 2018; Petersen et al., 2002; Zhong et al., 1997).

3.2. Asymmetric Cell Division and tumorigenesis

Stem cells play an essential role in the growth and development of multicellular organisms due to their capacity of generating by ACD both self-renewing stem cells as well as differentiated progeny. Despite all the mechanisms involved in regulating this process, failures can occur deleteriously affecting this delicate balance between self-renewal and differentiation, ultimately triggering proliferating deadly tumors (Reya et al., 2001; Neumüller & Knoblich, 2009; Li et al., 2014). Over time, *Drosophila* NBs have

been established as an excellent model to study the cellular and molecular mechanisms underlying stem cell function and the transition from normal stem cells to tumor-initiating stem cells due to the high degree of conservation with humans (Clevers, 2005; Chia et al., 2008; Homem & Knoblich, 2012). The asymmetric segregation of cell fate determinants in an ACD is a fundamental mechanism to ensure the generation of cell diversity, organ homeostasis and repair so when this segregation of apical/basal regulators fails, hyperproliferation, neoplastic growth and tumorigenesis can occur **(Figure 7)**. The connection between failures in the ACD process and tumorigenesis was first demonstrated in 2005, when it was observed neoplastic transformation of *Drosophila* larval brain mutant tissue for different ACD regulators after transplantation of the mutant tissue into the abdomen of wild-type (WT) adult hosts (Caussinus & González, 2005).

The link between failures in asymmetric NB division and tumor-like overgrowth described above was initially suggested when it was discovered that several well-known TS genes, such as *l(2)gl*, *dlg1* or *scribble* (*scrib*) act as well as regulators of asymmetric NB division (Jacob et al., 1987; Woods & Bryant, 1991; Bilder & Perrimon, 2000; Wodarz, 2005). L(2)gl/Dlg1/Scrib regulate several aspects of the NB ACD process. They show apical cortical enrichment during metaphase and regulate basal localization of cell-fate determinants such as Pros or Mira. These first studies showed that Dlg1 is required for the cortical enrichment of both Scrib and L(2)gl, however, Dlg1 localization does not depend on either Scrib or L(2)gl (Albertson & Doe, 2003). In addition, it was shown that all *dlg1*, *l(2)gl* and *scrib* mutants show a smaller apical domain than in WT conditions, resulting in symmetric or even inverted cell divisions, demonstrating the importance of these proteins not only in the regulation of cortical polarity, but also in the control of asymmetry in both daughter cell size and mitotic spindle size in NBs. (Peng et al., 2000; Bilder, 2000; Albertson et al., 2004; Lee, Robinson, et al., 2006b). Over the past years additional relevant functions for most of these regulators in the context of ACD have been unveiled (Rives-Quinto et al., 2017; Carmena, 2020 for a review).

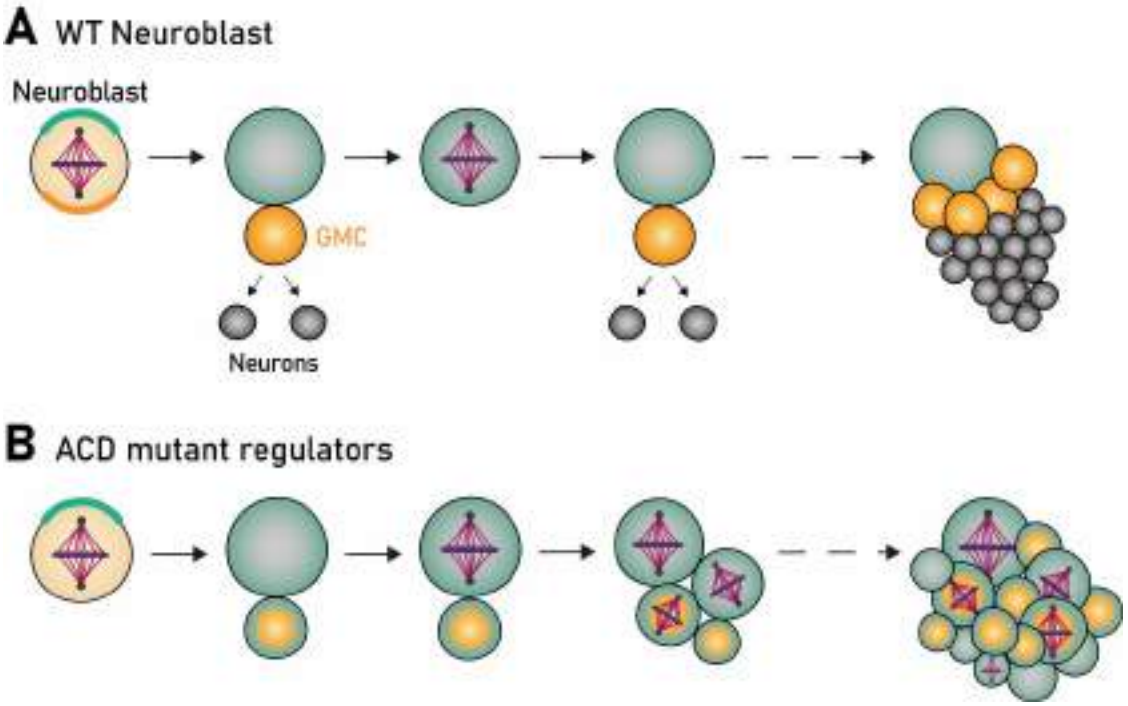

Figure 7. Mutations in ACD regulators can lead to tumor-like overgrowth. (A) In a normal situation, NBs divide asymmetrically, generating another NB (green cell), which continues self-renewing and a GMC (orange cell), which starts a differentiation program. **(B)** Mutations in some ACD regulators, such as the basal cell-fate determinants Brat, Numb or Pros cause failures in the identity of the daughter cell that would normally differentiate. These mutant daughter cells do not produce neurons, they revert to a NB-like identity and keep on proliferating producing tumor-like overgrowth.

Mutations in ACD regulatory genes are not always followed by tumor overgrowth; it all depends on the regulator that is altered, as well as the environment in which the cell develops (Carmena, 2018). In epithelia, it has been shown that, despite the fact that *dlg1/L(2)gl/Scrib* are TS genes, epithelial clones mutant for these TS genes do not cause tumor overgrowth; even more, in the case of *scrib* clones, they die by apoptosis (Igaki et al., 2006). This is caused by the activation of the Jun N-terminal kinase (JNK) signaling, induced by the WT cells surrounding the clone by a phenomenon called cell competition (Tamori & Deng, 2011). However, when an oncogenic and activated form of Ras (Ras^{V12}) is expressed, together with *scrib* (or another of the TS genes individually), cell death is prevented in these epithelial mutant clones by converting the pro-tumorigenic effect of JNK signaling in a pro-growth effect, developing large neoplastic tumor masses (Brumby & Richardson, 2003; Igaki et al., 2006; Humbert et al., 2015; La Marca & Richardson,

2020). In our lab, we observed that larval brain type II NBs mutants for the ACD regulators Cno, Scrib, L(2)gl or Dlg1 produce ectopic NBs but they do not induce tumor-like overgrowth. However, the simultaneous loss of *cno* and *scrib* do produce tumor-like overgrowth in type II NBs. This occurs through the activation of the Ras pathway (promoted by the loss of *cno*), which suppresses the cell death induced by the *scrib* mutation, plus the inactivation of two ACD regulators, Cno and Scrib (Rives-Quinto et al., 2017). These results lead us to design a pilot screening, taking advantage of the Ras^{V12} *scrib* sensitized genetic background, to search for new potential TS genes and ACD regulators (Wu et al., 2010; Rives-Quinto et al., 2017; Manzanero-Ortiz et al., 2021).

Apart of *l(2)gl*, *dlg1* or *scrib*, other well-known TS genes, such as *brat*, *AurA* or *polo*, have also shown a posteriori to regulate ACD (Gateff, 1994; Humbert et al., 2008; Zhong & Chia, 2008; Kelsom & Lu, 2012; Jiang & Reichert, 2014). Most TS genes are related to signal transduction pathways that trigger both cell-cycle arrest and apoptosis. In the context of NB ACD, as mentioned before, it has been demonstrated that mutations in some of these genes cause overproliferation of NBs during larval stages by inducing failures in the localization of cell-fate determinants in mitotic NBs and, consequently, malignant neoplastic formation (Wodarz, 2000; Chia et al., 2008).

4. *p53* tumor suppressor gene

The human TF *TP53* (*Trp53* in mice), discovered in 1979, is one of the most relevant TS genes (Kress et al., 1979; Lane & Crawford, 1979), as it is mutated in approximately 50% of all cancers and the p53 signaling pathway is disrupted in virtually all human cancers (Hollstein et al., 1991; Lane, 1992; Vogelstein et al., 2000). p53 is a key regulator of stress responses. Different stress factors such as DNA damage, nutrient deprivation, hypoxia or oncogene activation trigger a series of post-translational modifications that result in the stabilization, accumulation and activation of p53 (Brosh & Rotter, 2009; Oren, 2003). In response to these stress signals, p53 promotes cell cycle

arrest, DNA repair and apoptosis **(Figure 8)** (Schwartz & Rotter, 1998; Ventura et al., 2007; Xue et al., 2007; Hernández Borrero & El-Deiry, 2021) through its translocation to the nucleus and binding to specific DNA sequences of the genome (known as p53 response elements or p53-binding sites) (El-Deiry et al., 1992; Wang et al., 2010). Once in the nucleus, it activates or represses the transcription of adjacent genes, as well as more distant genes regulated by enhancers with p53-binding sites (Ginsberg et al., 1991; Wei et al., 2006; Riley et al., 2008; Beckerman & Prives, 2010). Failures in p53 result in the loss of its protective and tumor suppressive functions such as cell cycle regulation and apoptosis. This results in a permissive environment for tumorigenesis, allowing cancer cell proliferation and survival, promoting invasion, migration and metastasis (Mantovani et al., 2019).

Under unstressed situations, p53 is maintained at very low levels due to its rapid degradation, primarily mediated by the Murine doble minute 2 (Mdm2) protein **(Figure 8)**. This E3 ubiquitin ligase promotes phosphorylation and subsequent degradation of p53 (Haupt et al., 1997; Kubbutat et al., 1997; Vousden & Prives, 2005). Failures in both the activation and inactivation systems of Mdm2 are also linked to tumor development, since they prevent the correct degradation or stabilization, respectively, of p53 and, therefore, the correct functioning of p53 (Michael & Oren, 2002; Terzian et al., 2008). In addition, p53 is also degraded by other Mdm2-independent mechanisms, as well as inactivated by viral oncoproteins such as the E6 protein (Scheffner et al., 1990; Asher et al., 2001; Benetti et al., 2001).

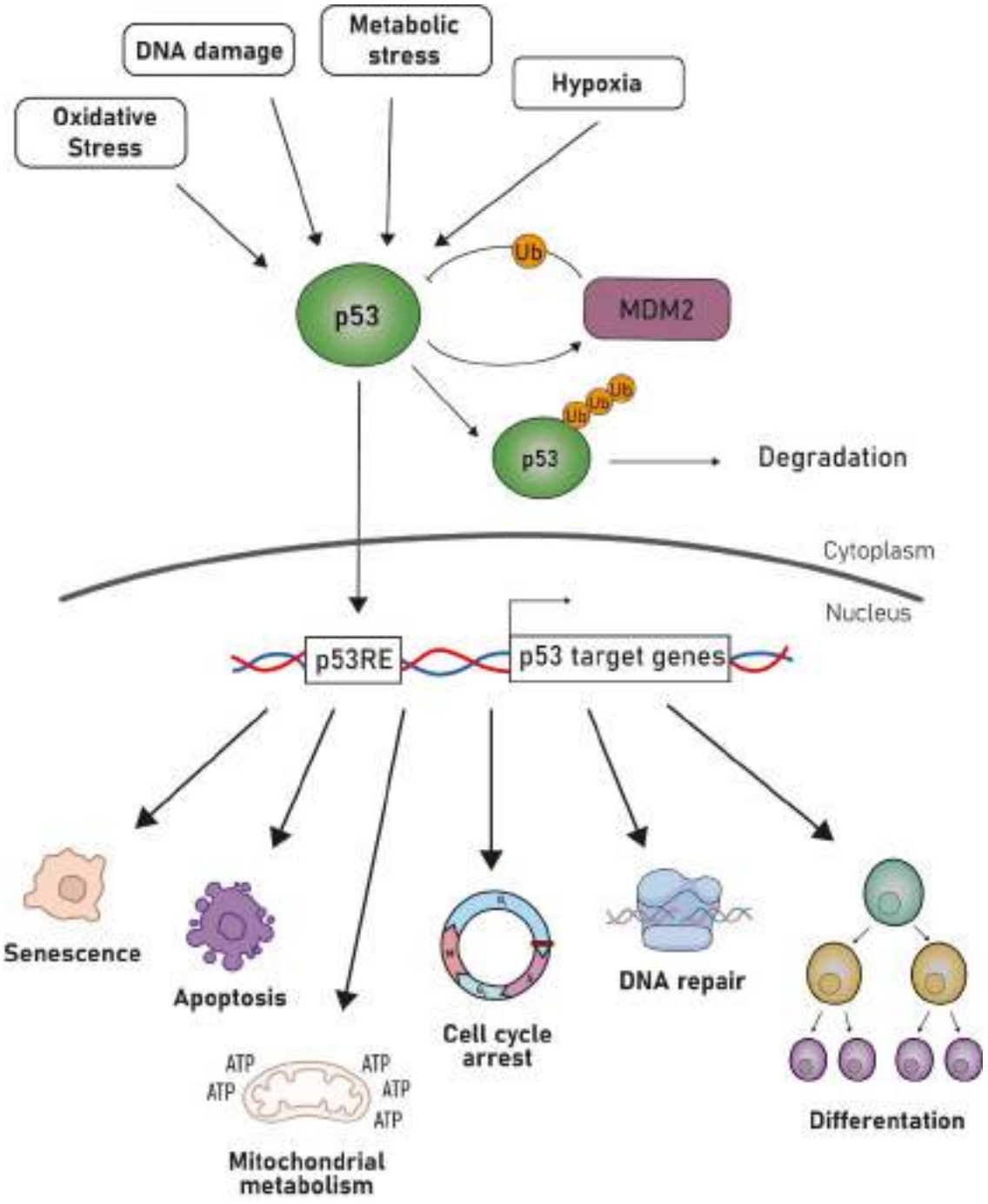

Figure 8. p53 activity in unstressed versus stressed cells. Under basal conditions, p53 is expressed at very low levels due to its ubiquitination by Mdm2 and subsequent degradation. Different cellular stresses trigger its activation and translocation to the nucleus, where p53 induces a transcriptional response by binding to DNA in a sequence-specific fashion at p53 response elements (p53RE), activating transcription of target genes involved in a wide range of cellular processes from cell cycle arrest until differentiation.

4.1. The *p53* gene family

In mammals, p53 belongs to a gene family formed by two other genes, *p63* and *p73*, both with a high degree of structural and functional similarity (Murray-Zmijewski et al., 2006). p63 and p73 are also TFs with key roles during development, although they possess specific functions that they do not share with p53. Because of their relevance in response to cellular stress, p53-like proteins are highly conserved in eukaryotes, including lower multicellular organisms (Derry et al., 2001; Schumacher et al., 2001; Cheng et al., 2015). The single *Drosophila p53* gene (*Dmp53*) encodes proteins homologous to the three members. Although the *Dmp53* gene structurally and functionally resembles mammalian p53, it has also been implicated in cell differentiation independently of its pro-apoptotic function (Ollmann et al., 2000; Stiewe, 2007; Fan et al., 2010). Furthermore, although *Dmp53* also contributes to cell-cycle arrest, it is not directly involved in this process as it occurs in mammals. In mammals, p53 directly activates the p21 cyclin-dependent kinase (Cdk) inhibitor in response to DNA damage leading to cell-cycle arrest (Harper et al., 1995; Xiong et al., 1993), while Dmp53 activates p21 (Dacapo in *Drosophila*) indirectly. Dmp53 regulates Cyclin E (CycE) levels through the activation of its transcriptional target Archipelago (Ago), which triggers proteasomal degradation of CycE. (Ouyang et al., 2011). This, in turn, leads to cell cycle arrest (Harper et al., 1995).

4.2. Non-canonical functions of p53

Despite its fundamental role as TS gene and in the maintenance of tissue homeostasis by regulating various cellular processes, over the past years p53 has been shown to display additional functions in non-canonical programs such as autophagy, inflammation and metabolism. p53 acts as a dual modulator, promoting autophagy in times of cellular stress while also inhibiting basal autophagy under normal conditions.

This dual role is attributed to its ability to transactivate autophagy-related genes like the DNA damage regulated autophagy modulator 1 (DRAM1) and Sestrin, while repressing the mammalian target of rapamycin (mTOR) signaling that is a negative regulator of autophagy (Tasdemir et al., 2008; Maiuri et al., 2010). Additionally, p53 exerts influence over inflammatory responses by modulating the nuclear factor-kappaB (NF-κB) pathway which, in turn, increases K-Ras to pathological levels (Daniluk et al., 2012), thereby impacting the expression of pro-inflammatory cytokines. While p53 actively aids in promoting immune responses, it conversely contributes to the establishment of chronic inflammation, a factor intertwined with the progression of cancer (Gudkov et al., 2011; Cooks et al., 2014; Agupitan et al., 2020). Furthermore, p53 influences cellular metabolism to maintain the metabolic homeostasis of cells and adapt them to stress by regulating glycolysis, oxidative phosphorylation, and lipid metabolism through interactions with various metabolic enzymes and transcription factors. In addition, recent studies have shown that gain-of-function (GOF) mutant p53 proteins drive metabolic reprogramming in cancer cells, contributing, in this way, to cancer progression (Contreras et al., 2018; Liu et al., 2019). The intricate interplay between p53 and these pathways underscores its multifaceted nature and highlights its significance in maintaining cellular integrity (Vousden & Prives, 2009).

In addition, in the last decade new functions of p53 have been emerging in unstressed cells, during embryonic development and differentiation, and in stem cell populations (Cicalese et al., 2009; Vousden & Prives, 2009; Ingaramo et al., 2018). One of the most captivating facets of p53 functions lies in its ability to modulate stem cell fate decisions. Studies have shown that p53 plays a dual role in this context, acting as both a suppressor and an activator of stem cell self-renewal. For instance, in the context of embryonic stem cells, p53 activation leads to differentiation by upregulating lineage-specific transcription factors and suppressing pluripotency markers, thereby driving cellular specialization and regulating stem cells homeostasis. On the contrary, in certain somatic stem cells, p53 prevents premature exhaustion by maintaining a delicate balance between self-renewal and differentiation, ensuring tissue homeostasis (Bonizzi et al., 2012; Meletis et al., 2006).

As discussed above, the ACD process in *Drosophila* neural stem cells, or NBs, functions as a mechanism of tumor suppression, since dysregulations in this process can cause loss of cell polarity and an increase in self-renewal stem cells, similar to the expansion of cancer cells (Pardal et al., 2003; Cicalese et al., 2009; Carmena, 2018). Thus, we wondered whether known TS genes could be regulating ACD. Given the relevance of *p53* as TS gene and given the involvement of p53 in modulating the mode of stem cell division, we aimed to investigate in deep in this thesis work a potential role of p53 as an ACD regulator and, eventually, the mechanisms by which p53 might be controlling this process.

II. OBJECTIVES

The general objective of this thesis project was to analyze the potential function of known TS genes in the ACD process. In particular, we were interested in determining the potential role of the TS gene *p53* in the context of ACD, using *Drosophila melanogaster* as a model system. To this end, and based on the available knowledge, we aimed to address the following specific objectives:

1. To characterize the endogenous expression/localization and loss of function phenotype of *p53* in the lineages of asymmetrically dividing stem/progenitor cells.

2. To analyze in detail the ACD on NBs in *p53* null mutants.

3. To study the mechanism of action of p53 in the ACD of NBs.

4. To analyze potential functional relationships between p53 and other ACD regulators in the context of tumorigenesis.

III. MATERIALS AND METHODS

1. *Drosophila* strains and genetics

1.1. *Drosophila* husbandry

The fly stocks used were from the Bloomington *Drosophila* Stock Center (BDSC) and Vienna *Drosophila* Resource Center (VDRC), unless otherwise stated. The following mutant stocks were used for the current work: *hs-FLP* (X-chromosome); $p53^{E8}$ (Lee et al., 2003); *p53::GFP* (BDSC: 60516); *Dll-Gal4 UAS-CD8::GFP; FRT82B tub-Gal80* (BDSC: 64307); *wor-Gal4 aseGal80* (Neumüller et al., 2011); *UAS-CD8::GFP* (BDSC: 5137); *FRT82B (BDSC)*; cno^{R2} (Sawyer et al., 2009); $Robo^{RNAi}$ (VDRC: 42241 and (Dimitrova et al., 2008); *FRT82B* $p53^{E8}$; *FRT82B* cno^{R2} $p53^{E8}$ (both for this work).

1.1.1. Balancer chromosomes

In *Drosophila melanogaster* there are a number of genetically modified chromosomes, known as balancer chromosomes, that have long been used for many purposes in genetics, such as stock construction or maintaining recessive deleterious alleles in populations (Beadle & Sturtevant, 1935; Novitski & Braver, 1954). These balancer chromosomes contain multiple inversions that suppress genetic exchange or result in aberrant meiotic products if crossing over occurs. They also contain dominant mutations to follow their presence (i.e., Tubby, Tb, "small and rounded fly body/larvae"), as well as recessive mutations, also as potential markers. In addition, most of the balancer chromosomes are lethal in homozygosis. There is a wide variety of balancers that are named according to the chromosome and the position in which they are located (e.g., FM

for the first chromosome, or TM for the third). This is one of the most powerful tools for genetic analysis in *Drosophila* (Hentges & Justice, 2004; Ashburner & Bergman, 2005; Miller et al., 2016). A part of the balancers, there are other dominant mutations that also act as markers such as sternopleural (Sp), irregular facts (If) and MKRS. For this work, the following balancer chromosomes were used: CyO, TM2 and TM6B, and the specific fly lines used were: *w; Sp/CyO Tb; TM2/TM6B; w; If/CyO lacZ; MKRS/TM6 lacZ; y w; MKRS/TM6B* (all of them from our laboratory).

1.2. Gal4-UAS system

The GAL4-UAS system was applied to achieve (ectopic/over) expression of genes or constructs of interest. It consists of two components: the *gal4* gene, which encodes the yeast GAL4 transcription activator protein, and the upstream activating sequence (UAS), which GAL4 specifically binds **(Figure 9)**. An advantage of this system is the separation of the GAL4 protein from its target gene in different transgenic lines, ensuring that the target gene remains silent until the introduction of GAL4 (Brand & Perrimon, 1993).

In *Drosophila*, GAL4 expression is under the control of a specific promoter/enhancer (ubiquitous of tissue-specific) and the gene of interest is under the control of *UAS*. When a GAL4 driver line is crossed to a line with the target gene under the control of UAS, the progeny expresses the gene of interest only in cells in which GAL4 is present.

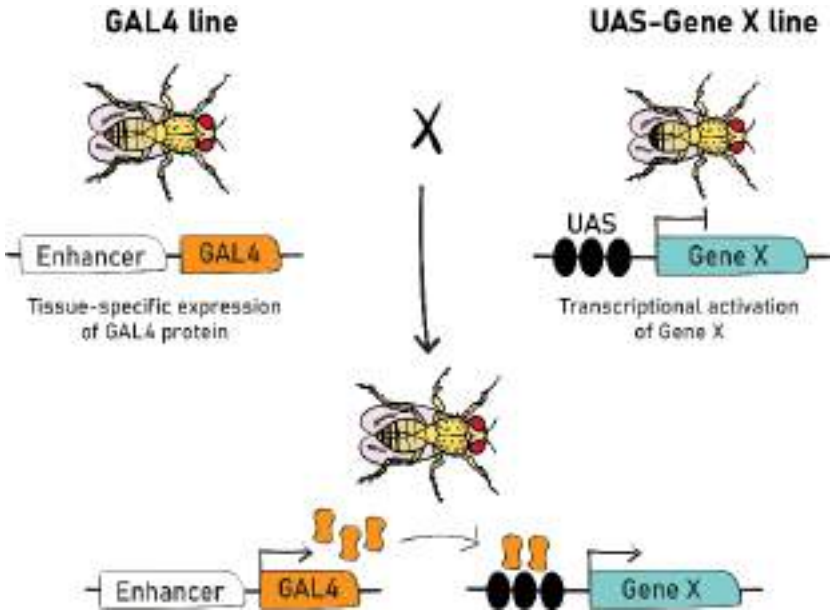

Figure 9. Schematic of the UAS-GAL4 system. Flies expressing GAL4 under the control of a specific promoter or enhancer are crossed with flies carrying the gene of interest under the control of UAS. In the offspring of the cross, the gene under the control of UAS is expressed in the presence of GAL4.

The following fly lines were used to drive the expression of GFP in the membranes of larval type II NBs: *DllGal4 UAS-CD8::GFP and wor-Gal4 aseGal80; UAS-CD8::GFP*. All GAL4-UAS crosses were carried out at 25ºC. A *white* (*w*-) fly strain was used as the reference control WT strain.

1.3. MARCM larval brain clones

To establish type II NB mutant clones in a WT surrounding environment, we used the Mosaic Analysis with a Repressible Cell Marker (MARCM) clone technique (Lee & Luo, 1999). This technique generates a subset of homozygous mutant cells from heterozygous progenitors through mitotic recombination. For that, the yeast recombinase flippase (FLP) and the FLP recombination target (FRT) sites are used in combination with

the GAL4/UAS system to positively label the mutant clones. The GAL80, a GAL4 repressor is key in this technique (see below) (Golic & Lindquist, 1989). The MARCM technique allows spatial control (by the use of tissue/cell-specific Gal4 lines), in addition to the temporal control of clone induction (by using an inducible flippase, i.e., with a heat shock promoter) at different developmental stages **(Figure 10)**.

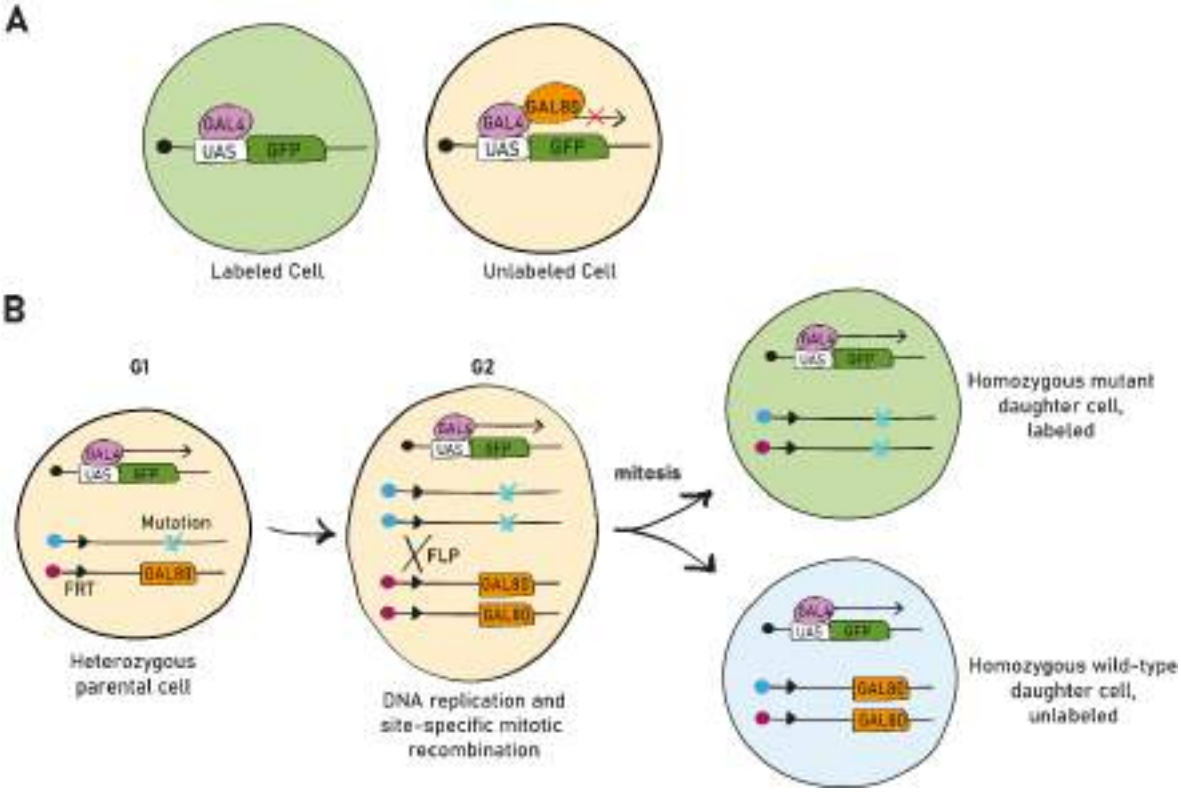

Figure 10. Schematic representation of the MARCM genetic system. (A) Cells containing the GAL4 express the UAS-gene (GFP, in green) whereas in cells in which the GAL4 repressor GAL80 is present the UAS-gene (GFP), GAL4-dependent, is not expressed. In this schematic, genes are denoted by colored boxes whereas proteins are denoted by colored ovals. (**B)** In the MARCM technique, after site-specific mitotic recombination induced by the FLP at the FRT sites (black arrowheads), a heterozygous mother cell can give rise to two daughter cells in which the chromosome arms distal to the recombination site become homozygous. The loss by recombination of the GAL4 repressor GAL80 in the homozygous mutant cells results in specific expression of (UAS-)GFP under the control of the GAL4 line.

Initially, parental cells are heterozygous for the GAL-80 transgene, which inhibits the activity of the GAL4 transcription factor, thus preventing the expression of a membrane-associated reporter (UAS-CD8::GFP). By FLP/FRT-mediated mitotic

recombination induced by heat shock, GAL-80 is removed from one of the daughter cells allowing the activity of the GAL4 and, thus, GFP expression. GFP can be visualized in all mutant clones if directed by a ubiquitous GAL4 driver, or only in a subset of cells when a tissue-specific GAL4 driver is used. Moreover, mitotic recombination can be induced at a specific time of development by selecting the timing of the heat shock, which results very useful to study and establish different patterns throughout the process of neurogenesis.

For this work we used the line *Dll-Gal4 UAS-CD8::GFP* , to drive GFP expression in type II NB lineages, combined with the FRT82B tub-Gal80 repressible system (chromosomes II and III, respectively). This line was crossed with flies containing hsFLP (chromosome X) combined with FRT82B followed by the mutation of interest (chromosome III) **(Figure 11)**.

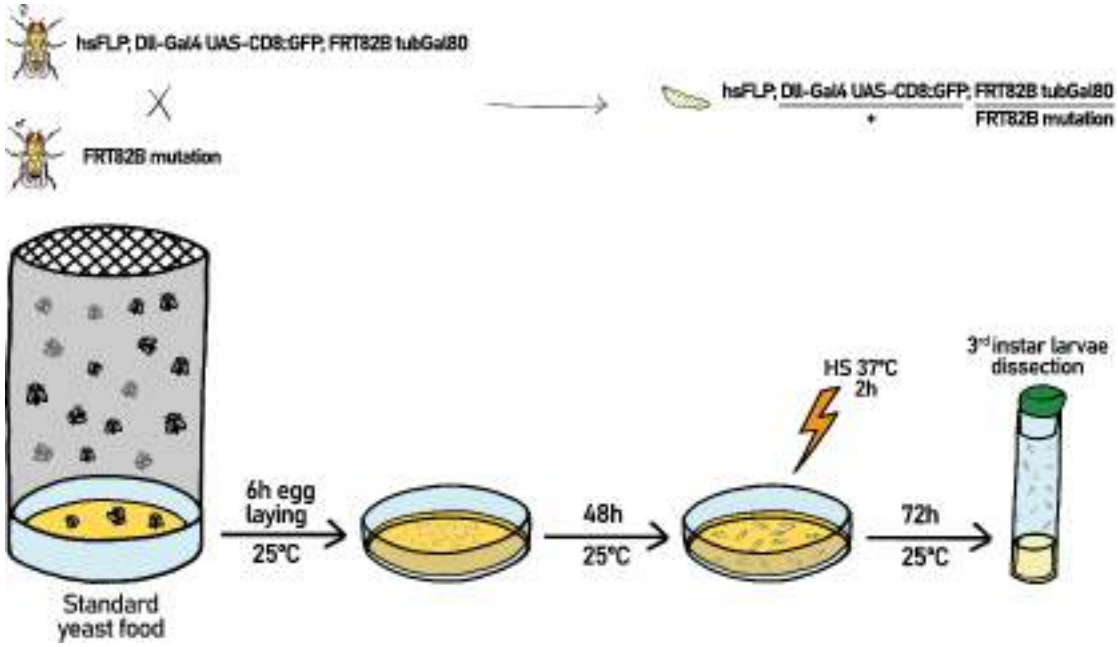

Figure 11. Schematic representation of the crosses and the protocol performed to obtain MARCM clones in larval brain type II NB lineages. Crosses were carried out in egg-laying cages with Petri dishes containing standard yeast food at 25°C for 6 hours. The adult flies were then removed from the laying cage and the eggs were incubated for 48 hours at 25ºC. At that moment (the end of the first/beginning of the second larval instar stage), a heat shock was induced at 37°C for 2 hours. The larvae were then placed at 25°C to develop for up to 72 hours more. Larvae were collected and dissected at the third larval instar stage (120h AEL).

1.4. Generation of *FRT82B p53^{E8}* recombinant flies

In order to induce *p53^{E8}* mitotic recombination clones, the presence of FRT sequences in the same chromosome arm as *p53* are mandatory. Hence, we generated in the lab ***FRT82B p53^{E8}*** recombinant flies using the following cross scheme:

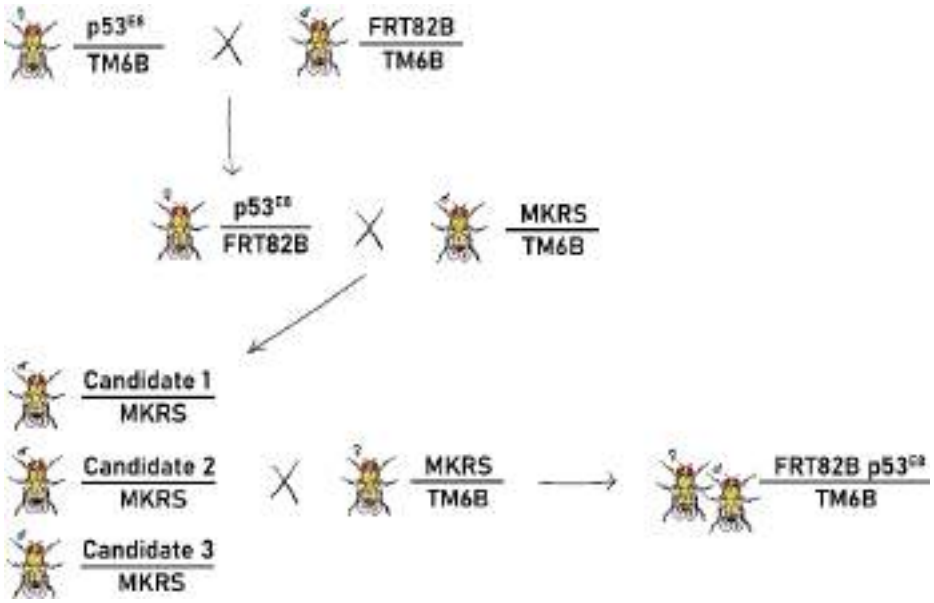

Figure 12. Schematic representation of the crosses performed to obtain the *FRT82B p53^{E8}* recombinant. Virgin *yw, hsFLP*; *FRT82B/TM6B* females were crossed with *w; p53^{E8}/TM6B* males. *FRT82B/p53^{E8}* virgin females from the F1 were selected and mated with males with balancer chromosomes. Then, different recombinant male candidates were mated one last time with females-containing balancer chromosomes.

The offspring from these crosses was tested for the presence of both FRT and *p53^{E8}*, as explained below.

1.4.1. FRT validation

FRT sequences are integrated into a P-element that in many cases contains a neomycin gene (*hs-neo*) to allow antibiotic selection of FRT-containing chromosomes (Xu & Rubin, 1993; Theodosiou & Xu, 1998). In this way only flies carrying this *hs-neo* element can grow and develop on Geneticin medium (*G418-Sulfate*, *Thermofisher*) due to their resistance. 50 mg of antibiotic was dissolved in 2 ml of sterilized water and added to the standard yeast food mixture to prepare fly food tubes. After a 24h set at 25ºC, the adults were removed and the tubes were incubated for a further 24h at 25ºC. Then a heat shock was induced at 37°C for 40 min and finally incubated at 25ºC until the development of new adults. *W-* strain was used as the negative reference control and a known/already validated FRT strain was used as a positive reference control.

1.4.2. *p53* validation

Genomic DNA extraction from potential recombinants was carried out in eppendorfs with an adult fly of our interest in 50 µl of STE buffer. After adding 1µl of proteinase K (20 mg/ml), the tissue was homogenized mechanically with a pestle. The sample was then incubated 30 min at 37°C followed by 5 min at 95°C to inactivate the enzyme activity. Finally, the samples were centrifuged and transferred to a new eppendorf to be stored at -20°C or used directly for PCR amplification. The absence of *p53* in the potential recombinants was confirmed by PCR. PCR reaction is shown in **table 1**. PCR conditions are shown in **table 2**.

Primers used:

Forward 5'- CAT GCA AGG TTT CTA CTG TTC G

Reverse 5'- GCT GCA TTA TCA TAT GTC TGC

PCR reaction mix (25 µl volume)	Final concentration
5x Green GoTaq Flexi Buffer	1x
$MgCl_2$ Solution, 25 mM	2.4 mM
PCR Nucleotide Mix, 10 mM each	0.2 mM each dNTP
Forward primer 10 µM	1.6 µM
Reverse primer 10µM	1.6 µM
GoTaq DNA Polymerase (5 u/µl)	1.25 u
p53 cDNA	20 ng

Table 1. PCR reaction mix for *p53* amplification using GoTaq Flexi DNA Polymerase (*Promega*)

Process	Temperature	Time	Cycles
Initial Denaturation	95ºC	2 min	1x
Denaturation	95ºC	30 sec	30x
Annealing	52ºC	30 sec	30x
Extension	72ºC	1 min	30x
Final Extension	72ºC	5 min	1x
Soak	4ºC	Indefinite	1x

Table 2. PCR thermal cycling using GoTaq Flexi DNA Polymerase (*Promega*)

2. *Drosophila* dissection and fixation

2.1. Embryo collection and dechorionation

All embryos were collected from a mix of grape juice with agar laying plates daubed with yeast paste at intervals of 0-16 hours at 25ºC depending on required embryo stage. For the embryo collection, materials such as small sieves, a paintbrush and a small scraper were used. Before the collection, yeast traces can be removed with a scraper to facilitate the process. For embryo dechorionation, small sieves were employed using 100% commercial bleach for 2 minutes at room temperature (RT), until the chorion was

completely eliminated. Embryos were well washed several times with distilled water to remove any trace of bleach.

2.2. Embryo formaldehyde fixation

Dechorionated embryos were transferred into glass vials with 1 volume of heptane and 1 volume of 4% formaldehyde (FA) in phosphate-buffered saline (PBS, pH 7.4). Before transferring the embryos, the vials were well-shaked to allow the formation of an interphase with FA-saturated heptane, in which the embryos are going to be fixed. After that, embryos were transferred into the vials and fixed for 20 minutes at RT in an orbital shaker. Then, any trace of FA (bottom phase), as well as heptane (upper phase), were well-removed by using a Pasteur pipette. Embryos were washed two times with heptane, leaving them with 1 volume of fresh heptane. To remove embryo vitelline membranes, 1 volume of methanol was added to the heptane, vigorously shaking the vials. Embryos that lose the vitelline membrane fall down to the bottom of the vial (methanol). The interphase methanol:heptane with the rest of embryos that have not lost their vitelline membrane, as well as the upper phase (heptane), was completely removed. After 2 rinses of 100% methanol, embryos were transferred to 0.5 ml Eppendorf tube and then were stored in methanol at -20ºC or directly used for immunostaining experiments.

2.3. Larval brain dissection and paraformaldehyde fixation

*Drosophil*a larval brains were dissected under the scope in wells filled with cold PBS. Larval brains were transferred to 600 µl of 4% paraformaldehyde (PFA) in PBT to fix them for 20 minutes at RT in the orbital shaker.

3. Immunohistochemistry and immunofluorescence

Fixed tissue was rinsed twice with PBS containing 0.3% Triton X-100 (PBT, pH 7.4). Then, embryos or larval brains were washed 3 times with 500 µl of PBT pH 7.4 for 15 minutes at RT. All washes and incubations were done in a rotator for embryos or in an orbital shaker for larval brains. PBT was replaced by 500 µl of PBT containing 0.1% of Bovine Serum Albumin (BSA, *Sigma*) and incubated for 1 hour at RT, followed by an over-night (ON) incubation at 4ºC with the primary antibody (Ab). This last incubation can also be done at RT for 2 hours (in the case of embryos) or during 3 hours (for larval brains). All Abs (primary and secondary Abs) were always diluted in PBT 0.1% BSA. After incubation with the primary Ab, embryos or larval brains were washed with PBT (pH 7.4): two quick rinses followed by three 15 minutes-washes. Then, tissue was incubated with the secondary Ab (1:200-1:400) at RT (1 hour for embryos and 2 hours for larval brains). Finally, tissue was washed three times for 15 minutes in PBT followed by 10 minutes with PBS and mounted in the proper media: Epon, for embryo DAB immunohistochemistry (see below) or Vectashield (*Linaris*), for both embryo and larval brain immunofluorescence. The Vectashield was directly added to the tissue after the last washing. Preparations were set up in microscope slides with larval brains placed in dorsal position organized in a single row, between two glue pieces of adhesive tape, and protected with a cover glass. Embryos were mounted in 5 rows, with 5 embryos in each row, in a lateral or ventral position between two glue pieces of adhesive tape and protected with a cover glass.

3.1. DAB histochemistry

Fixed embryos were incubated with primary and biotin-conjugated secondary Abs (see below). After incubation in an Avidin Biotin mixture (described below) and washing steps, embryos were transferred to a small collection basket. Almost all PBT was removed

and replaced by 200 µl of 0.5 mg/ml of diaminobenzidine solution (DAB) in PBS pH 7.4 for 2-3 minutes. Protein expression was detected through oxidation of DAB by using 0.01% of peroxidase. This oxidation results in an orange-brown color. Addition of Ni^{2+} ions to DAB prior to the oxidation reaction resulted in a dark blue color. Those two colors helped to distinguish between patterns of different proteins. Embryos were then dehydrated through a graded series of ethanol solutions including 1 time for 10 minutes in 70% ethanol and 2 times for 10 min in 100% ethanol. Then, embryos were incubated 2 times for 10 min in acetone and left in a mix of Acetone/Epon (1:1). After Acetone evaporation, embryos were mounted with a drop of Epon in microscope slides and heated to solidify the Epon. Finally, a small amount of Epon and a cover glass was added on the embryos. After heating the slide to solidify the Epon, the slide was ready to analyze under the microscope.

The following primary Abs were used: rabbit anti-Ase 1:100 (Rives-Quinto et al., 2017), guinea pig anti-Dpn 1:2000 (Rives-Quinto et al., 2017), chicken anti-GFP 1:3000 (*Aves Labs*), guinea pig anti-L'sc 1:100 (Stagg et al., 2011), mouse anti-Wg 1:50 (*DSHB*), mouse anti-γtubulin from 1:100 and 1:400 (for larval and embryo staining, respectively; *Sigma-Aldrich*, *T5326*), rabbit anti-phospho-histone H3 from 1:400 to 1:1000 (for embryo and larval staining, respectively; *Millipore*, *06-570*), mouse anti-phospho-histone-H3 1:2000 (*Millipore*, *05-806*), mouse anti-Dlg 1:25 (*DSHB*), mouse anti-β-galactosidase from 1:200 to 1:8000 (for immunofluorescence and DAB staining, respectively; *Promega*, *Z3781*), rabbit anti-Eve 1:3000 (Frasch et al., 1987), rabbit anti-Zfh1 1:1250 (Lai et al., 1991), guinea pig anti-Runt 1:400 (Kosman et al., 1998), rabbit anti-PKCζ 1:100 (*Santa Cruz Biotechnology*, *sc-216*), goat anti-Numb 1:200 (*Santa Cruz Biotechnology*, *sc-23579*), guinea pig anti Par-6 1:1000 (Petronczki & Knoblich, 2001) and rabbit anti-Brat 1:200 (Betschinger et al., 2006).

The following secondary Abs conjugated with fluorescent dyes were used with the concentrations described above (1:400): Alexa Fluor 488 (green), Alexa Fluor 546 (red), Alexa Fluor 633 (blue), Alexa Fluor 647 (blue) (*Invitrogen*), Cy3 (*Jackson ImmunoResearch*), Phalloidin 633 1:40 (blue) (*Sigma, 68825-10NMOL*).

Biotinylated secondary Abs (*Vector labs*) were used 1:200 for embryo immunohistochemistry and incubated as described previously. After two rinses and three times for 15 minutes washes in PBT pH 7.4, embryos were incubated in Avidin and Biotin mixture (Vectastain ABC kit, *Vector labs*) for 40 minutes at RT. Then embryos were washed with PBT three times for 15 minutes at RT (all the incubation steps were carried out in the rotator).

4. Imaging

HRP immunohistochemistry from figure 15 was visualized using Nomarski Optics on a Carl Zeiss microscope (Axio Imager.A1). Images of ventral view embryos were taken with 63x/1.25 oil objective. Images were assembled using Adobe Photoshop CS6 program.

Fluorescence images from figures 14, 16, 17 (except figure 17C) and 22A were recorded by using an Inverted Leica laser-scanning spectral confocal microscope TCS SP2 (Leica Spectral Confocal acquisition software). The rest of fluorescence images from figures (including figure 17C) were recorded using a Super-resolution Inverted Confocal Microscope Zeiss LSM 880-Airyscan Elyra PS.1. Images were analyzed using the image processing package FIJI from ImageJ and assembled using Adobe Photoshop CS6 program.

5. Viability curve

To establish the survival rate of *p53* mutants, we performed a viability curve, following this procedure **(Figure 13)**: After a 4-hour egg laying in Petri dishes with a mixture of agar and grape juice, approximately 100 embryos were collected and placed in a new Petri dish with the same mixture. After 24h, hatched embryos were counted and first instar larvae (L1) were collected and transferred to a new Petri dish. This process was repeated at 48 h after larval hatching (ALH) (second instar larvae, L2) and 72h ALH (third instar larvae, L3). Finally, L3 larvae were transferred into glass tubes with food and left until the adult stage (all incubations were performed at 25ºC).

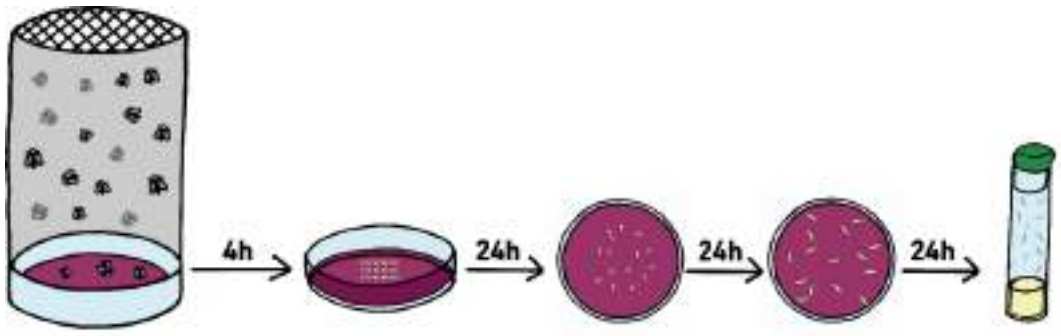

Figure 13. Viability curve scheme. Following a 4-hour laying, 100 embryos were selected and tracked until adulthood to establish the survival rate.

6. Quantitative RT-PCR

To quantify RNA levels, total RNA was extracted from 16 halved *Drosophila* larvae using TRI Reagent (*Invitrogen, AM9738*). Briefly, samples were incubated 5 min at RT, 100 µl BCP (1-bromo-3-chloropropane) / mL TRI Reagent was added and incubated again for 15 min at RT. After centrifugation, the aqueous phase was collected and 0.7 volumes of isopropanol / mL TRI Reagent were added. After a centrifugation, pellet was

washed with 70% Ethanol, resuspended in TE and quantified using a Nanodrop (*Thermo Scientific, ND-1000*). RNA was treated with DNAse (*Thermo Scientific*, *EN0521*) and reverse transcripted with NZY Reverse Transcriptase (*NZYTech, MB12401*). For Numb PCRs, SuperScript III Reverse Transcriptase (*Invitrogen*, *1808044*) was used. Oligo(dT) primer mix (*NZYTech, MB12801* or *Invitrogen*, *184181-020* in the case of Numb) were used. Quantitative real time PCR (qRT-PCR) was performed using NZY Supreme qPCR Green Master Mix, ROX Plus (*NZYTech, MB440022*) or Power SYBR Green PCR Master Mix (*Applied Biosystems, PN4367218*) in the case of Numb amplification, following established protocols in **Tables 3, 4** on an QuantStudio™ 3 apparatus (*Applied Biosystems*). Act88F and GADPH primers were used for mRNA normalization. Comparative qPCRs were performed in at least three replicates and the relative expression was calculated using the comparative ΔΔCt method.

Primer sequences:

Brat:

Forward 5'- GCA AGG TGA TGC GTG TGA TC

Reverse 5'- TGT CGC TGA TGA AGA TCT CC

Numb:

Forward 5'- GCA GCA TTA ATC AGA ACA TC

Reverse 5'- ATG GAG CGT CTG ATA TGT GG

Traf4:

Forward 5'- GCA CTC TGT TGT GGA AGA TC

Reverse 5'- AGT GTG AAG GTG ATG GAG TGC

Act88F:

Forward 5'- TCG ATC ATG AAG TGC GAC GT

Reverse 5'- CGG AGT ACT TCC TCT CGG GT

GADPH:

Forward 5'- TAA ATT CGA CTC GAC TCA CGG T

Reverse 5'- CTC CAC CAC ATA CTC GGC TC

PCR reaction mix (20 µl volume)	**Final concentration**
2x Master Mix	1x
Forward primer	50 to 400 nM
Reverse primer	50 to 400 nM
Template	1 to 100 ng
Nuclease-free water	-

Table 3. qRT-PCR reaction mix for *p53* amplification using NZY Supreme qPCR Green Master Mix, ROX Plus (*NZYTech*) for *brat* and *Traf4* genes or Power SYBR® Green PCR Master Mix for *numb* gene.

	brat, Traf4			***numb***		
Process	**Tº**	**Time**	**Cycles**	**Tº**	**Time**	**Cycles**
Polymerase activation	95ºC	20 sec	1x	95ºC	4 min	1x
Denaturation	95ºC	5 sec	40x	95ºC	10 sec	40x
Annealing/ extension	60ºC	20 sec		60ºC	35 sec	

Table 4. qRT-PCR thermal cycling using NZY Supreme qPCR Green Master Mix for *brat* and *Traf4* genes or Power SYBR Green PCR Master Mix for *numb* gene.

7. Statistical analyses

Statistical analyses were carried out with SigmaPlot 12.0 Software. To assume statistical significance, p-values were determined below 0.05. The data were first analyzed using the Shapiro-Wilk test to determine whether the sample followed a normal

distribution. Parametric t-test or a nonparametric two-tailed Mann Whitney U test for those that did not follow a normal distribution were used to compare statistical differences between two different groups. To determine the equality of proportion between different groups, a Chi-squared test with Yates correction was applied.

For most experiments, images data graphic representation was done using simple bars or box plots with whiskers. For spindle orientation analysis, angles were calculated using ImageJ, measuring the angle between a line linking both centrosomes and the planar apical surface. To avoid overcorrection, only mitoses with centrosomes in the same or in two consecutive Z-planes were considered for quantification. The specific test used, experimental sample size (n) and the *p*-value are indicated in the figure or figure legend; * $P < 0.05$, * $P < 0.01$, *** $P < 0.001$, ns: not significant ($P > 0.05$).

IV. RESULTS

1. p53 is expressed in neural progenitor cells

Previous works have shown that p53, a very well-known TS gene, can suppress the self-renewal capacity of stem cells (Cicalese et al., 2009). In this thesis work, we wanted to investigate whether p53 could be acting as an ACD regulator, using the *Drosophila* NBs as a model system. Therefore, we first analyzed p53 expression in embryonic type I NBs and in larval type II NB lineages. We took advantage of transgenic flies carrying a GFP-tagged endogenous *p53* gene that allowed us to see its entire expression profile. Early stage 9 *p53::GFP* embryos were labeled with GFP, to increase the signal, and specific markers of NBs, such as the proneural protein L'sc, a TF that is expressed in all NBs (Martín-Bermudo et al., 1991), and the cytoplasmic and secretable protein Wingless (Wg), expressed only in a specific group of NBs **(Figure 14A)** (Chu-LaGraff & Doe, 1993).

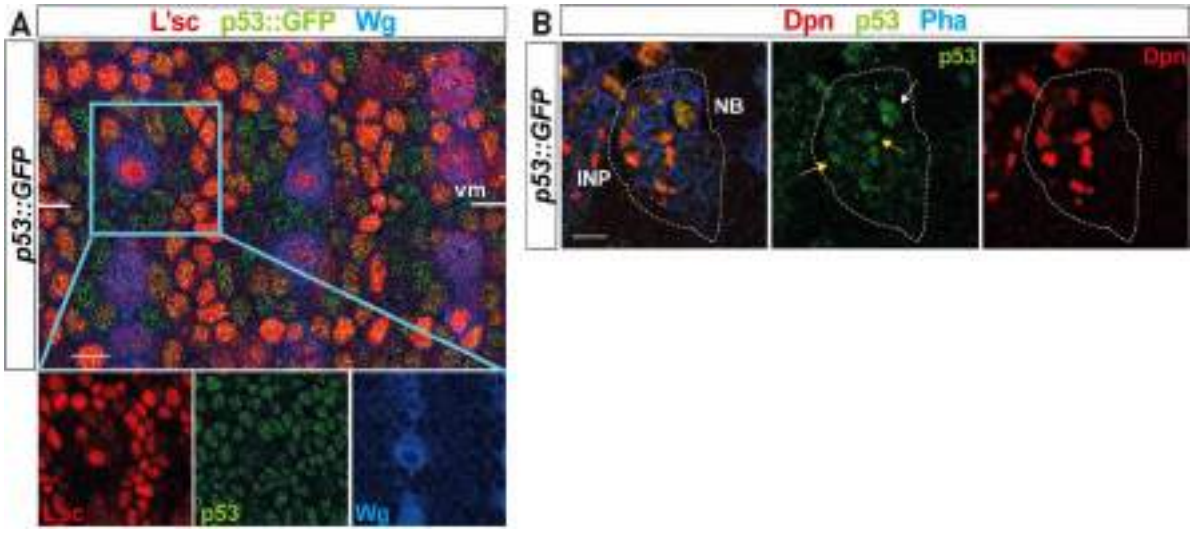

Figure 14. Expression of p53 in neural progenitor cells. (A) Embryo ventral view at stage 9 stained with GFP (green) to label the GFP-tagged endogenous p53, L'sc (red) and Wg (blue). L'sc shows a nuclear expression like p53 while Wg shows a cytoplasmic expression in the NB. **(B)** In larval type II NB lineages, p53 (GFP, in green) is expressed in NB (white arrow) and INPs (yellow arrows), Dpn (red) labels the NB and INPs, and Phalloidin (blue) labels the membranes. vm=ventral midline, NB=neuroblast, INP=intermediate neural progenitor. Scale bar: 10 µm

We next wanted to determine whether p53 accumulates asymmetrically in metaphase NB, as it has been reported for other TFs (Knoblich et al., 1995; Fuerstenberg et al., 1998). For this analysis, we used phospho-histone H3 (PH3), to label mitotic cells, as well as γ-tubulin to label the centrosomes. However, we were not able to observe any asymmetric distribution of p53 in mitotic NBs (data not shown). To assess the expression of p53 in the larval brain type II NB lineages, we used as a marker Deadpan (Dpn), which is a TF present in all NBs and other progenitor cells (INPs). We observed a strong expression of p53 in NBs and INPs of type II NBs lineages **(Figure 14B)**.

2. p53 is required for proper neuronal lineage formation

As a first approach to analyze the potential function of p53 in ACD, we examined the asymmetric division of the *Drosophila* embryonic ganglion mother cell type I (GMC-1), whose neuronal lineage has been extensively studied and very well characterized **(Figure 15)** (Bhat & Schedl, 1994; Bossing et al., 1996). At stage 11, the NB 7-3 divides asymmetrically, generating another NB and the GMC-1, in which the expression of the TF Even-skipped (Eve) begins (Isshiki et al., 2001) **(Figure 15A)**. By stage 12, the GMC-1 divides giving rise to two neurons called RP2 and RP2-sibling (RP2sib), both of which will initially express Eve. However, at late stages of neurogenesis, stages 16-17, only the RP2 neuron maintains Eve expression; in RP2sib Eve expression completely disappears. Therefore, only one RP2 neuron (Eve^{+}) is present per hemisegment at these later stages in the embryonic CNS. Defects in the number of RP2 neurons (i.e., either duplications or losses) at these later stages are used as an indicator of failures in the ACD process in this GMC-1 lineage (Broadusa et al., 1995). We observed that $p53^{E8}$ null mutant homozygous embryos (n=99) displayed defects in the number of RP2 in 3.4% of the hemisegments analyzed (n=1830), while in control embryos (n=90), 0.3% of the total hemisegments analyzed (n=1685) showed failures **(Figure 15C, D)**. This result strongly suggested that p53 might be somehow regulating the ACD within the GMC-1 neuronal lineage.

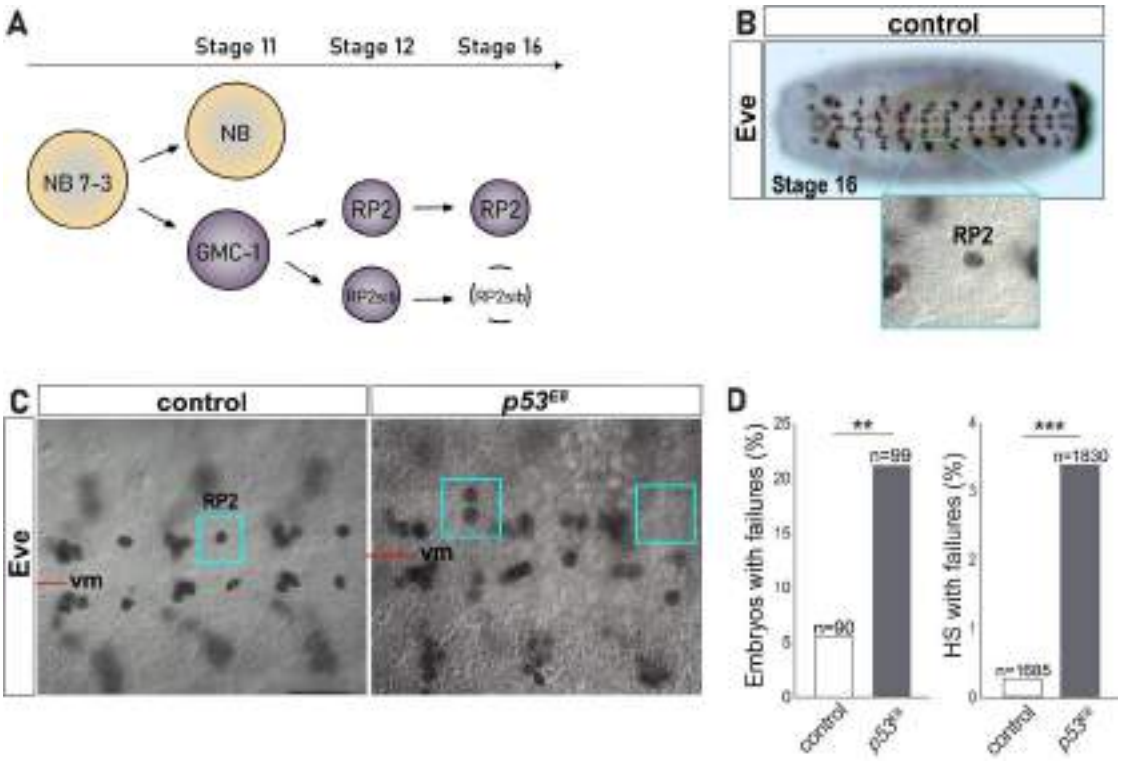

Figure 15. The GMC-1 neuronal lineage is altered in *p53^{E8}* null mutants. (A) GMC-1 neuronal lineage. Eve expression appears in the GMC-1 and maintains its expression after its division in RP2 and RP2sib neurons. At late stages only the RP2 neuron keeps the Eve expression. **(B)** Ventral view of *Drosophila* embryo CNS at stage 16. In a higher magnification of one hemisegment (HS) the RP2 neuron is shown. **(C)** Ventral view of the WT CNS stained with Eve Ab, where one RP2 neuron is present per HS (blue square). *p53^{E8}* null mutants show defects in the number of RP2 neurons, either duplications or losses (blue squares). **(D)** Bar graphs showing the percentage of failures of RP2 neurons in *p53^{E8}* null mutant embryos and total HS compared to the control. The analysis was done using a Chi-square test with Yate's correction; ** P<0.01, *** P<0.001. vm=ventral midline n= number of embryos or HS, respectively, analyzed. Scale bar: 20 μm

3. The linage formation of *Drosophila* embryonic muscle/heart progenitors are impaired in *p53^{E8}* null mutants

To further support a potential role of p53 regulating ACD, we wondered whether p53 could be functioning regulating this process in other tissues apart from the CNS (GMC-1 lineage). Thus, we decided to study whether p53 affects the asymmetric division

of embryonic muscle and heart progenitor, specifically of two muscle/heart lineages that have been very well characterized: those from progenitors 2 (P2) and 15 (P15) that express the TF Eve (Carmena et al., 1995, 1998) **(Figure 16)**. We focused for a detailed analysis on the P2 lineage, as there are specific markers to distinguish its progeny. For example, the TF Runt is only expressed in one of the P2 daughter cells, the muscle founder cell of the dorsal oblique 2 (DO2) muscle (F_{DO2}), and the TF Zfh-1 is exclusively expressed in the other daughter cell, the founder of the Eve Pericardial cells (F_{EPCS}). This daughter cell will give rise to two Eve-positive pericardial cells. By stage 11 there are usually three cells per hemisegment, two of them co-localizing Eve and Zfh-1, one expressing only Eve and one expressing only Runt **(Figure 16B)**.

We observed that $p53^{E8}$ null mutant homozygous embryos (n=18) displayed clear defects in the lineage generation of P2 in 7.53% of the hemisegments analyzed (n=146), compared to control embryos (n=23), in which 0.48% of the total hemisegments analyzed (n=210) showed failures. Specifically, supernumerary progeny of P2 were observed in several cases **(Figure 16 C, D)**. However, this result did not clearly involve p53 in the ACD of P2. Even though the P2 lineage was altered, the result also suggested a potential function of p53 regulating progenitor (P2) specification. Thus, we decided to focus exclusively on the NBs of the CNS as a model to characterize in detail the function of p53 in ACD.

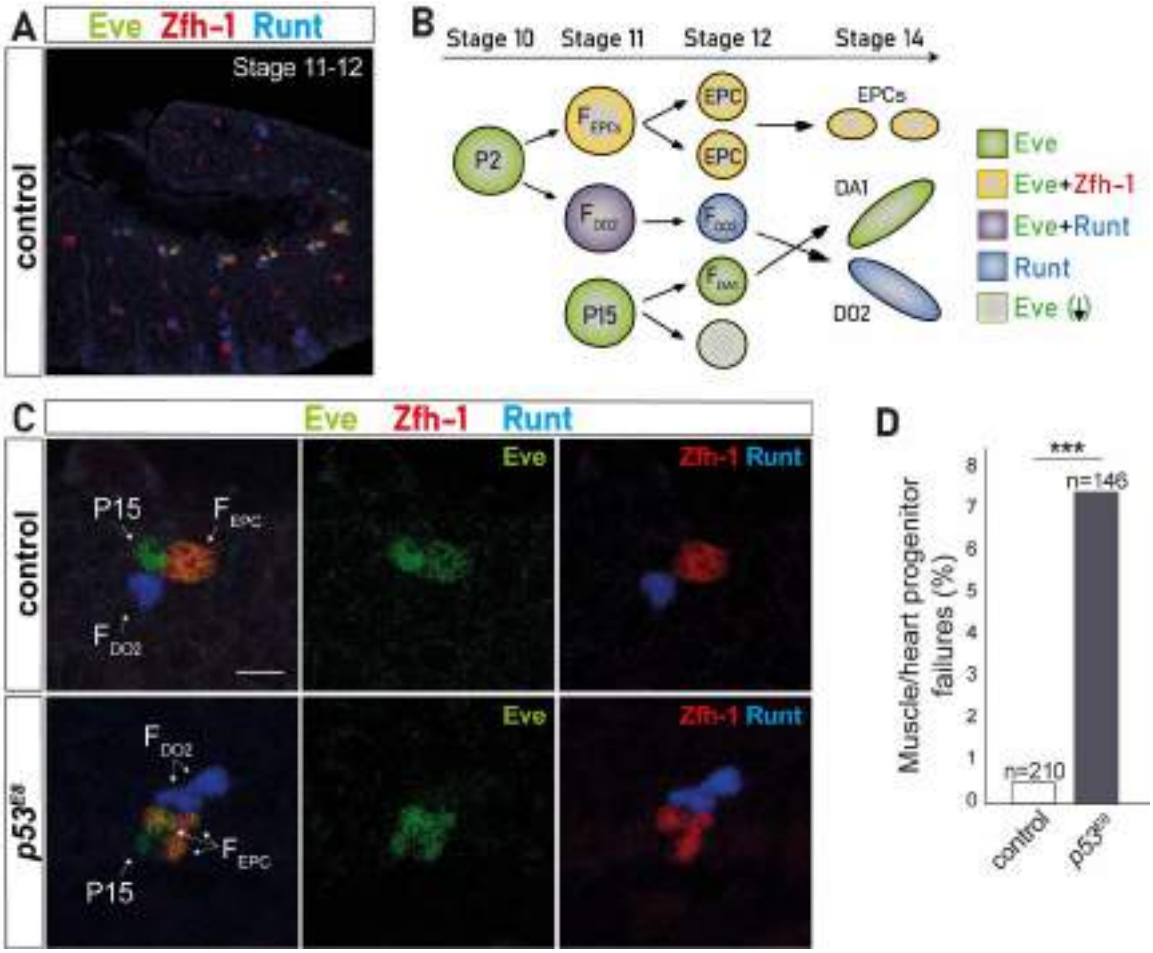

Figure 16. Muscle and heart P2 and P15 lineages. (A-B) At stage 11, P2 divides asymmetrically into two muscle and heart founder cells, F_{EPCs}, which expresses Eve and Zfh-1 and F_{DO2}, which expresses Eve and Runt. At the same time, the P15 is specified and expresses Eve. By stage 12, F_{EPCs} divide symmetrically into two pericardial cells (EPCs) and the Eve expression disappears from the F_{DO2}. At that time, P15 divides giving rise to the muscle founder cell F_{DA1}. **(C)** Magnification of a lateral view of *Drosophila* control embryo at stage 11 stained with the markers Eve (green), Zfh-1 (red) and Runt (blue). Zfh-1 and Eve are co-expressed in the F_{EPC} daughter cell, Runt is expressed in F_{DO2} daughter cell and Eve is expressed in P15 progenitor. In *Drosophila* $p53^{E8}$ null mutant there are two F_{DO2} cells expressing Runt and three F_{EPCs} co-expressing Eve and Zfh-1. **(D)** Bar graph showing the percentage of muscle/heart progenitor cells with failures in their lineages in $p53^{E8}$ null mutant compared to the control. The analysis was done using a Chi-square test with Yate's correction *** P<0.001). n=number of progenitors analyzed. Scale bar: 5µm

4. p53 modulates some key processes of ACD

4.1. The localization of the ACD regulators Numb and Pins in mitotic NBs is altered in $p53^{E8}$ mutant embryos

To investigate in detail the function of p53 in the ACD process we decided to concentrate the study in the embryonic NBs, established as an excellent paradigm to dissect ACD. We started analyzing the localization of different ACD regulators in mitotic NBs, such as the apical complex proteins aPKC and Pins, as well as the cell-fate determinant Numb in $p53^{E8}$ mutant embryos. In control metaphase NBs, both aPKC and Pins form apical crescents, while Numb accumulates at the basal pole of the NB **(Figure 17)**. In $p53^{E8}$ null mutant embryos, no significant defects were detected in the apical localization of aPKC in metaphase NBs (n=245 NBs; 24 embryos) compared to control NBs (n=232; 27 embryos) **(Figure 17A, B)**. However, the apical localization of Pins showed defects in 64% of the $p53^{E8}$ null mutant NBs (n=132, 25 embryos) compared to control NBs (n=161; 27 embryos). The defects observed were both cortical mislocalization (93%, 14 NBs) and "absence" of protein (34.8%, 8 NBs) **(Figure 17C, D)**. The basal localization of the cell-fate determinant Numb was also compromised in 79.2% of the cases (n=157, 24 embryos) compared to control NBs (n=159, 28 embryos). In fact, in 96.1% of all mutant NBs Numb was absent **(Figure 17E, F)**. This last data suggested that p53 might be directly or indirectly regulating the expression of Numb.

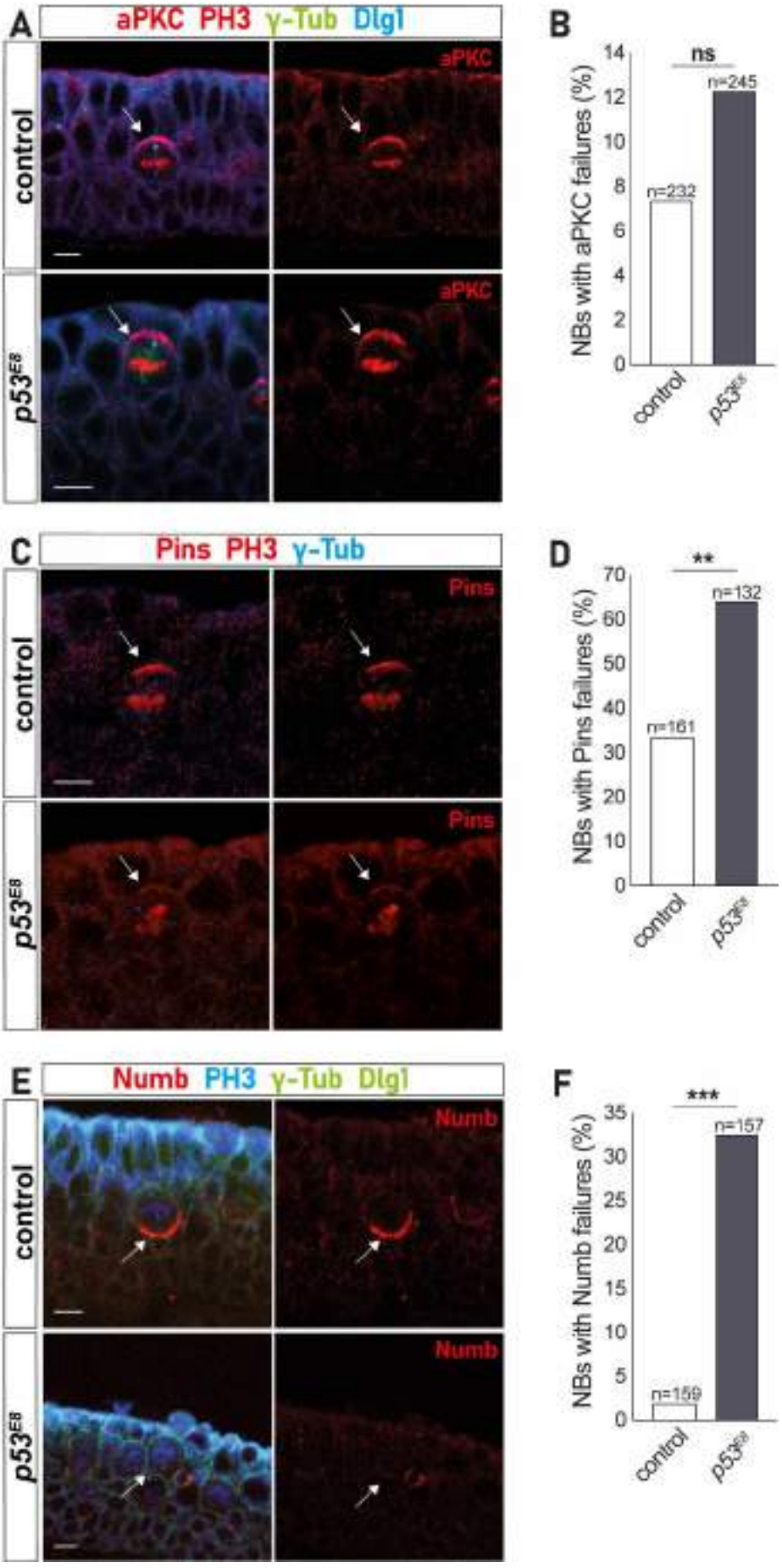
A
aPKC PH3 γ-Tub Dlg1
control
$p53^{E8}$
aPKC
B
NBs with aPKC failures (%)
ns
n=232
n=245
control
$p53^{E8}$
C
Pins PH3 γ-Tub
Pins
D
NBs with Pins failures (%)
**
n=161
n=132
E
Numb PH3 γ-Tub Dlg1
Numb
F
NBs with Numb failures (%)
***
n=159
n=157

Figure 17. The localization of the ACD regulators Pins and Numb is compromised in *p53^{E8}* null mutant embryonic NBs at metaphase. (A) Lateral view of a stage 11 embryo stained with aPKC (red, white arrows) that forms apical crescents in mitotic WT NBs, PH3 (red), γ-tub (green) that label DNA and centrosomes, respectively, and Dlg1 (blue) to label membranes. **(B)** Bar graph showing no significant failures in aPKC localization in *p53^{E8}* null mutant mitotic embryonic NB compared to control. **(C)** Lateral view of a stage 11 embryo stained with Pins (red, white arrows) that forms apical crescents in mitotic WT NBs, PH3 (red) and γ-tub (blue) that label DNA and centrosomes, respectively. **(D)** Bar graph showing a significant increase in the failures of Pins localization in mitotic NBs of *p53^{E8}* null mutant embryos compared to the control. **(E)** Lateral view of a stage 11 embryo stained with Numb (red, white arrows) that forms basal crescents in mitotic WT NBs, PH3 (blue) and γ-tub (green) that label DNA and centrosomes, respectively, and Dlg1 (green) to label cellular membranes. **(F)** Bar graph showing a significant increase in the failures of Numb localization in mitotic NBs of *p53^{E8}* null mutant embryos compared to control. The analysis was done using a Chi-square test with Yate's correction; ns=not significant, ** P<0.01, *** P<0.001. n=number of metaphase NBs analyzed. Scale bar: 5 μm

4.2. Mitotic spindle orientation is not affected in *p53^{E8}* mutant NBs

Next, as the localization of Pins was altered in *p53^{E8}* null mutant embryonic NBs and since this protein is involved in the correct orientation of the mitotic spindle (see introduction), we decided to analyze whether the lack of p53 could be affecting the spindle orientation during metaphase. For this analysis, we used aPKC as an apical marker, γ-tubulin as a centrosome marker, which allows us to determine the spindle position, and PH3 to label the DNA of mitotic NBs. Taking as a reference the epithelial cells from the neuroepithelium (NE), in control NBs the spindle is oriented perpendicular (90º) to the plane of this NE, and any fluctuations in this orientation can lead to defects in the ACD of the NB **(Figure 18)**. Some spindle orientation failures were found in NBs of *p53^{E8}* null mutant homozygous embryos (n=164 NBs; 16 mutant embryos analyzed), compared to the control (n=154 NBs; 22 embryos). However, the result was not statistically significant **(Figure 18B)**. Thus, we conclude that p53 is not involved in the orientation of the mitotic spindle.

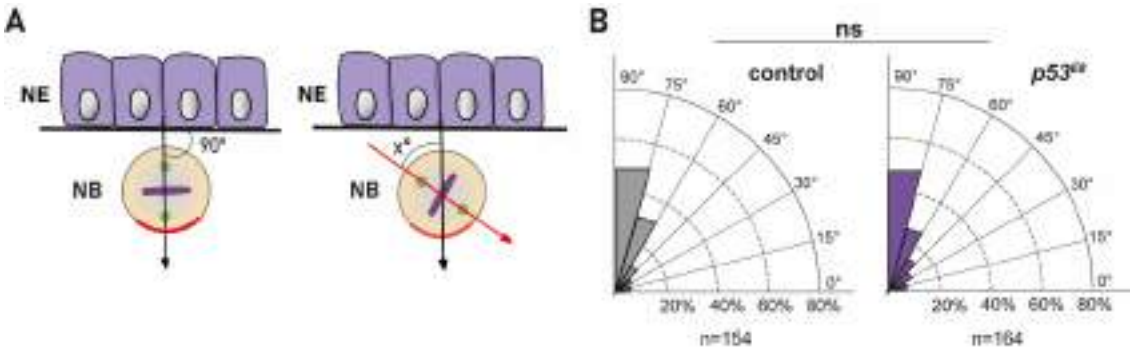

Figure 18. The mitotic spindle orientation is not altered in *p53*^{E8} null mutant embryonic NBs. (A) Failures in the perpendicular location of the mitotic spindle with respect to the NE results in incorrect segregation of daughter cells. **(B)** The orientation of the mitotic spindle does not show significant defects in *p53*^{E8} null mutant embryos compared to control according to Chi-square with Yate's correction; ns=not significant. NE=neuroepithelium, NB=neuroblast.

5. *Drosophila* homologs of conserved human/mice predicted p53 targets regulate ACD

Next, we wondered whether, in addition to Numb and Pins, other ACD regulators could be regulated by p53. Instead of randomly analyzing other ACD regulators, we decided to follow an in-silico approach, taking advantage of published data-sets about potential p53 target genes. We found particularly interesting a recent meta-analysis of transcriptomic and ChIP-seq data sets in which the author unveiled a subset of 86 direct p53 target genes that appears to be common in mice and humans (Fischer, 2019). Therefore, we decided to look for those human/mice genes whose closest counterparts in *Drosophila* are known ACD regulators. We focused on three of those genes for further analyses: *TRIM32*, *PARD6G* and *TRAF4*. TRIM32 is related to *Drosophila* Brat, an atypical TRIM-NHL protein and, like Numb, a key cell-fate determinant during asymmetric NB division. It is polarized at the basal part of the NB during mitosis and secreted to the most basal daughter cell where Brat contributes to inhibit proliferation and to induce differentiation (see introduction). PARD6G is homologue of *Drosophila* Par-6, which forms part of the apical complex in dividing NBs and the TRAF4 counterpart in

Drosophila, Traf4 is another apical regulator required in the Insc-independent telophase rescue pathway during asymmetric NB division.

5.1. The localization of the cell-fate determinant Brat fails in $p53^{E8}$ mutant mitotic NBs

Thus, we started analyzing the localization of those *Drosophila* regulators (Brat, Par-6 and Traf4) in metaphase NBs. The apical localization of Par-6 was not affected in mitotic NBs of $p53^{E8}$ null mutant embryos (n=89 NBs, 14 embryos) **(Figure 19A, B)**. However, we detected a significant number of failures in the basal localization of Brat in 31.4% of metaphase NBs (n=66 NBs, 11 embryos) of $p53^{E8}$ null mutant embryos compared with the 1.1% of defective NBs found in control embryos (n=95 NBs, 16 embryos) **(Figure 19C, D)**. Regarding the specific defects observed, in 42.9% of the cases the Brat crescent was mislocalized while in 47.6% of the cases Brat was absent. We could not analyze Traf4 localization as we were not able to generate appropriate antibodies to reproduce the published expression of Traf4 in NBs (Wang et al., 2006).

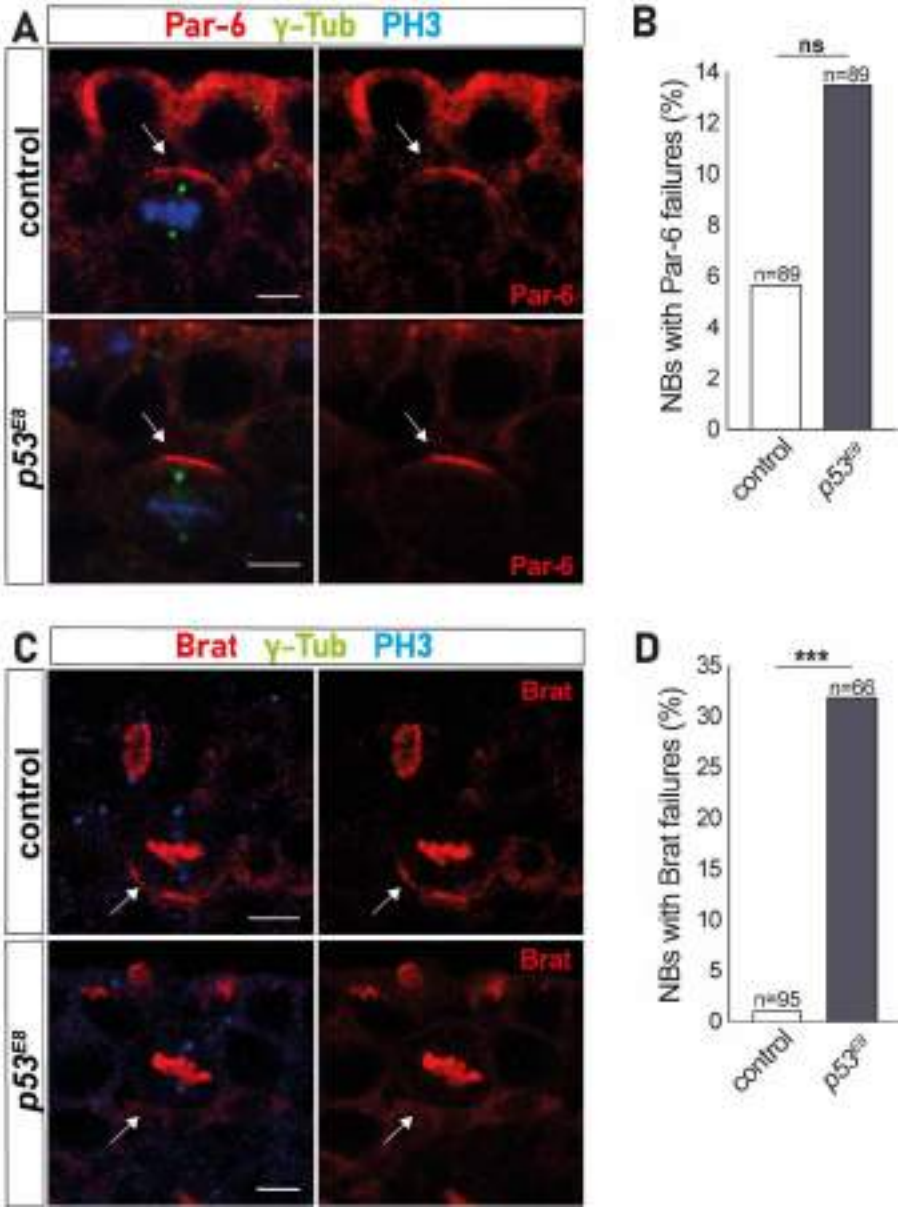

Figure 19. Brat localization is altered in *p53^{E8}* null mutant embryonic NBs at metaphase. (A) Lateral view of a stage 11 embryo stained with Par-6 (red, white arrows) that forms apical crescents in mitotic WT NBs, PH3 (blue) and γ-tub (green) that label DNA and centrosomes, respectively. **(B)** Bar graph showing no significant failures in Par-6 localization in *p53^{E8}* null mutant mitotic embryonic NB compared to control. **(C)** Lateral view of a stage 11 embryo stained with Brat (red, white arrows) that forms basal crescents in mitotic WT NBs, PH3 (blue) and γ-tub (green) that label DNA and centrosomes, respectively. **(D)** Bar graph showing a significant increase in the failures of Brat localization in mitotic NBs of *p53^{E8}* null mutant embryos compared to the control. The analysis was done using a Chi-square with Yate's correction; ns=not significant, *** P<0.001. n=number of metaphase NBs analyzed. Scale bar: 5 μm

We classified the phenotypes that we observed in metaphase NBs into three major groups depending on the protein location: (1) Absent or much less expressed, (2) Cortical mislocalization, and (3) Cytoplasmic. See **Table 5** for a summary of the observed phenotypes, and **Table 6** for the summary of the detailed phenotypes.

ACD proteins	WT N=NBs	WT failures %	$p53^{E8}$ N=NBs	$p53^{E8}$ failures %
aPKC	232	7.3	245	12.2
Pins	161	6.8	132	**17.4**
Par-6	89	3.4	89	10.1
Numb	159	1.9	157	**32.5**
Brat	95	1.1	66	**31.8**

Table 5. Summary of ACD proteins distribution in $p53^{E8}$ null mutants (in bold are highlighted those ACD regulators that show a significant number of failures in $p53^{E8}$ mutants, see above).

Phenotype	Pins	Numb	Brat
Absent or less	34.8%	**96.1%**	**47.6%**
Cortical mislocalized	**60.9%**	3.9%	42.9%
Cytoplasmic	4.4%	0%	9.5%

Table 6. Characteristics of the phenotype of the ACD proteins in $p53^{E8}$ null mutants.

With all these data, we conclude that p53 is modulating the process of ACD in embryonic NBs at least by regulating the localization of the ACD regulators Pins and the cell-fate determinants Numb and Brat.

6. *Drosophila* p53 regulates the expression of the ACD regulators Numb, Brat and Traf4

To more directly determine whether p53 was regulating the cell-fate determinants Numb and Brat at a transcriptional level, we performed quantitative polymerase chain reaction (qPCR) analyses. We compared Numb and Brat expression levels in $p53^{E8}$ homozygous mutant versus control larval brain. We also included Traf4 in this set of experiments. Compared to controls, we observed a significant reduction in all Numb (29%), Brat (58%) and Traf4 (42%) mRNA expression levels in $p53^{E8}$ homozygous mutant larval brains **(Figure 20)**. These results strongly supported that p53 is directly or indirectly activating the ACD regulators Numb, Brat and Traf4.

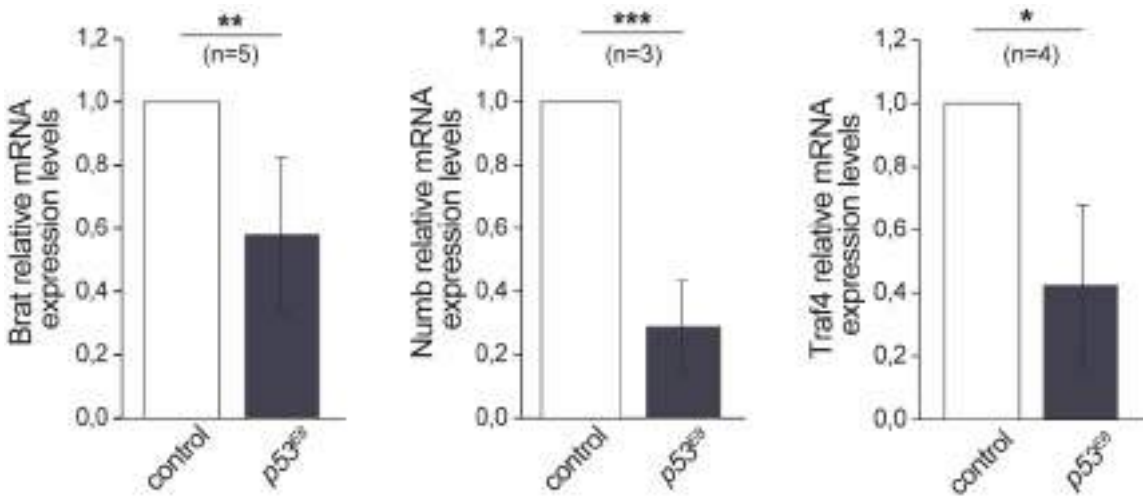

Figure 20. mRNA expression levels of Brat, Numb and Traf4 are reduced in *Drosophila* $p53^{E8}$ null mutant. qRT-PCRs reveal a significant decrease in the level of expression of the indicated genes in $p53^{E8}$ homozygous mutants relative to the control. In Brat and Traf4 experiments, GADPH was used for mRNA normalization while Numb was normalized with respect to Act88F. The analysis was done using a Mann-Whitney U non parametric test for Brat and Traf4 and a t-test for Numb; * P<0.05, ** P<0.01, *** P<0.001. n=number of experiments.

7. The cellular composition of larval type II NBs linages is not altered in *p53^{E8}* null mutant clones

Drosophila larval type II NBs have been established as a powerful system to study how failures in the process of ACD can lead to tumor-like overgrowth. Thus, we next decided to analyze the effect of mutating *p53* in these larval type II NBs by performing clonal analysis (MARCM clones). We started analyzing the cellular composition of these lineages using specific markers, such as the transcription factors Dpn and Ase to label both NBs (Dpn^+ Ase^-) and mINPs (Dpn^+ Ase^+). In WT lineages there is only one cell expressing Dpn, the NB, and several cells expressing both Dpn and Ase, the mINPs. We were not able to detect significant differences in the composition of control and *p53^{E8}* null mutant clones **(Figure 21)**. Two potential explanations for this result, not necessarily exclusive, were: (1) Given that ACD is a highly redundant process, no phenotype is visible unless you further compromise the system (i.e., it is necessary that other ACD regulators also fail – (Rives-Quinto et al., 2017; Carmena, 2018) and (2) the WT cells surrounding the *p53* mutant clones could somehow compete with the latter avoiding their growth and defects inside the clone (i.e. we should look at larval type II NB *p53* mutant clones but in a *p53* homozygous background). We started analyzing this second possibility.

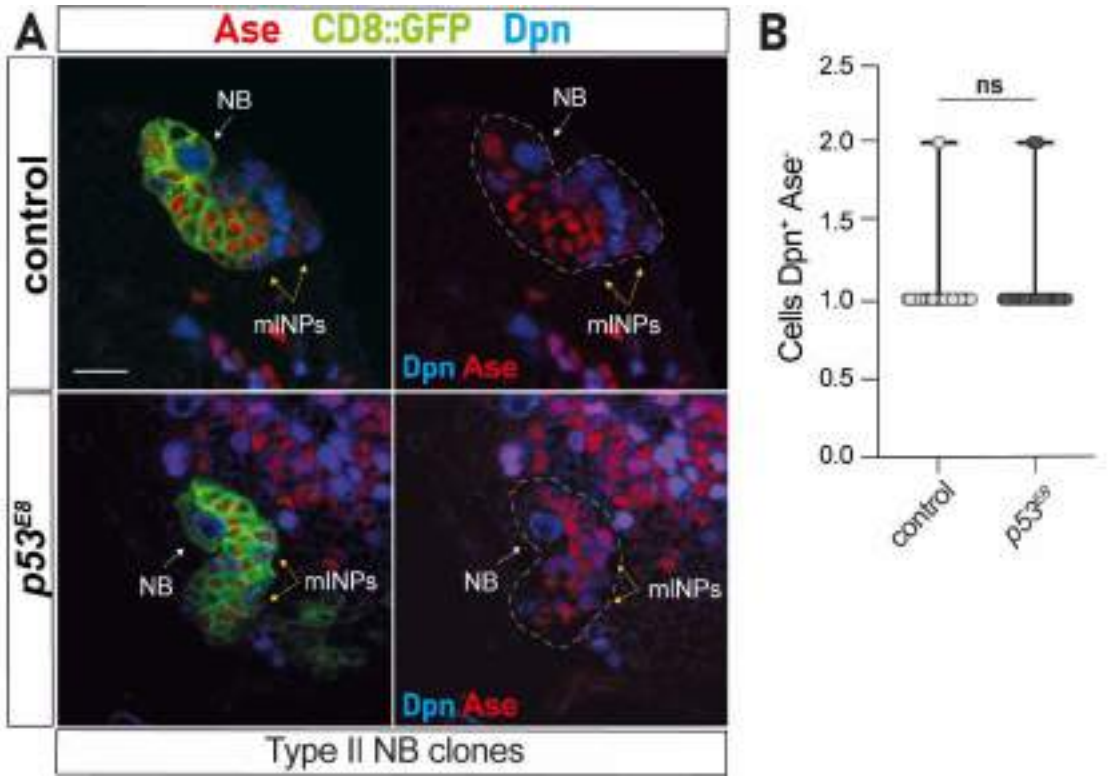

Figure 21. *p53^{E8}* NBII null mutant clones do not show ectopic NBs. (A) Confocal images showing type II NB clones of the indicated genotypes stained with Dpn (blue) and Ase (red). Each lineage is composed of one NB (Dpn^{+} Ase^{-}, white arrow) and several mINPS (Dpn^{+} Ase^{+}, yellow arrows). **(B)** No significant failures were found in the number of Dpn^{+} Ase^{-} cells (NBs) in *p53^{E8}* null mutant clones compared to control. The analysis was done using a Mann-Whitney U non parametric test; ns=not significant. NB=neuroblast, mINP= mature intermediate neural progenitor. Scale bar: 10 µm

8. The cellular composition of larval type II NB lineages is not altered in *p53^{E8}* null mutant homozygotes

Given that we did not find any significant defects in the composition of *p53^{E8}* larval type II NBs mutant clones, we decided to perform this study in a *p53^{E8}* homozygous background, instead of in a WT background. However, we did not find either significant difference in the cellular composition of the type II NB lineages in this condition (i.e., in a *p53* homozygous background) **(Figure 22A, B)**. In fact, Numb localization was not significantly affected in these larval type II NBs lineages in a *p53^{E8}* homozygous

background **(Figure 22C, D)**, in contrast with the phenotype observed in embryonic NBs in $p53^{E8}$ homozygotes. Thus, we next decided to analyze whether *p53* homozygotes develop properly from embryo to adult life.

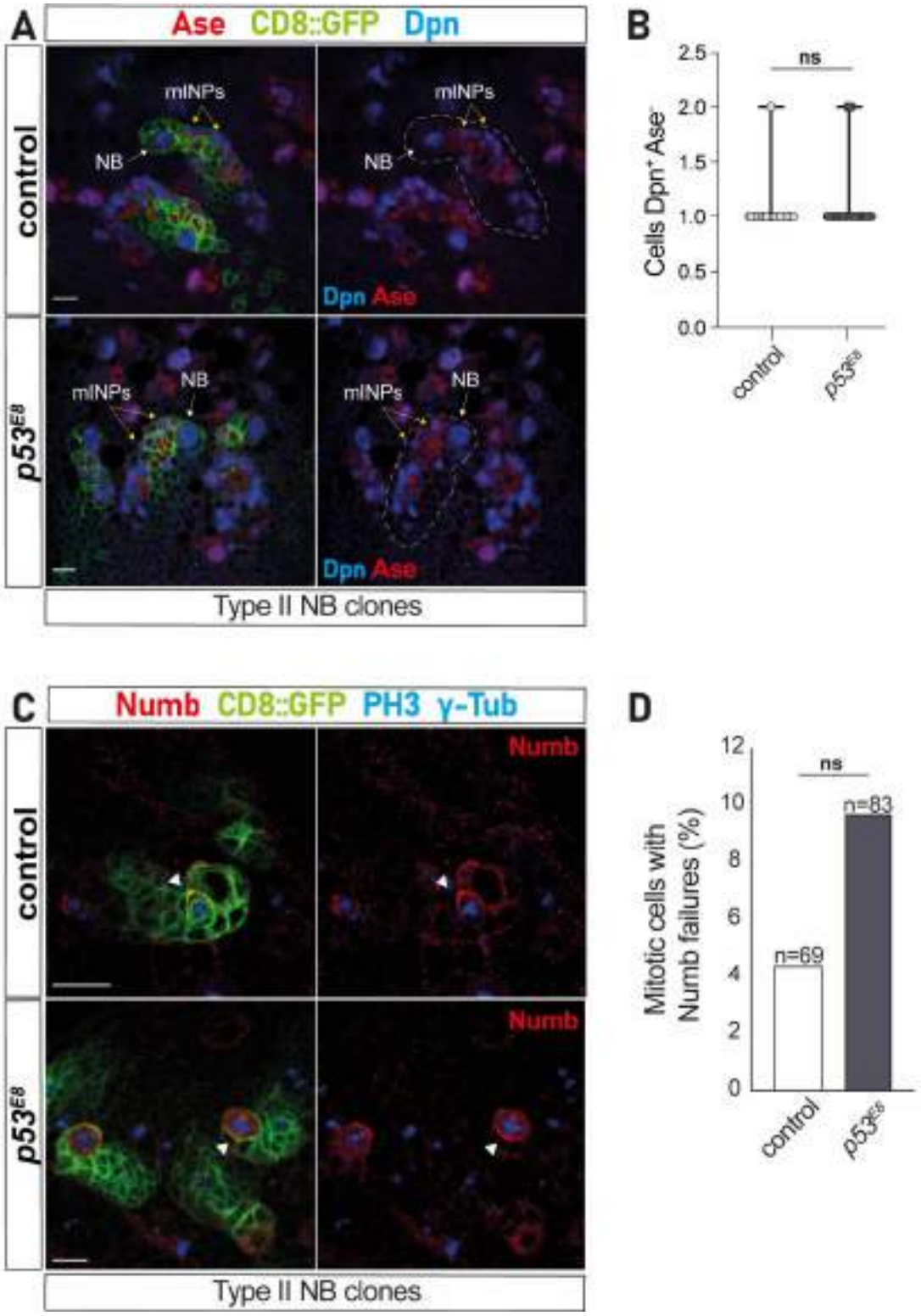

Figure 22. Type II NB *p53^{E8}* mutant clones do not show ectopic NBs in a *p53^{E8}* homozygous mutant background. (A) Confocal images showing type II lineages of the indicated genotypes stained with Dpn (blue) and Ase (red). Each lineage is composed by one NB (Dpn^{+} Ase^{-}, white arrow) and several mINPS (Dpn^{+} Ase^{+}, yellow arrows). **(B)** Box plot showing no significant failures in the number of NBs (Dpn^{+} Ase^{-}) in *p53^{E8}* null mutant lineages compared to control. The analysis was done using a Mann-Whitney U non parametric test. **(C)** Confocal images showing type II NB lineages of the indicated genotypes stained with Numb, which forms basal crescents in mitotic progenitor cells (red, white arrowheads), PH3 and γ-tub (blue) labeling DNA in mitotic cells and centrosomes, respectively. **(D)** Bar graph showing no significant failures in Numb localization in *p53^{E8}* null mutant mitotic cells compared to control. The analysis was done using a Chi-square with Yate's correction; ns=not significant. NB=neuroblast, mINP= mature intermediate progenitor. Scale bar:10 μm

9. *p53^{E8}* null homozygous mutants fail to develop properly

As we did not observe significant differences in the cellular composition or in the Numb localization in larval NB lineages of *p53^{E8}* null mutant homozygotes, we decided to perform a viability curve to better understand the behavior and fitness of *p53* homozygotes (**Figure 23**). Starting with n=100 control or *p53* mutant embryos, while in the control 92.5% of the hatching embryos (n=89/100 embryos) pupated, in the case of *p53^{E8}* null homozygous mutants only 62.2% of the hatching embryos (n=69/100 embryos) did so. We also observed a substantial difference in the number of pupae that hatched into adults in both genotypes: 97.5% in the control versus 67% in *p53^{E8}* null mutant homozygotes. Thus, from embryo hatching to adulthood, *p53^{E8}* null homozygous mutants undergo a 47% reduction of viability with respect to the control. We could then hypothesize that the *p53* homozygous larvae in which we performed the analyses and did not show a significant phenotype are the ones that are in "better conditions" (i.e., most *p53* homozygotes, which could have shown a phenotype, died during embryogenesis or early larval life).

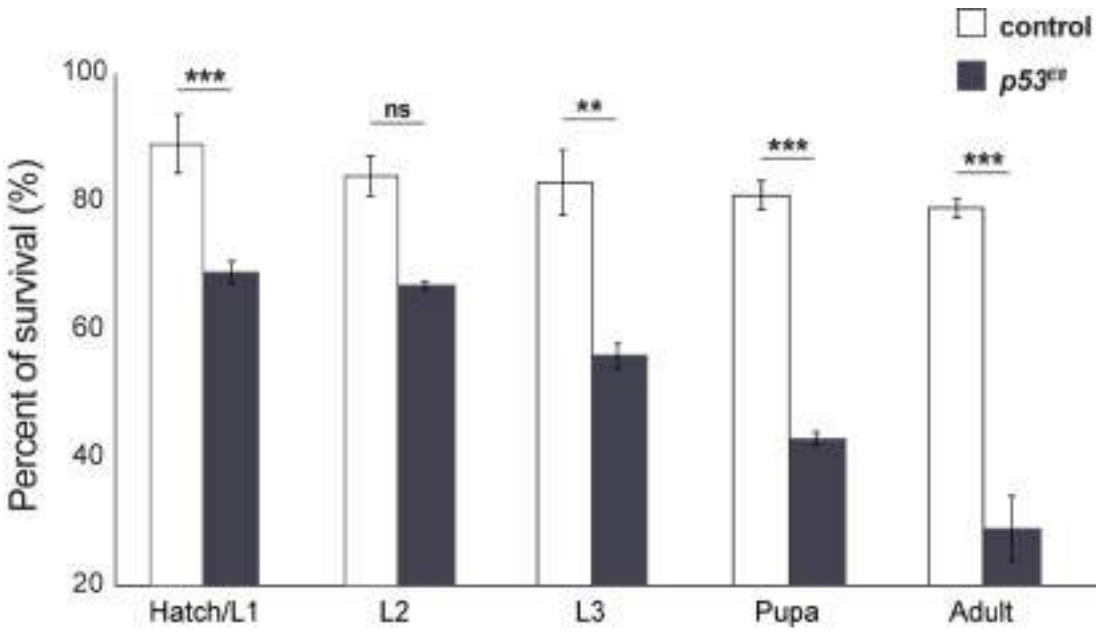

Figure 23. *Drosophila* development is impaired in $p53^{E8}$ homozygous null mutants. Histogram of the percentage of survival at different stages of development from embryo until adult flies. In $p53^{E8}$ null mutants, the number of embryos reaching adulthood is reduced to 29%, while the control is 79%. The analysis was done using a Chi-square with Yate's correction; ns=not significant, ** P<0.01, *** P<0.001.

10. Interaction of p53 with other ACD regulators/TS genes

Previous work in the lab showed a compelling phenomenon in type II NBs mutant clones in the larval brain for some ACD regulators, including Cno, Scrib, L(2)gl and Dlg1. These mutant clones did not show tumor overgrowth despite displaying the presence of ectopic NBs (Rives-Quinto et al., 2017). However, *cno scrib* double-mutant NB clones led to tumor-like overgrowth. This intriguing result suggested that the confluence of alterations in Cno and Scrib regulators is critical in triggering such overgrowth. In addition to the alteration of these ACD regulators, upregulation of the Ras oncogene was detected in the context of the double mutant *cno scrib*. In fact, under normal conditions, Cno restraints Ras activation (Carmena et al., 2006). Given the substantial redundancy inherent in the ACD process, those findings led us to infer that the manifestation of a pronounced effect in overgrowth may require the alteration of more than one ACD

regulator, highlighting the intricate interplay within these regulatory networks, and allowing us to set up a pilot screen to look for novel ACD regulators, as mentioned before (Manzanero-Ortiz et al., 2021).

10.1. *cno* and *p53* mutations did not show a synergistic interaction similar to that shown by *cno* and *scrib*

Due to the involvement of Cno in ACD, we wanted to determine whether *cno* could be synergistically interacting with *p53*, as it has been established with *scrib* (Rives-Quinto et al., 2017). Since in both *cno* and *p53* single mutants some of the proteins involved in the ACD process are altered, we decided to analyze whether in the double mutant type II NB lineages there was any significant alteration in their composition, compared to the lineages in the single mutants, using the MARCM clone technique. Although we did not observe significant number of ectopic "NB-like" (Dpn^+ Ase^-) **(Figure 24A, B)** in any of the genotypes, we did observe a significant decrease in the number of mINPS (Dpn^+ Ase^+) in both the cno^{R2} mutants (n=19 clones) and the cno^{R2} $p53^{E8}$ double mutants (n=27 clones) compared to the control (n=18 clones) and the $p53^{E8}$ single mutant (n=17 clones) **(Figure 24B)**. This data agrees with what was previously reported, since the size of the cno^{R2} mutant clones is smaller with respect to the control (Rives-Quinto et al., 2017). However, given that there were no significant differences between the cno^{R2} single mutant and the cno^{R2} $p53^{E8}$ double mutant, the phenotype of the double mutant was only caused by the loss of *cno* and not to any particular interaction with p53 in this aspect.

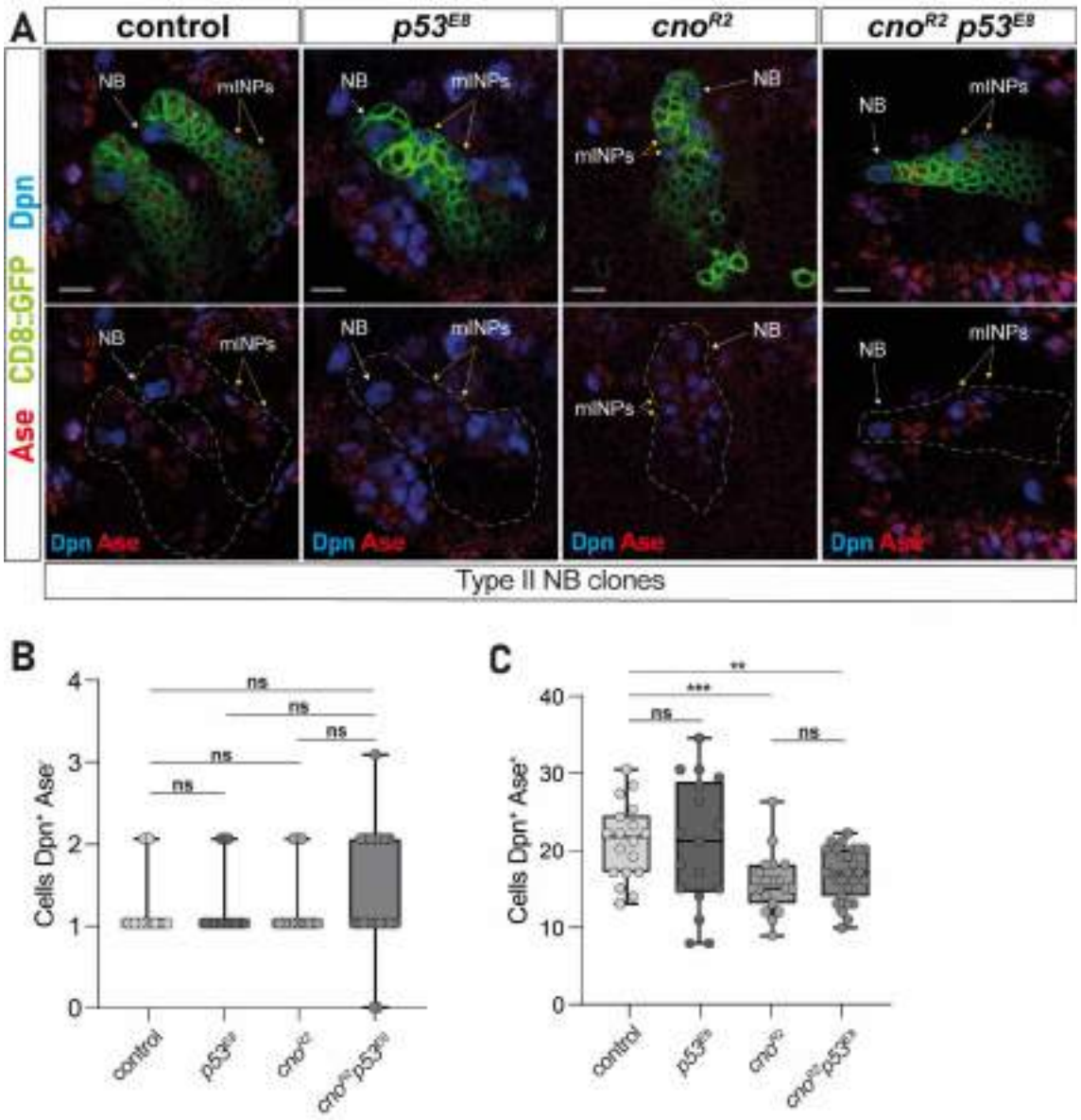

Figure 24. *p53* and *cno* mutations do not synergistically interact. (A) Confocal images showing type II NB clones of the indicated genotypes stained with Dpn (blue) and Ase (red). Each lineage is composed of one NB (Dpn^+ Ase^-, white arrow) and several mINPS (Dpn^+ Ase^+, yellow arrows). **(B)** Box plot with whiskers showing no significant failures in the number of Dpn^+ Ase^- cells (NBs) in $p53^{E8}$ null mutant clones compared to control. **(C)** Box plot with whiskers showing significant failures were found in the number of Dpn^+ Ase^+ cells (mINPS) in double mutants and cno^{R2} single mutants compared to the control (P=0.002), but no differences were found between both mutants (P=0.282). The analysis was done using a Mann-Whitney U non parametric test and the parametric t-test; ns=not significant, ** P<0.01, *** P<0.001. NB=neuroblast, mINP= mature intermediate neural progenitor. Scale bar: 10 µm

We did observe a significant reduction in the size of the NBs of type II double mutant clones with respect to the NBs of the control lineages **(Figure 25)**. While the mean of the control is 8.72 ±1.19 µm in diameter (n=18 clones), in the cno^{R2} $p53^{E8}$ double mutant (n=26 clones), the diameter was reduced to 7.20 ±1.30 µm. The difference was also significant with respect to the $p53^{E8}$ single mutant (n=17 clones), whose diameter is 8.52 ± 1.43 µm and with respect to the cno^{R2} single mutant (n=19 clones), in which the NB is even smaller, 5.53 ± 10.4 µm. Thus, the deletion of *p53* in the double mutant cno^{R2} $p53^{E8}$ tends to suppress the *cno* phenotype related to the small size of the NB, although in the double mutant the NB is still significantly smaller than in control NB lineages.

In conclusion, the simultaneous loss of *cno* and *p53* in Type II NB clones did not cause overgrowth or any strong phenotype that could support at all any synergistic interaction similar to that observed between *cno* and *scrib* (Rives-Quinto et al., 2017).

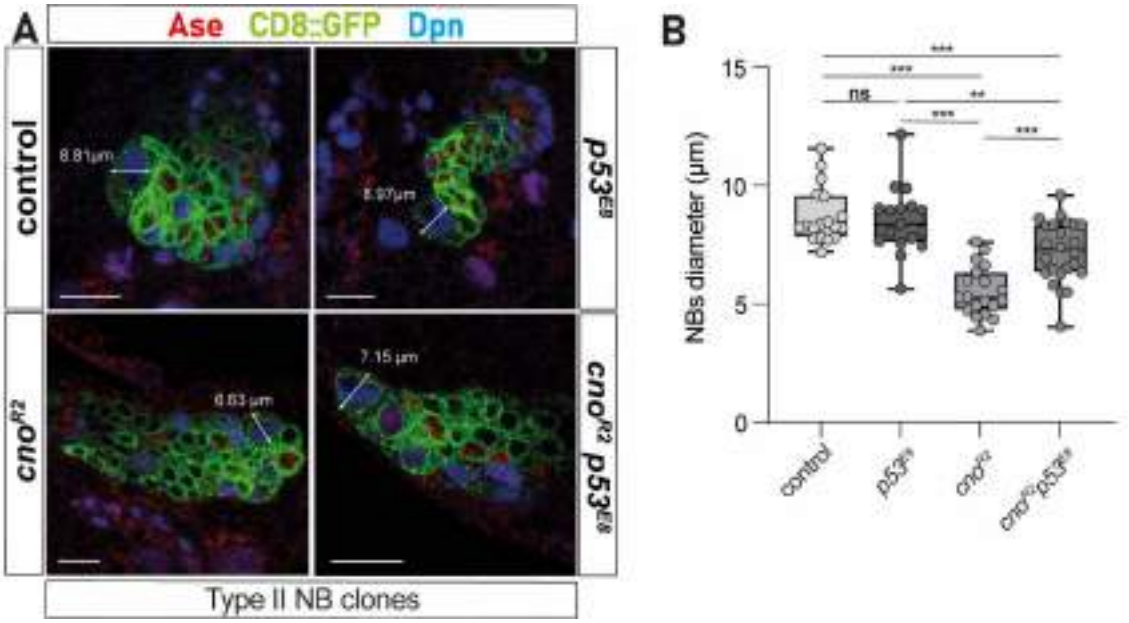

Figure 25. cno^{R2} $p53^{E8}$ double mutant clones show bigger NBs than cno^{R2} single mutant clones. (A) Confocal images showing type II NB clones of the indicated genotypes stained with Dpn (blue) and Ase (red) showing the diameter of the NB (white arrow). **(B)** Box plot showing a significant NB diameter reduction in cno^{R2} null mutants compared to the control (P<0.001). The same phenotype was observed in cno^{R2} $p53^{E8}$ double mutants, compared to control (P<0.001). The NB diameter in cno^{R2} $p53^{E8}$ double mutant was also significantly increased compared to the single mutant cno^{R2} (P<0.001). The analysis was done using a Mann-Whitney U non parametric test and the parametric t-test; ns=not significant, ** P<0.01, *** P<0.001. Scale bar: 10 µm

10.2. *p53* mutation suppressed the ectopic NB phenotype observed in *robo1* mutant NB lineages

The transmembrane receptor Roundabout1 (Robo1) regulates the NB ACD through impinging on the correct localization of ACD intrinsic factors (de Torres-Jurado et al., 2022). For example, in *robo1* mutants the cell fate determinant Numb, as it occurs in *p53* mutants, shows an altered localization (de Torres-Jurado et al., 2022). Therefore, we also decided to study a potential synergistic interaction between *robo1* and *p53*. For that, we started analyzing the presence of ectopic NBs in MARCM clones of larval brain type II NB lineages in the single and double mutant conditions **(Figure 26)**. We found no significant differences in the number of NBs in the double mutant (n=21 clones) with respect to the control (n=24 clones) or the $p53^{E8}$ null mutant (n=24 clones). However, the ectopic NB phenotype observed after downregulating *robo1* in NB lineages **(Figure 26B)** (de Torres-Jurado et al., 2022) was suppressed in the double mutant $robo1^{RNAi}$ *p53* **(Figure 26)**. We did not detect significant differences in the number of mINPs in control lineages with respect to the different mutants nor between the $robo1^{RNAi}$ $p53^{E8}$ double mutant and the $robo1^{RNAi}$ and $p53^{E8}$ single mutants **(Figure 26C)**.

In conclusion, simultaneous loss of *robo1* and *p53* in type II NB clones did not cause overgrowth that could support any synergistic interaction. However, the suppression in the double mutant *robo1 p53* of the ectopic NB phenotype, present in the single *robo1* NB clones, suggests some kind of interaction between *p53* and *robo1* (see discussion).

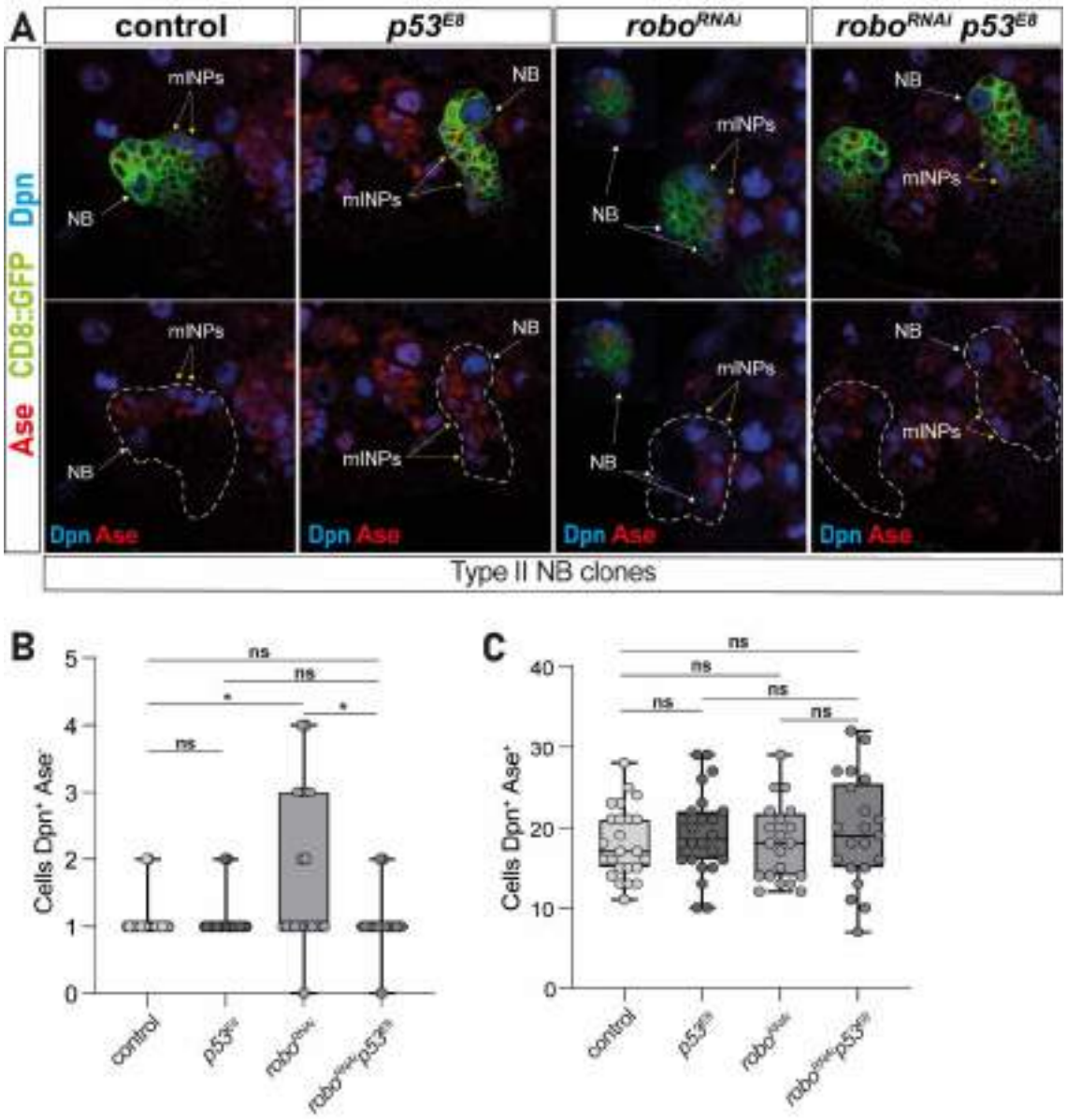

Figure 26. *p53* mutation suppressed the ectopic *robo1* mutant NB phenotype. (A) Confocal images showing type II NB clones of the indicated genotypes stained with Dpn (blue) and Ase (red). Each lineage is composed mainly of one NB (Dpn^+ Ase^-, white arrow) and several mINPS (Dpn^+ Ase^+, yellow arrows). **(B)** Box plot with whiskers showing no significant failures in the number of Dpn^+ Ase^- cells (NBs) in *robo1* $p53^{E8}$ double mutant clones compared to control (P=0.754). However, significant differences are shown between the control and the $p53^{E8}$ null mutant with respect to the *robo1* mutant (P=0.029). There are also significant differences between the *robo1* mutant and the *robo1* $p53^{E8}$ double mutant (P=0.032) **(C)** Box plot with whiskers showing no significant failures in the number of Dpn^+ Ase^+ cells (mINPS) in double mutants and single mutants compared to the control. The analysis was done using a Mann-Whitney U non parametric test and the parametric t-test; ns=not significant, * P<0.05. NB=neuroblast, mINP= mature intermediate neural progenitor. Scale bar: 10 µm

V. DISCUSSION

p53 is one of the most relevant tumor suppressor genes, since it is mutated in about 50% of all human tumors. Apart from the extensively studied canonical functions of p53 related to DNA damage response and apoptosis, thus preventing the propagation of damaged genetic material, novel non-canonical processes modulated by p53 have been unveiled over the past years, extending beyond its conventional scope. However, the mechanisms by which p53 is modulating these processes remain still poorly understood (Spike & Wahl, 2011; Jain & Barton, 2018; Boutelle & Attardi, 2021). For example, recent studies have highlighted the intricate role of p53 in stem cell maintenance, fate determination, and differentiation. Comparative studies across species, including human, mice, and *Drosophila melanogaster*, have revealed both conserved and divergent roles of p53 in stem cell biology. While the core functions of p53 are conserved, species-specific differences have been observed in terms of the regulatory networks and pathways that p53 interacts with to influence these processes. These differences highlight the complex interplay between p53 and other molecular players in different organisms (Horvath et al., 2007; Brandt et al., 2009; Jegga et al., 2008; Ingaramo et al., 2018). In the context of stem cells, the functions of p53 are not solely limited to tumor suppression. It has been observed that p53 can influence stem cell self-renewal and differentiation through its regulatory effects on key signaling pathways that are crucial for stem cell maintenance (Molchadsky et al., 2010). The fine balance between the effects of p53 on maintaining genomic stability and its impact on stem cell behavior adds complexity to the stem cell regulatory network.

1. p53 regulates ACD by directly activating ACD regulators

In this study we have shown that p53 regulates the process of ACD. Given that p53 is a transcription factor we hypothesized that p53 might be directly regulating the

expression levels of ACD regulators. Interestingly, some among the 86 direct p53 target genes commonly predicted in mice and humans in a recent in silico study, such as *TRIM32* and *TRAF4,* are homologs of *Drosophila* ACD regulators Brat and Traf4, respectively (Fischer, 2019). We were aware that the mechanisms by which ACD regulators operate, or at least those that have been predominantly described, rely mainly on protein-protein interactions and post-translational modifications, largely phosphorylation events. However, the relevance of ACD regulation at the transcriptional level is coming on stage over the past years (Deffie et al., 1993; Wang et al., 2009; Polager & Ginsberg, 2009; Menendez et al., 2013; Su et al., 2015; Senitzki et al., 2021). In fact, we have found that *Drosophila* p53 is activating the expression of key ACD regulators: Numb, Brat and Traf4.

Numb, which is one of the most relevant cell-fate determinants involved in NB differentiation, has been traditionally associated to the inhibition of the transmembrane Notch receptor and the consequent induction of differentiation in the daughter cell in which is asymmetrically segregated, as it has been shown in *Drosophila* nervous system, in mammals and in human carcinogenesis (Mosner et al., 1995; Benetka et al., 2008; Sousa-Nunes & Somers, 2010). Interestingly, the tumor suppressor effect of human NUMB has also been linked to its capacity to stabilize p53 in human mammary gland, preventing the E3 ubiquitin ligase HDM2 (MDM2)-mediated ubiquitination and consequent p53 degradation (Krahn et al., 2010). Moreover, p53 has been shown to favor an asymmetric mode of cell division in isolated human mammary stem cells (Cicalese et al., 2009). Likewise, Numb, in mouse mammary epithelial stem cells, ensures high p53 activity in the cell in which is asymmetrically segregated, and the loss of Numb promotes *p53* loss of function-induced tumorigenesis (Cai et al., 2001). Intriguingly, here we have found that *Drosophila* p53, in turn, activates the expression of Numb, establishing a positive feedback loop that can reinforce the regulatory function of the Numb-p53 pathway (Rust & Wodarz, 2021).

*Drosophil*a TRIM-NHL protein Brat is related to human TRIM proteins (TRIM2, TRIM3 and TRIM32), especially closer to TRIM3, a tumor suppressor gene also involved in regulating ACD (Chang et al., 2010). The function of human TRIM32 appears to be contingent upon the specific cell type and context, being a target of p53. It interacts with

and degrades p53 through ubiquitination (Rust & Wodarz, 2021), implying an oncogenic role for TRIM32. Conversely, TRIM32 has also been proven to trigger ACD in neuroblastoma cells and other precursor cells, acting as a tumor suppressor gene (Guo et al., 1996; Spana & Doe, 1996; McGill & McGlade, 2003). A comparable pattern emerges in mouse TRIM32, which curbs self-renewal in neural precursors, thereby facilitating differentiation through the mediation of microRNAs (Pece et al., 2004).

Finally, the function of human TRAF4 in the context of ACD has not been reported. It has been described that the expression levels of TRAF4 are elevated in many human cancers, normally associated with gene amplification (Colaluca et al., 2008; Tosoni et al., 2015). In vivo experiments in mice also suggest an oncogenic role for TRAF4 (Faraldo & Glukhova, 2015). Thus, in the case of TRAF4 it is not yet clear a potential tumor suppressor role in particular contexts or cell types.

Intriguingly, very recent work in our lab has shown that all *numb*, *brat* and *Traf4* are direct targets of p53 (Manzanero-Ortiz et al., unpublished results). Thus, taking all data together, and given the conservation of all these *Drosophila* genes *numb*, *brat* and *Traf4*, in humans and mice, it would be very interesting to assess whether these genes are also direct targets of p53 in vertebrates in the context of ACD, They might represent potential targets for cancer therapy. This could impact on our understanding of the high complexity of p53 pleiotropic effects to achieve its tumor suppressor activity.

Despite the remarkable decrease in Brat, Traf4 and Numb mRNA levels, there are significant failures in Numb localization and expression in embryos but not in larvae (Brat localization, which fails in embryos, has not been analyzed in larvae). We were unable to test Traf4 localization in either embryos or larvae due to problems with the Ab. This result can be explained by the low survival of *p53* mutant homozygotes **(Figure 23)**. For example, while in embryos we can observe a wide range of failures, only those embryos with best fitness would be able to reach the larval stage. And, therefore, these larvae would not show significant defects. Future work will further clarify this question.

2. p53 may cooperate with other ACD regulators to modulate the process

As discussed in the introduction, dysregulation of ACD plays a pivotal role in the complex landscape of tumorigenesis, as it can lead to the accumulation of undifferentiated progenitor cells and genetic mutations, creating a fertile ground for tumor initiation and progression. Indeed, the function of all these well-known determinants of *Drosophila*, Pros, Brat and Numb, repressing self-renewal and activating differentiation, can easily explain their loss-of-function phenotype, resulting in tumor-like overgrowth, with an overproduction of "NB-like" cells in detriment of differentiated cells (Januschke & Gonzalez, 2008; Reichert, 2011). Nevertheless, the loss of many ACD regulators does not cause tumor-like overgrowth (Rives-Quinto et al., 2017; Carmena, 2018). That was also the case for *p53* whose loss did not cause tumor overgrowth in type II NB clones. The fact that ACD is a highly regulated and redundant process can explain this phenomenon, as mentioned before. Thus, only the simultaneous deletion of different ACD regulators display more drastic effects (Rives-Quinto et al., 2017). We took advantage of this finding to design a screening looking for novel tumor suppressor genes and ACD regulators (Manzanero-Ortiz et al., 2021). Specifically, we used the sensitized genetic background Ras^{V12} *scrib* which does not cause overgrowth per se, to randomly screen a collection of RNAi lines, finding potential novel ACD regulators (Manzanero-Ortiz et al., 2021). Based on this study and given that we did not find an overgrowth phenotype in *p53* NB mutant clones, we are currently combining *p53* with Ras^{V12} *scrib* to determine potential interactions with this sensitized genetic background. We did start analyzing other potential interactions between p53 and other ACD regulators, such as Cno and Robo1 (Rives-Quinto et al., 2017; de Torres-Jurado et al., 2022). However, these combinations, *p53 cno* or *p53 robo1* double mutants, did not render strong or synergistic interactions, at least in their effect in causing tumor-like overgrowth. Nevertheless, some subtle interactions were found in the double mutant *p53 cno*, regarding the size of the NB of the clone. In *cno* type II NB single mutant clones, the NB is always smaller than in the control clones (Rives-Quinto et al., 2017); in the double mutant *p53 cno*, the loss of *p53* partially suppressed this phenotype. The mechanisms involved in this effect is something to

investigate in the future. Likewise, in the double mutants *p53 robo1*, the ectopic NB phenotype observed in *robo1* Type II NB single mutant clones was suppressed. One possibility to interpret this result is that p53 is normally repressing *robo1* levels, so that in the double mutant $robo^{RNAi}$ $p53^{E8}$, the increase in the *robo1* levels due to the loss of *p53* is compensating the downregulation of *robo1* caused by the $robo^{RNAi}$. This is intriguing as we may have indirectly found another possible target of p53. It is interesting since we have seen that Robo1 is involved in the control of the ACD process (de Torres-Jurado et al., 2022). Future work might also clarify this point.

In conclusion, in this work we have shown that *Drosophila* p53 directly regulates the ACD of NBs by activating the expression of key ACD regulators. Given the conservation of these p53 target genes in mammals, it could be an evolutionary conserved mechanism by which p53 is regulating the mode of stem cell division in other organisms, including humans. Additional studies must be carried out to get a deeper understanding of the role of p53 in ACD both in *Drosophila* and in vertebrates. This will help to shed light on how p53 integrates its multiple functions to drive its tumor suppressor activity.

VI. CONCLUSIONS

1. The tumor suppressor p53 is required for the proper formation of embryonic neural progenitor lineages.

2. p53 is necessary for the correct localization of some critical regulators of NB ACD, including the apical protein Pins and the cell-fate determinants Numb and Brat. However, p53 is not required for the proper orientation of the mitotic spindle in dividing NBs.

3. p53 transcriptionally activates the expression of the ACD regulatory proteins Brat, Numb and Traf4.

4. The loss of *p53* leads to a significant decrease in survival along the *Drosophila melanogaster* life cycle.

5. The loss of *p53* causes neither overgrowth nor failures in the cellular composition of larval type II NB lineages.

6. *p53* might be functionally interacting with other ACD regulators to modulate ACD.

CONCLUSIONES

1. El supresor de tumores p53 es necesario para la correcta formación de los linajes de progenitores neurales embrionarios.

2. p53 es necesario para la correcta localización de algunos reguladores críticos del proceso de DCA de los NBs, incluyendo la proteína apical Pins y los determinantes del destino celular Numb y Brat. Sin embargo, p53 no es necesario para la correcta orientación del huso mitótico en los NB en división.

3. p53 activa transcripcionalmente la expresión de las proteínas reguladoras del DCA Brat, Numb y Traf4.

4. La pérdida de *p53* conduce a una disminución significativa de la supervivencia a lo largo del ciclo vital de *Drosophila melanogaster*.

5. La pérdida de *p53* no causa ni sobrecrecimiento ni fallos en la composición celular de los linajes larvarios de NB de tipo II.

6. *p53* podría estar interactuando funcionalmente con otros reguladores del DCA para modularlo.

VII. BIBLIOGRAPHY

Adams, M. D., Celniker, S. E., Holt, R. A., Evans, C. A., Gocayne, J. D., Amanatides, P. G., Scherer, S. E., Li, P. W., Hoskins, R. A., Galle, R. F., George, R. A., Lewis, S. E., Richards, S., Ashburner, M., Henderson, S. N., Sutton, G. G., Wortman, J. R., Yandell, M. D., Zhang, Q., … Pfeiffer, B. D. (2000). The Genome Sequence of *Drosophila melanogaster*. Science, 287(5461), 2185–2195. doi: 10.1126/science.2875461.2185

Agupitan, A. D., Neeson, P., Williams, S., Howitt, J., Haupt, S., & Haupt, Y. (2020). P53: A guardian of immunity becomes its saboteur through mutation. Int J Mol Sci, 21(10), 3452. doi: 10.3390/ijms21103452

Albertson, R., Chabu, C., Sheehan, A., & Doe, C. Q. (2004). Scribble protein domain mapping reveals a multistep localization mechanism and domains necessary for establishing cortical polarity. J Cell Sci, 117(25), 6061–6070. doi: 10.1242/jcs.01525

Albertson, R., & Doe, C. Q. (2003). Dlg, Scrib and Lgl regulate neuroblast cell size and mitotic spindle asymmetry. Nat Cell Biol, 5(2), 166–170. doi: 10.1038/ncb922

Arama, E., Dickman, D., Kimchie, Z., Shearn, A., & Lev, Z. (2000). Mutations in the b-propeller domain of the *Drosophila* brain tumor (brat) protein induce neoplasm in the larval brain. Oncogene, 19(33), 3706-3716. doi: 10.1038/sj.onc.1203706

Ashburner, M., & Bergman, C. M. (2005). *Drosophila melanogaster*: A case study of a model genomic sequence and its consequences. Genome Res, 15(12), 1661–1667. doi: 10.1101/gr.3726705

Asher, G., Lotem, J., Cohen, B., Sachs, L., & Shaul, Y. (2001). Regulation of p53 stability and p53-dependent apoptosis by NADH quinone oxidoreductase 1. Proc Natl Acad Sci U S A, 98(3), 1188–1193. doi:10.1073/pnas.98.3.1188

Atwood, S. X., Chabu, C., Penkert, R. R., Doe, C. Q., & Prehoda, K. E. (2007). Cdc42 acts downstream of Bazooka to regulate neuroblast polarity through Par-6-aPKC. J Cell Sci, 120(18), 3200–3206. doi:10.1242/jcs.014902

Atwood, S. X., & Prehoda, K. E. (2009). aPKC Phosphorylates Miranda to Polarize Fate Determinants during Neuroblast Asymmetric Cell Division. Curr Biol, 19(9), 723–729. doi: 10.1016/j.cub.2009.03.056

Baumgardt, M., Karlsson, D., Salmani, B. Y., Bivik, C., MacDonald, R. B., Gunnar, E., & Thor, S. (2014). Global Programmed Switch in Neural Daughter Cell Proliferation Mode Triggered by a Temporal Gene Cascade. Dev Cell, 30(2), 192–208. doi: 10.1016/j.devcel.2014.06.021

Beadle, G. W., & Sturtevant, A. H. (1935). X Chromosome Inversions and Meiosis in *Drosophila Melanogaster*. Proc Natl Acad Sci U S A, 21(6), 384–390. doi: 10.1073/pnas.21.6.384

Beckerman, R., & Prives, C. (2010). Transcriptional regulation by p53. Cold Spring Harb Perspect Biol, 2(8). doi: 10.1101/cshperspect.a000935

Bellaïche, Y., Radovic, A., Woods, D. F., Hough C D, Parmentier M L, O'Kane C J, Bryant P J, & Schweisguth F. (2001). The Partner of Inscuteable/Discs-Large Complex Is Required to Establish Planar Polarity during Asymmetric Cell Division in *Drosophila*. Cell, 106(3), 355–366. doi: 10.1016/s0092-8674(01)00444-5

Bellen, H. J., Tong, C., & Tsuda, H. (2010). 100 years of *Drosophila* research and its impact on vertebrate neuroscience: A history lesson for the future. Nat Rev Neurosci, 11(7), 514–522. doi: 10.1038/nrn2839

Bello, B., Reichert, H., & Hirth, F. (2006). The brain tumor gene negatively regulates neural progenitor cell proliferation in the larval central brain of *Drosophila*. Development, 133(14), 2639–2648. doi: 10.1242/dev.02429

Bello, B. C., Izergina, N., Caussinus, E., & Reichert, H. (2008). Amplification of neural stem cell proliferation by intermediate progenitor cells in *Drosophila* brain development. Neural Dev, 3(1). doi: 10.1186/1749-8104-3-5

Benetka, W., Mehlmer, N., Maurer-Stroh, S., Sammer, M., Koranda, M., Neumüller, R., Betschinger, J., Knoblich, J. A., Teige, M., & Eisenhaber, F. (2008). Experimental testing of predicted myristoylation targets involved in asymmetric cell division and calcium-dependent signalling. Cell Cycle, *7*(23), 3709–3719. doi: 10.4161/cc.7.23.7176

Benetti, R., Del Sal, G., Monte, M., Paroni, G., Brancolini, C., & Schneider, C. (2001). The death substrate Gas2 binds m-calpain and increases susceptibility to p53-dependent apoptosis. EMBO J, 20(11), 2702–2714. doi: 10.1093/emboj/20.11.2702

Berdnik, D., Török, T., GonzáLez-Gaitán, M., & Knoblich, J. A. (2002). The Endocytic Protein alpha-Adaptin Is Required for Numb-Mediated Asymmetric Cell Division in *Drosophila*. Dev Cell, 3(2), 221-231. doi: 10.1016/s1534-5807(02)00215-0

Bertet, C., Li, X., Erclik, T., Cavey, M., Wells, B., & Desplan, C. (2014). Temporal patterning of neuroblasts controls notch-mediated cell survival through regulation of hid or reaper. Cell, 158(5), 1173–1186. doi: 10.1016/j.cell.2014.07.045

Betschinger, J., Mechtler, K., & Knoblich, J. A. (2003). The Par complex directs asymmetric cell division by phosphorylating the cytoskeletal protein Lgl. Nature, 422(6929), 326–330. doi: 10.1038/nature01486

Betschinger, J., & Knoblich, J. A. (2004). Dare to be different: Asymmetric cell division in *Drosophila*, *C. elegans* and vertebrates. Curr Biol, 14(16), 674-685. doi: 10.1016/j.cub.2004.08.017

Betschinger, J., Mechtler, K., & Knoblich, J. A. (2006). Asymmetric Segregation of the Tumor Suppressor Brat Regulates Self-Renewal in Drosophila Neural Stem Cells. Cell, 124(6), 1241–1253. doi: 10.1016/j.cell.2006.01.038

Bhat, K. M., & Schedl, P. (1994). The Drosophila miti-mere gene, a member of the POU family, is required for the specification of the RP2/sibling lineage during neurogenesis. Development, 120(6), 1483–1501. doi: 10.1242/dev.120.6.1483

Bier, E. (2005). Drosophila, the golden bug, emerges as a tool for human genetics. Nat Rev Genet, 6(1), 9-23. doi: 10.1038/nrg1503

Bilder, D. (2000). Cooperative Regulation of Cell Polarity and Growth by Drosophila Tumor Suppressors. Science, 289(5476), 113–116. doi: 10.1126/science.289.5476.113

Bilder, D., & Perrimon, N. (2000). Localization of apical epithelial determinants by the basolateral PDZ protein Scribble. Nature, 403(6770), 676–680. doi: 10.1038/35001108

Bilen, J., & Bonini, N. M. (2005). Drosophila as a model for human neurodegenerative disease. Annu Rev Genet, 39, 153–171. doi: 10.1146/annurev.genet.39.110304.095804

Bonizzi, G., Cicalese, A., Insinga, A., & Pelicci, P. G. (2012). The emerging role of p53 in stem cells. Trends Mol Med, 18(1), 6–12. doi: 10.1016/j.molmed.2011.08.002

Boone, J. Q., & Doe, C. Q. (2008). Identification of *Drosophila* type II neuroblast lineages containing transit amplifying ganglion mother cells. Dev Neurobiol, 68(9), 1185–1195. doi: 10.1002/dneu.20648

Bossing, T., Udolph, G., Doe, C. Q., & Technau, G. M. (1996). The Embryonic Central Nervous System Lineages of Drosophila melanogaster I. Neuroblast Lineages

Derived from the Ventral Half of the Neuroectoderm. Dev Biol, 179(1), 41-64. doi: 10.1006/dbio.1996.0240

Boulay, J. L., Stiefel, U., Taylor, E., Dolder, B., Merlo, A., & Hirth, F. (2009). Loss of heterozygosity of TRIM3 in malignant gliomas. BMC Cancer, 9(71). doi: 10.1186/1471-2407-9-71

Boutelle, A. M., & Attardi, L. D. (2021). p53 and Tumor Suppression: It Takes a Network. Trends Cell Biol, 31*(4),* 298–310. doi: 10.1016/j.tcb.2020.12.011

Bowman, S. K., Neumüller, R. A., Novatchkova, M., Du, Q., & Knoblich, J. A. (2006). The Drosophila NuMA Homolog Mud Regulates Spindle Orientation in Asymmetric Cell Division. Developmental Cell, 10(6), 731–742. doi: 10.1016/j.devcel.2006.05.005

Bradley, J. R., & Pober, J. S. (2001). Tumor necrosis factor receptor-associated factors (TRAFs). Oncogene, *20*(44), 6482–6491. doi: 10.1038/sj.onc.1204788

Brand, H., & Perrimon, N. (1993). Targeted gene expression as a means of altering cell fates and generating dominant phenotypes. Development, 118(2), 401–415. doi: 10.1242/dev.118.2.401

Brand, A. H., & Livesey, F. J. (2011). Neural Stem Cell Biology in Vertebrates and Invertebrates: More Alike than Different? Neuron, 70(4), 719–729. doi: 10.1016/j.neuron.2011.05.016

Brandt, T., Petrovich, M., Joerger, A. C., & Veprintsev, D. B. (2009). Conservation of DNA-binding specificity and oligomerisation properties within the p53 family. BMC Genomics, 10, 628. doi: 10.1186/1471-2164-10-628

Britton, J. S., & Edgar, B. A. (1998). Environmental control of the cell cycle in *Drosophila*: nutrition activates mitotic and endoreplicative cells by distinct mechanisms. Development, 125, 2149–2158. doi: 10.1242/dev.125.11.2149

Broadusa, J., Skeathb, J. B., Spanab, E. P., Bossingc, T., Technaw, G., & Doe&b, C. Q. (1995). New neuroblast markers and the origin of the aCC/pCC neurons in the *Drosophila* central nervous system. Mech Dev, 53(3), 393-402. doi: 10.1016/0925-4773(95)00454-8

Brosh, R., & Rotter, V. (2009). Transcriptional control of the proliferation cluster by the tumor suppressor p53. Mol Biosyst, 6(1), 17–29. doi:10.1039/b911416e

Brumby, A. M., & Richardson, H. E. (2003). scribble mutants cooperate with oncogenic Ras or Notch to cause neoplastic overgrowth in *Drosophila*. EMBO J, 22(21), 5769–5779. doi: 10.1093/emboj/cdg548

Cabernard, C., & Doe, C. Q. (2009). Apical/Basal Spindle Orientation Is Required for Neuroblast Homeostasis and Neuronal Differentiation in *Drosophila*. Developmental Cell, 17(1), 134–141. doi: 10.1016/j.devcel.2009.06.009

Cabernard, C. (2012). Cytokinesis in *Drosophila melanogaster*. Cytoskeleton, 69(10), 791–809. doi: 10.1002/cm.21060

Cabrera, C. V, Martinez-Arias, A., & Bate, M. (1987). The Expression of Three Members of the achaete-scute Gene Complex Correlates with Neuroblast Segregation in *Drosophila*. Cell, 50(3), 425-433. doi: 10.1016/0092-8674(87)90496-x

Cai, Y., Chia, W., & Yang, X. (2001). A family of Snail-related zinc finger proteins regulates two distinct and parallel mechanisms that mediate *Drosophila* neuroblast asymmetric divisions. EMBO J, 20(7), 1704–1714. doi: 10.1093/emboj/20.7.1704

Cai, Y., Yu, F., Lin, S., Chia, W., & Yang, X. (2003). Apical Complex Genes Control Mitotic Spindle Geometry and Relative Size of Daughter Cells in *Drosophila* Neuroblast and pI Asymmetric Divisions. Cell, 112(1), 51–62. doi: 10.1016/s0092-8674(02)01170-4

Carmena, A., Bate, M., & Jimenez, F. (1995). Lethal of scute, a proneural gene, participates in the specification of muscle progenitors during *Drosophila* embryogenesis. Genes Dev, 9(19), 2373–2383. doi: 10.1101/gad.9.19.2373

Carmena, A., Murugasu-Oei, B., Menon, D., Nez, F. J., & Chia, W. (1998). Inscuteable and numb mediate asymmetric muscle progenitor cell divisions during *Drosophila* myogenesis. Genes Dev, 12(3), 304–315. doi:10.1101/gad.12.3.304

Carmena, A., Speicher, S., & Baylies, M. (2006). The PDZ Protein Canoe/AF-6 links ras-MAPK, Notch and Wingless/Wnt signaling pathways by directly interacting with Ras, Notch and Dishevelled. PLoS One, 1(1). doi: 10.1371/journal.pone.0000066

Carmena, A., Makarova, A., & Speicher, S. (2011). The Rap1-Rgl-Ral signaling network regulates neuroblast cortical polarity and spindle orientation. J Cell Biol, 195(4), 553–562. doi: 10.1083/jcb.201108112

Carmena, A. (2018). Compromising asymmetric stem cell division in *Drosophila* central brain: Revisiting the connections with tumorigenesis. Fly, 12(1), 71–80. doi: 10.1080/19336934.2017.1416277

Carmena, A. (2020). The case of the scribble polarity module in asymmetric neuroblast division in development and tumorigenesis. Int J Mol Sci, 21(8), 2865. doi: 10.3390/ijms21082865

Carter, A. P., Okumura, M., Natsume, T., Kanemaki, M. T., & Kiyomitsu, T. (2018). Dynein-Dynactin-NuMA clusters generate cortical spindle-pulling forces as a multi-arm ensemble. Elife, 7. doi: 10.7554/eLife.36559

Caussinus, E., & González, C. (2005). Induction of tumor growth by altered stem-cell asymmetric division in *Drosophila melanogaster*. Nat Genet, 37(10), 1125–1129. doi: 10.1038/ng1632

Chang, K. C., Garcia-Alvarez, G., Somers, G., Sousa-Nunes, R., Rossi, F., Lee, Y. Y., Soon, S. B., Gonzalez, C., Chia, W., & Wang, H. (2010). Interplay between the Transcription Factor Zif and aPKC Regulates Neuroblast Polarity and Self-Renewal. Dev Cell, 19(5), 778–785. doi: 10.1016/j.devcel.2010.10.007

Chell, J. M., & Brand, A. H. (2010). Nutrition-responsive glia control exit of neural stem cells from quiescence. Cell, 143(7), 1161–1173. doi: 10.1016/j.cell.2010.12.007

Cheng, Z., Zhu, S., Wang, L., Liu, F., Tian, H., Pengsakul, T., & Wang, Y. (2015). Identification and characterisation of Emp53, the homologue of human tumor suppressor p53, from *Echinococcus multilocularis*: Its role in apoptosis and the oxidative stress response. Int J Parasitol, 45(8), 517–526. doi:10.1016/j.ijpara.2015.02.010

Chia, W., Somers, W. G., & Wang, H. (2008). *Drosophila* neuroblast asymmetric divisions: Cell cycle regulators, asymmetric protein localization, and tumorigenesis. J Cell Biol, 180(2), 267–272. doi: 10.1083/jcb.200708159

Choksi, S. P., Southall, T. D., Bossing, T., Edoff, K., de Wit, E., Fischer, B. E. E., van Steensel, B., Micklem, G., & Brand, A. H. (2006). Prospero Acts as a Binary Switch between Self-Renewal and Differentiation in *Drosophila* Neural Stem Cells. Dev Cell, 11(6), 775–789. doi: 10.1016/j.devcel.2006.09.015

Chu-LaGraff, Q., & Doe, C. Q. (1993). Neuroblast Specification and Formation Regulated by wingless in the *Drosophila* CNS. Science, 261(5128), 1594–1597. doi: 10.1126/science.8372355

Cicalese, A., Bonizzi, G., Pasi, C. E., Faretta, M., Ronzoni, S., Giulini, B., Brisken, C., Minucci, S., Fiore, P. P. Di, & Pelicci, P. G. (2009). The Tumor Suppressor p53 Regulates Polarity of Self-Renewing Divisions in Mammary Stem Cells. Cell, 138(6), 1083–1095. doi: 10.1016/j.cell.2009.06.048

Clevers, H. (2005). Stem cells, asymmetric division and cancer. Proc. Natl. Acad. Sci. USA, 37(10), 1027-1028. doi: 10.1038/ng1005-1027

Colaluca, I. N., Tosoni, D., Nuciforo, P., Senic-Matuglia, F., Galimberti, V., Viale, G., Pece, S., & Di Fiore, P. P. (2008). NUMB controls p53 tumour suppressor activity. Nature, 451(7174), 76–80. doi: 10.1038/nature06412

Contreras, E. G., Sierralta, J., & Glavic, A. (2018). P53 is required for brain growth but is dispensable for resistance to nutrient restriction during *Drosophila* larval development. PLoS ONE, 13(4). doi: 10.1371/journal.pone.0194344

Cooks, T., Harris, C. C., & Oren, M. (2014). Caught in the crossfire: p53 in inflammation. Carcinogenesis, 35(8), 1680–1690. doi: 10.1093/carcin/bgu134

Couturier, L., Vodovar, N., & Schweisguth, F. (2012). Endocytosis by Numb breaks Notch symmetry at cytokinesis. Nat Cell Biol, 14(2), 131–139. doi: 10.1038/ncb2419

Daniluk, J., Liu, Y., Deng, D., Chu, J., Huang, H., Gaiser, S., Cruz-Monserrate, Z., Wang, H., Ji, B., & Logsdon, C. D. (2012). An NF-κB pathway-mediated positive feedback loop amplifies Ras activity to pathological levels in mice. J Clin Inves, 122(4), 1519–1528. doi: 10.1172/JCI59743

de Torres-Jurado, A., Manzanero-Ortiz, S., & Carmena, A. (2022). Glial-secreted Netrins regulate Robo1/Rac1-Cdc42 signaling threshold levels during *Drosophila* asymmetric neural stem/progenitor cell division. Curr Biol, 32(10), 2174-2188. doi: 10.1016/j.cub.2022.04.001

Deffie, A., Wu, H., Reinke, V., & Lozano, G. (1993). The tumor suppressor p53 regulates its own transcription. Mol Cell Biol, 13(6), 3415–3423. doi: 10.1128/mcb.13.6.3415-3423.1993

Derry, W. B., Putzke, A. P., & Rothman, J. H. (2001). *Caenorhabditis elegans* p53: Role in apoptosis, meiosis, and stress resistance. Science, 294(5542), 591–595. doi: 10.1126/science.1065486

Dimitrova, S., Reissaus, A., & Tavosanis, G. (2008). Slit and Robo regulate dendrite branching and elongation of space-filling neurons in *Drosophila*. Dev Biol, 324(1), 18–30. doi: 10.1016/j.ydbio.2008.08.028

Doe, C. Q., Chu-LaGraff, Q., Wright, D. M., & Scott, M. P. (1991). The prospero gene specifies cell fates in the *Drosophila* central nervous system. Cell, 65(3), 451–464. doi: 10.1016/0092-8674(91)90463-9

Doe, C. Q. (1992). Molecular markers for identified neuroblasts and ganglion mother cells in the *Drosophila* central nervous system. Development, 116(4), 855–863. doi: 10.1242/dev.116.4.855

Egger, B., Chell, J. M., & Brand, A. H. (2008). Insights into neural stem cell biology from flies. Philos Trans R Soc Lond B Biol Sci, 363(1489), 39–56. doi: 10.1098/rstb.2006.2011

Egger, B., Gold, K. S., & Brand, A. H. (2010). Notch regulates the switch from symmetric to asymmetric neural stem cell division in the *Drosophila* optic lobe. Development, 137(18), 2981–2987. doi:10.1242/dev.051250

El-Deiry, W. S., Kern, S. E., Pietenpop, J. A., Kinzler, K. W., & Vogelstein, B. V. (1992). Definition of a consensus binding site for p53. Nat Genet, 1(1), 45–49. doi: 10.1038/ng0492-45

Fan, Y., Lee, T. V, Xu, D., Chen, Z., Lamblin, A.-F., Steller, H., & Bergmann, A. (2010). Dual roles of *Drosophila* p53 in cell death and cell differentiation. Cell Death Differ, 17(6), 912–921. doi: 10.1038/cdd.2009.182

Faraldo, M. M., & Glukhova, M. A. (2015). Regulating the regulator: Numb acts upstream of p53 to control mammary stem and progenitor cell. J Cell Biol, 211(4), 737–739. doi: 10.1083/jcb.201510104

Fernández-Moreno, M. Á., Farr, C. L., Kaguni, L. S., & Garesse, R. (2007). *Drosophila melanogaster* as a Model System to Study Mitochondrial Biology. Methods Mol Biol, 372, 33–49. doi: 10.1007/978-1-59745-365-3_3

Fischer, M. (2019). Conservation and divergence of the p53 gene regulatory network between mice and humans. Oncogene, 38(21), 4095–4109. doi: 10.1038/s41388-019-0706-9

Fortini, M. E., & Bonini, N. M. (2000). Modeling human neurodegenerative diseases in *Drosophila*. Trends Genet, 16(4), 161–167. doi: 10.1016/s0168-9525(99)01939-3

Frank, D. J., Edgar, B. A., & Roth, M. B. (2002). The *Drosophila melanogaster* gene brain tumor negatively regulates growth and ribosomal RNA synthesis. Development, 129(2), 399–407. doi: 10.1242/dev.129.2.399

Frasch, M., Hoey, T., Rushlow, C., Doyle, H., Levine, M., & Noll, M. (1987). Characterization and localization of the even-skipped protein of *Drosophila*. EMBO J, 6(3), 749–759. doi: 10.1002/j.1460-2075.1987.tb04817.x

Frise, E., Knoblich, J. A., Younger-shepherd, S., Jan, L. Y., & Nung Jan, Y. (1996). The *Drosophila* Numb protein inhibits signaling of the Notch receptor during cell-cell interaction in sensory organ lineage. Proc Natl Acad Sci USA, 93(21), 11925-11932. doi: 10.1073/pnas.93.21.11925

Fuerstenberg, S., Broadus, J., & Doe, C. Q. (1998). Asymmetry and cell fate in the *Drosophila* embryonic CNS. In Int. J. Dev. Biol, 42(3), 379-383. Available in https://ijdb.ehu.eus/article/9654022

García-Bellido, A., & Santamaría, P. (1978). Developmental analysis of the achaete-scute system of *Drosophila melanogaster*. Genetics, 88(3), 469–486. doi: 10.1093/genetics/88.3.469

García-Heredia, J. M., & Carnero, A. (2018). NUMB and NUMBL differences in gene regulation. Oncotarget, 9(10), 9219-9234. Doi: 10.18632/oncotarget.24186

Gateff, E. (1994). Tumor suppressor and overgrowth suppressor genes of *Drosophila* melanogaster: developmental aspects. Int J Dev Biol, *38*(4), 565–590. Available in https://ijdb.ehu.eus/article/7779680

Ginsberg, D., Mechta, F., Yaniv, M., & Oren, M. (1991). Wild-type p53 can down-modulate the activity of various promoters. Proc. Natl. Acad. Sci. USA, 88(22), 9979–9983. doi: 10.1073/pnas.88.22.9979

Golic, K. G., & Lindquist, S. (1989). The FLP Recombinase of Yeast Catalyzes Site-Specific Recombination in the Drosophila Genome. Cell, 59(3), 499–509. doi: 10.1016/0092-8674(89)90033-0

Gómez-López, S., Lerner, R. G., & Petritsch, C. (2014). Asymmetric cell division of stem and progenitor cells during homeostasis and cancer. Cell Mol Life Sci, 71(4), 575–597). doi: 10.1007/s00018-013-1386-1

González, C. (2013). *Drosophila melanogaster*: A model and a tool to investigate malignancy and identify new therapeutics. Nat Rev Cancer, 13(3), 172-183. doi: 10.1038/nrc3461

Gudkov, A. V., Gurova, K. V., & Komarova, E. A. (2011). Inflammation and p53: A tale of two stresses. Genes Cancer, 2(4), 503–516. doi: 10.1177/1947601911409747

Guo, M., Jan, L. Y., & Jan, Y. N. (1996). Control of Daughter Cell Fates during Asymmetric Division: Interaction of Numb and Notch. Neuron, 17(1), 27–41. doi: 10.1016/s0896-6273(00)80278-0

Haenfler, J. M., Kuang, C., & Lee, C. Y. (2012). Cortical aPKC kinase activity distinguishes neural stem cells from progenitor cells by ensuring asymmetric segregation of Numb. Dev Biol, 365(1), 219–228. doi: 10.1016/j.ydbio.2012.02.027

Harper, W. J., Elledge, S. J., Keyomarsi, K., Dynlacht, B., Tsai, L.-H., Zhang, P., Dobrowolski, S., Bai, C., Connell-Crowley, L., Swindell, E., Pat Fox, M., Wei, N., & McLean, M. (1995). Inhibition of Cyclin-dependent Kinases by p21. Mol Biol Cell, 6(4), 387–400. doi: 10.1091/mbc.6.4.387

Hartenstein, V., & Campos-Ortega, J. A. (1984). Early neurogenesis in wild-type *Drosophila melanogaster*. Wilehm Roux Arch Dev Biol, 193(5), 308-325. doi: 10.1007/BF00848159

Haupt, Y., Maya, R., Kazaz, A., & Oren, M. (1997). Mdm2 promotes the rapid degradation of p53. Nature, 387(6630), 296–299. doi: 10.1038/387296a0

Heitzler, P., Bourouis, M., Ruel, L., Carteret, C., & Simpson, P. (1995). Genes of the Enhancer of split and achaete-scute complexes are required for a regulatory loop between Notch and Delta during lateral signalling in *Drosophila*. Development, 122(1), 161–171. doi: 10.1242/dev.122.1.161

Hentges, K. E., & Justice, M. J. (2004). Checks and balancers: Balancer chromosomes to facilitate genome annotation. Trends Genet, 20(6), 252–259. doi: 10.1016/j.tig.2004.04.004

Hernández Borrero, L. J., & El-Deiry, W. S. (2021). Tumor suppressor p53: Biology, signaling pathways, and therapeutic targeting. Biochim Biophys Acta Rev Cancer, 1876(1). doi: 10.1016/j.bbcan.2021.188556

Holguera, I., & Desplan, C. (2018). Neuronal specification in space and time. Science, 362(6411), 176–180. doi: 10.1126/science.aas9435

Hollstein, M., Sidransky, D., Vogelstein, B., & Harris, C. C. (1991). p53 Mutations in Human Cancers. Science, 253(5015), 49–53. doi: 10.1126/science.1905840

Homem, C. C. F., & Knoblich, J. A. (2012). *Drosophila* neuroblasts: A model for stem cell biology. Development, 139(23), 4297–4310. doi: 10.1242/dev.080515

Horvath, M. M., Wang, X., Resnick, M. A., & Bell, D. A. (2007). Divergent evolution of human p53 binding sites: Cell cycle versus apoptosis. PLoS Genetics, 3(7), 1284–1295. doi: 10.1371/journal.pgen.0030127

Horvitz, H. R., & Herskowitzt, I. (1992). Mechanisms of Asymmetric Cell Division: Two Bs or Not Two Bs, That Is the Question. Cell, 68(2), 237-255. doi: 10.1016/0092-8674(92)90468-r

Humbert, P. O., Grzeschik, N. A., Brumby, A. M., Galea, R., Elsum, I., & Richardson, H. E. (2008). Control of tumourigenesis by the Scribble/Dlg/Lgl polarity module. In Oncogene, 27(55) 6888–6907. doi: 10.1038/onc.2008.341

Humbert, P. O., Russell, S. M., Smith, L., & Richardson, H. E. (2015). The scribble–Dlg–Lgl module in cell polarity regulation. Essays Biocem, 53, 141-168. doi: 10.1007/978-3-319-14463-4_4

Igaki, T., Kanda, H., Yamamoto-Goto, Y., Kanuka, H., Kuranaga, E., Aigaki, T., & Miura, M. (2002). Eiger, a TNF superfamily ligand that triggers the *Drosophila* JNK pathway. EMBO J, (12), 3009–3018. doi: 10.1093/emboj/cdf306

Igaki, T., Pagliarini, R. A., & Xu, T. (2006). Loss of Cell Polarity Drives Tumor Growth and Invasion through JNK Activation in Drosophila. Curr Biol, 16(11), 1139–1146. doi: 10.1016/j.cub.2006.04.042

Ingaramo, M. C., Sánchez, J. A., & Dekanty, A. (2018). Regulation and function of p53: A perspective from Drosophila studies. In *Mechanisms of Development* (Vol. 154, pp. 82–90). Elsevier Ireland Ltd. https://doi.org/10.1016/j.mod.2018.05.007

Isshiki, T., Pearson, B., Holbrook, S., & Doe, C. Q. (2001). *Drosophila* Neuroblasts Sequentially Express Transcription Factors which Specify the Temporal Identity of Their Neuronal Progeny. Cell, 106(4), 511-521. Doi: 10.1016/s0092-8674(01)00465-2

Izumi, Y., Ohta, N., Hisata, K., Raabe, T., & Matsuzaki, F. (2006). *Drosophila* Pins-binding protein Mud regulates spindle-polarity coupling and centrosome organization. Nat Cell Biol, 8(6), 586–593. doi: 10.1038/ncb1409

Jacob, L., Opper, M., Yetrroth, B., Phannavong, B., & Mechler, B. M. (1987). Structure of the l(2)gl Gene of *Drosophila* and Delimitation of Its Tumor Suppressor Domain. Cell, 50(2), 215-225. doi: 10.1016/0092-8674(87)90217-0

Jain, A. K., & Barton, M. C. (2018). P53: Emerging roles in stem cells, development and beyond. Development, 145(8). doi: 10.1242/dev.158360

Januschke, J., & Gonzalez, C. (2008). *Drosophila* asymmetric division, polarity and cancer. Oncogene, 27(55), 6994–7002. doi: 10.1038/onc.2008.349

Jegga, A. G., Inga, A., Menendez, D., Aronow, B. J., & Resnick, M. A. (2008). Functional evolution of the p53 regulatory network through its target response elements. Proc Natl Acad Sci USA, 105(3), 944–949. doi: 10.1073/pnas.0704694105

Jiang, Y., & Reichert, H. (2014). *Drosophila* neural stem cells in brain development and tumor formation. J Neurogenet, 28(3-4), 181-189. doi: 10.3109/01677063.2014.898639

Kaltschmidt, J. A., Davidson, C. M., Brown, N. H., & Brand, A. H. (2000). Rotation and asymmetry of the mitotic spindle direct asymmetric cell division in the developing central nervous system. Nat Cell Biol, 2(1), 7-12. doi: 10.1038/71323

Kang, K. H., & Reichert, H. (2015). Control of neural stem cell self-renewal and differentiation in Drosophila. Cell Tissue Res, 359(1), 33–45. doi: 10.1007/s00441-014-1914-9

Keder, A., Rives-Quinto, N., Aerne, B. L., Franco, M., Tapon, N., & Carmena, A. (2015). The Hippo pathway core cassette regulates asymmetric cell division. Curr Biol, 25(21), 2739–2750. doi: 10.1016/j.cub.2015.08.064

Kelsom, C., & Lu, W. (2012). Uncovering the link between malfunctions in *Drosophila* neuroblast asymmetric cell division and tumorigenesis. Cell Biosci, 2(1), 38. doi: 10.1186/2045-3701-2-38

Knoblich, J. A., Jan, L. Y., & Jan, Y. N. (1995). Asymmetric segregation of Numb and Prospero during cell division. Nature, 377(6550), 624–627. doi: 10.1038/377624a0

Knoblich, J. A. (2001). Asymmetric cell division during animal development. Nat Rev Mol Cell Biol, 2(1), 11–20. doi; 10.1038/35048085

Knoblich, J. A. (2008). Mechanisms of Asymmetric Stem Cell Division. Cell, 132(4), 583–597. doi: 10.1016/j.cell.2008.02.007

Knoblich, J. A. (2010). Asymmetric cell division: Recent developments and their implications for tumour biology. Nat Rev Mol Cell Biol, 11(12), 849–860. doi: 10.1038/nrm3010

Knust, E., Bremer, K. A., Vässin, H., Ziemer, A., Tepass, U., & Campos-Ortega, J. A. (1987). The Enhancer of Split Locus and Neurogenesis in *Drosophila melanogaster*. Dev Biol, 122(1), 262-73. doi: 10.1016/0012-1606(87)90351-4

Kosman, D., Small, S., & Reinitz, J. (1998). Rapid preparation of a panel of polyclonal antibodies to *Drosophila* segmentation proteins. Dev Genes Evo, 208(5), 290–294. doi: 10.1007/s004270050184

Krahn, M. P., Egger-Adam, D., & Wodarz, A. (2009). PP2A Antagonizes Phosphorylation of Bazooka by PAR-1 to Control Apical-Basal Polarity in Dividing Embryonic Neuroblasts. Dev Cell, 16(6), 901–908. doi: 10.1016/j.devcel.2009.04.011

Krahn, M. P., Klopfenstein, D. R., Fischer, N., & Wodarz, A. (2010). Membrane Targeting of Bazooka/PAR-3 Is Mediated by Direct Binding to Phosphoinositide Lipids. Curr Biol, 20(7), 636–642. doi: 10.1016/j.cub.2010.01.065

Kraut, R., & Campos-Ortega, J. A. (1996). inscuteable, a neural precursor gene of *Drosophila*, encodes a candidate for a cytoskeleton adaptor protein. Dev Biol, 174(1), 65–81. doi: 10.1006/dbio.1996.0052

Kress, M., May, E., Cassingena, R., & May, P. (1979). Simian Virus 40-Transformed Cells Express New Species of Proteins Precipitable by Anti-Simian Virus 40 Tumor Serum. J Virol, 31(2), 472–483. doi: 10.1128/JVI.31.2.472-483.1979

Krieger, J. R., Taylor, P., Gajadhar, A. S., Guha, A., Moran, M. F., & McGlade, C. J. (2013). Identification and selected reaction monitoring (SRM) quantification of endocytosis factors associated with Numb. Mol Cell Proteomics, 12(2), 499–514. doi: 10.1074/mcp.M112.020768

Kubbutat, M. H., Jones, S. N., & Vousden, K. H. (1997). Regulation of p53 stability by Mdm2. Nature, 387(6630), 299–303. doi: 10.1038/387299a0

Kuchinke, U., Grawe, F., & Knust, E. (1998). Control of spindle orientation in *Drosophila* by the Par-3-related PDZ-domain protein Bazooka. Curr Biol, 8(25), 1357–1365. doi: 10.1016/s0960-9822(98)00016-5

La Marca, J. E., & Richardson, H. E. (2020). Two-Faced: Roles of JNK Signalling During Tumourigenesis in the *Drosophila* Model. Front Cell Dev Biol, 8. doi: 10.3389/fcell.2020.00042

Lai, Z., Fortini, M. E., & Rubin, G. M. (1991). The embryonic expression patterns of zfh-1 and zfh-2, two Drosophila genes encoding novel zinc-finger homeodomain proteins. Mech Dev, 34(2-3), 123-134. doi: 10.1016/0925-4773(91)90049-c

Lane, D. P., & Crawford, L. V. (1979). T antigen is bound to a host protein in SV40-transformed cells. Nature, 278(5701), 261–263. doi: 10.1038/278261a0

Lane, D. P. (1992). p53, guardian of the genome. Nature, 358(6381), 15–16. doi: 10.1038/358015a0

Lee, C. Y., Andersen, R. O., Cabernard, C., Manning, L., Tran, K. D., Lanskey, M. J., Bashirullah, A., & Doe, C. Q. (2006a). *Drosophila* Aurora-A kinase inhibits neuroblast self-renewal by regulating aPKC/Numb cortical polarity and spindle orientation. Genes Dev, 20(24), 3464–3474. doi: 10.1101/gad.1489406

Lee, C. Y., Robinson, K. J., & Doe, C. Q. (2006b). Lgl, Pins and aPKC regulate neuroblast self-renewal versus differentiation. Nature, 439(7076), 594–598. doi: 10.1038/nature04299

Lee, C. Y., Wilkinson, B. D., Siegrist, S. E., Wharton, R. P., & Doe, C. Q. (2006c). Brat is a Miranda cargo protein that promotes neuronal differentiation and inhibits neuroblast self-renewal. Dev Cell, 10(4), 441–449. doi: 10.1016/j.devcel.2006.01.017

Lee, J. H., Lee, E., Park, J., Kim, E., Kim, J., & Chung, J. (2003). In vivo p53 function is indispensable for DNA damage-induced apoptotic signaling in *Drosophila*. FEBS Letters, 550(1–3), 5–10. doi: 10.1016/S0014-5793(03)00771-3

Lee, T., & Luo, L. (1999). Mosaic Analysis with a Repressible Neurotechnique Cell Marker for Studies of Gene Function in Neuronal Morphogenesis. Neuron*, 22*(3), 451–461. doi: 10.1016/s0896-6273(00)80701-1

Li, P., Yang, X., Wasser, M., Cai, Y., & Chia, W. (1997). Inscuteable and Staufen Mediate Asymmetric Localization and Segregation of prospero RNA during *Drosophila* Neuroblast Cell Divisions. Cell, 90(3), 437–447. doi: 10.1016/s0092-8674(00)80504-8

Li, S., Wang, H., & Groth, C. (2014). *Drosophila* neuroblasts as a new model for the study of stem cell self-renewal and tumour formation. Biosci Rep, 34(4), 401–414. doi: 10.1042/BSR20140008

Lin, Z., Lin, X., Zhu, L., Huang, J., & Huang, Y. (2020). TRIM2 directly deubiquitinates and stabilizes Snail1 protein, mediating proliferation and metastasis of lung adenocarcinoma. Cancer Cell Int, 20(1). doi: 10.1186/s12935-020-01316-6

Liu, J., Zhang, C., Hu, W., & Feng, Z. (2019). Tumor suppressor p53 and metabolism. J Mol Cell Biol, 11(4), 284–292. doi: 10.1093/jmcb/mjy070

Liu, Y., Raheja, R., Yeh, N., Ciznadija, D., Pedraza, A. M., Ozawa, T., Hukkelhoven, E., Erdjument-Bromage, H., Tempst, P., Gauthier, N. P., Brennan, C., Holland, E. C., & Koff, A. (2014). TRIM3, a tumor suppressor linked to regulation of p21 Waf1/Cip1. Oncogene, 33(3), 308–315. doi: 10.1038/onc.2012.596

Loedige, I., & Filipowicz, W. (2009). TRIM-NHL Proteins Take on miRNA Regulation. Cell, 136(5), 818–820. doi: 10.1016/j.cell.2009.02.030

Lu, B., Ackerman, L., Jan, L. Y., & Jan Y N. (1999). Modes of Protein Movement that Lead to the Asymmetric Localization of Partner of Numb during *Drosophila* Neuroblast Division. Mol Cell, 4(6), 883–891. doi: 10.1016/s1097-2765(00)80218-x

Lu, B., Rothenberg, M., Jan, L. Y., & Jan, Y. N. (1998). Partner of Numb Colocalizes with Numb during Mitosis and Directs Numb Asymmetric Localization in *Drosophila* Neural and Muscle Progenitors. Cell, 95(2), 225–235. doi: 10.1016/S0092-8674(00)81753-5

Lu, M. S., & Johnston, C. A. (2013). Molecular pathways regulating mitotic spindle orientation in animal cells. Development, 140(9), 1843–1856. doi: 10.1242/dev.087627

Maiuri, M. C., Galluzzi, L., Morselli, E., Kepp, O., Malik, S. A., & Kroemer, G. (2010). Autophagy regulation by p53. Curr Opin Cell Biol, 22(2), 181–185. doi: 10.1016/j.ceb.2009.12.001

Mantovani, F., Collavin, L., & Del Sal, G. (2019). Mutant p53 as a guardian of the cancer cell. Cell Death Differ, 26(2), 199-212. doi: 10.1038/s41418-018-0246-9

Manzanero-Ortiz, S., de Torres-Jurado, A., Hernández-Rojas, R., & Carmena, A. (2021). Pilot RNAi screen in *Drosophila* neural stem cell lineages to identify novel tumor suppressor genes involved in asymmetric cell division. Int J Mol Sci, 22(21). doi: 10.3390/ijms222111332

Martín-Bermudo, M. D., Martínez, C., Rodríguez, A., & Jiménez, F. (1991). Distribution and function of the lethal of scute gene product during early neurogenesis in *Drosophila*. Development, 113(2), 445-454. doi: 10.1242/dev.113.2.445

Martín-Bermudo, M. D., Carmena, A., & Jiménez, F. (1995). Neurogenic genes control gene expression at the transcriptional level in neurogenesis and in mesectoderm specification. Development, 121(1), 219–224. doi: 10.1242/dev.121.1.219

Matsuzaki, F., Koizumi, K., Hamal, C., Yoshioka, T., & Nabeshimal, Y. (1992). Cloning of the *Drosophila* prospero gene and its expression in ganglion mother cells. Biochem Biophys Res Comm, 182(3), 1326–1332. doi: 10.1016/0006-291x(92)91878-t

Mauser, J. F., & Prehoda, K. E. (2012). Inscuteable regulates the pins-mud spindle orientation pathway. PLoS ONE, 7(1). doi: 10.1371/journal.pone.0029611

McGill, M. A., & McGlade, C. J. (2003). Mammalian Numb proteins promote Notch1 receptor ubiquitination and degradation of the Notch1 intracellular domain. J Biol Chem, 278(25), 23196–23203. doi: 10.1074/jbc.M302827200

Meletis, K., Wirta, V., Hede, S. M., Nistér, M., Lundeberg, J., & Frisén, J. (2006). p53 suppresses the self-renewal of adult neural stem cells. Development, 133(2), 363–369. doi: 10.1242/dev.02208

Menendez, D., Nguyen, T. A., Freudenberg, J. M., Mathew, V. J., Anderson, C. W., Jothi, R., & Resnick, M. A. (2013). Diverse stresses dramatically alter genome-wide p53 binding and transactivation landscape in human cancer cells. Nucleic Acids Research, 41(15), 7286–7301. doi: 10.1093/nar/gkt504

Michael, D., & Oren, M. (2002). The p53 and Mdm2 families in cancer. Curr Opin Genet Dev, 12(1), 53–59. doi: 10.1016/s0959-437x(01)00264-7

Miller, D. E., Cook, K. R., Kazemi, N. Y., Smith, C. B., Cockrell, A. J., Hawley, R. S., & Bergman, C. M. (2016). Rare recombination events generate sequence diversity among balancer chromosomes in *Drosophila melanogaster*. Proc Natl Acad Sci USA, 113(10), E1352–E1361. doi: 10.1073/pnas.1601232113

Molchadsky, A., Rivlin, N., Brosh, R., Rotter, V., & Sarig, R. (2010). P53 is balancing development, differentiation and de-differentiation to assure cancer prevention. Carcinogenesis, 31(9), 1501-1508. doi: 10.1093/carcin/bgq101

Morante, J., & Desplan, C. (2011). Dissection and staining of *Drosophila* optic lobes at different stages of development. Cold Spring Harb Protoc, 6(6), 652–656. doi:10.1101/pdb.prot5629

Mosner, J., Mummenbrauer, T., Bauer, C., Sczakiel, G., Grosse, F., & Deppert, W. (1995). Negative feedback regulation of wild-type p53 biosynthesis. EMBO J, 14(18), 4442–4449. doi: 10.1002/j.1460-2075.1995.tb00123.x

Murray-Zmijewski, F., Lane, D. P., & Bourdon, J. C. (2006). p53/p63/p73 isoforms: An orchestra of isoforms to harmonise cell differentiation and response to stress. Cell Death Differ, 13(6), 962-972. doi: 10.1038/sj.cdd.4401914

Neumüller, R. A., & Knoblich, J. A. (2009). Dividing cellular asymmetry: Asymmetric cell division and its implications for stem cells and cancer. Genes Dev, 23(23), 2675–2699). doi: 10.1101/gad.1850809

Neumüller, R. A., Richter, C., Fischer, A., Novatchkova, M., Neumüller, K. G., & Knoblich, J. A. (2011). Genome-wide analysis of self-renewal in *Drosophila* neural stem cells by transgenic RNAi. Cell Stem Cell, 8(5), 580–593. doi: 10.1016/j.stem.2011.02.022

Nipper, R. W., Siller, K. H., Smith, N. R., Doe, C. Q., & Prehoda, K. E. (2007). G alpha i generates multiple Pins activation states to link cortical polarity and spindle orientation in *Drosophila* neuroblasts. Proc Natl Acad Sci U S A, 104(36), 14306-14311. doi: 10.1073/pnas.0701812104

Novitski, E., & Braver, G. (1954). An analysis of crossing over within a heterozygous inversion in *Drosophila melanogaster*. Genetics, 39(2), 197–209. doi: 10.1093/genetics/39.2.197

Ogawa, H., Ohta, N., Moon, W., & Matsuzaki, F. (2009). Protein phosphatase 2A negatively regulates aPKC signaling by modulating phosphorylation of Par-6 in *Drosophila* neuroblast asymmetric divisions. J Cell Sci, 122(18), 3242–3249. doi: 10.1242/jcs.050955

Ohshiro, T., Yagami, T., Zhang, C., & Matsuzaki, F. (2000). Role of cortical tumour-suppressor proteins in asymmetric division of *Drosophila* neuroblast. Nature, 408(6812), 593–596. doi: 10.1038/35046087

Ollmann, M., Young, L. M., Di Como, C. J., Karim, F., Belvin, M., Robertson, S., Whittaker, K., Demsky, M., Fisher, W. W., Buchman, A., Duyk, G., Friedman, L.,

Prives, C., & Kopczynski, C. (2000). *Drosophila* p53 Is a Structural and Functional Homolog of the Tumor Suppressor p53. Cell, 101(1), 91–101. doi: 10.1016/S0092-8674(00)80626-1

Oren, M. (2003). Decision making by p53: Life, death and cancer. Cell Death Differ, 10(4), 431-442. doi: 10.1038/sj.cdd.4401183

Ouyang, Y., Song, Y., & Lu, B. (2011). dp53 restrains ectopic neural stem cell formation in the *Drosophila* brain in a non-apoptotic mechanism involving archipelago and cyclin E. PLoS ONE, 6(11). doi: 10.1371/journal.pone.0028098

Pardal, R., Clarke, M. F., & Morrison, S. J. (2003). Applying the principles of stem-cell biology to cancer. Nat Rev Cancer, 3(12), 895-902. doi: 10.1038/nrc1232

Pece, S., Serresi, M., Santolini, E., Capra, M., Hulleman, E., Galimberti, V., Zurrida, S., Maisonneuve, P., Viale, G., & Di Fiore, P. P. (2004). Loss of negative regulation by Numb over Notch is relevant to human breast carcinogenesis. J Cell Biol, 167(2), 215–221. doi: 10.1083/jcb.200406140

Peng, C. Y., Manning, L., Albertson, R., & Doe, C. Q. (2000). The tumour-suppressor genes lgl and dlg regulate basal protein targeting in *Drosophila* neuroblasts. Nature, 408, 596–600. doi: 10.1038/35046094

Petersen, P. H., Zou, K., Hwang, J. K., Jan, Y. N., & Zhong Weimin. (2002). Progenitor cell maintenance requires numb and numblike during mouse neurogenesis. Nature, 419(6910), 925–929. doi: 10.1038/nature01124

Petronczki, M., & Knoblich, J. A. (2001). DmPAR-6 directs epithelial polarity and asymmetric cell division of neuroblasts in *Drosophila*. Nat Cell Biol, 3(1), 43-49. doi: 10.1038/35050550

Plant, P. J., Fawcett, J. P., Lin, D. C. C., Holdorf, A. D., Binns, K., Kulkarni, S., & Pawson, T. (2003). A polarity complex of mPar-6 and atypical PKC binds, phosphorylates and regulates mammalian Lgl. Nat Cell Bio, 5(4), 301–308. doi: 10.1038/ncb948

Polager, S., & Ginsberg, D. (2009). P53 and E2f: Partners in life and death. Nature Rev Cancer, 9(10), 738–748. doi: 10.1038/nrc2718

Preiss, A., Johannes, B., Nagel, A. C., Maier, D., Peters, N., & Wajant, H. (2001). Dynamic expression of *Drosophila* TRAF1 during embryogenesis and larval development. Mech Dev, 100(1), 109–113. doi: 10.1016/s0925-4773(00)00506-2

Qin, Y., Ye, J., Zhao, F., Hu, S., & Wang, S. (2018). TRIM2 regulates the development and metastasis of tumorous cells of osteosarcoma. Int J Onc, 53(4), 1643–1656. doi: 10.3892/ijo.2018.4494

Reichardt, I., Bonnay, F., Steinmann, V., Loedige, I., Burkard, T. R., Meister, G., & Knoblich, J. A. (2018). The tumor suppressor Brat controls neuronal stem cell lineages by inhibiting Deadpan and Zelda. EMBO Rep, 19(1), 102–117. doi: 10.15252/embr.201744188

Reichert, H. (2011). *Drosophila* neural stem cells: cell cycle control of self-renewal, differentiation, and termination in brain development. Results Probl Cell Differ, 53, 529-546. doi: 10.1007/978-3-642-19065-0_21

Reya, T., Morrison, S. J., Clarke, M. F., & Weissman, I. L. (2001). Stem cells, cancer, and cancer stem cells. Nature, 414, 105–111. doi: 10.1038/35102167

Rhyu, M. S., Yeh Jan, L., & Nung Jan, Y. (1994). Asymmetric Distribution of Numb Protein during Division of the Sensory Organ Precursor Cell Confers Distinct Fates to Daughter Cells. In Cell, 76(3), 477-491. doi: 10.1016/0092-8647(94)90112-0

Riley, T., Sontag, E., Chen, P., & Levine, A. (2008). Transcriptional control of human p53-regulated genes. Nat Rev Mol Cell Biol, 9(5), 402–412. doi: 10.1038/nrm2395

Rives-Quinto, N., Franco, M., de Torres-Jurado, A., & Carmena, A. (2017). Synergism between canoe and scribble mutations causes tumor-like overgrowth via Ras activation in neural stem cells and epithelia. Development, 144(14), 2570–2583. doi: 10.1242/dev.148171

Romani, S., Campuzano, S., & Modolell, J. (1987). The achaete-scute complex is expressed in neurogenic regions of *Drosophila* embryos. EMBO J, 6(7), 2085-2092. doi: 10.1002/j.1460-2075.1987.tb02474.x

Rust, K., & Wodarz, A. (2021). Transcriptional control of apical-basal polarity regulators. Int J Molecular Sci, 22(22), 12340. doi: 10.3390/ijms222212340

Sarute, N., Ibrahim, N., Fagla, B. M., Lavanya, M., Cuevas, C., Stavrou, S., Otkiran-Clare, G., Tyynismaa, H., Henao-Mejia, J., & Ross, S. R. (2019). TRIM2, a novel member of the antiviral family, limits new world arenavirus entry. PLoS Biol, 17(2). doi: 10.1371/journal.pbio.3000137

Sawyer, J. K., Harris, N. J., Slep, K. C., Gaul, U., & Peifer, M. (2009). The *Drosophila* afadin homologue Canoe regulates linkage of the actin cytoskeleton to adherens junctions during apical constriction. J Cell Biol, 186(1), 57–73. doi: 10.1083/jcb.200904001

Schaefer, M., Shevchenko, A., Shevchenko, A., & Knoblich, J. A. (2000). A protein complex containing Inscuteable and the Gα-binding protein Pins orients asymmetric cell divisions in *Drosophila*. Curr Biol, 10(7), 353–362. doi: 10.1016/S0960-9822(00)00401-2

Scheffer, L. K., Xu, C. S., Januszewski, M., Lu, Z., Takemura, S. Y., Hayworth, K. J., Huang, G. B., Shinomiya, K., Maitin-Shepard, J., Berg, S., Clements, J., Hubbard, P. M., Katz, W. T., Umayam, L., Zhao, T., Ackerman, D., Blakely, T., Bogovic, J., Dolafi, T., … Plaza, S. M. (2020). A connectome and analysis of the adult drosophila central brain. ELife, 9. doi: 10.7554/ELIFE.57443

Scheffner, M., Werness, B. A., Huibregtse, J. 54, Levine, A. J., & Howley', P. M. (1990). The E6 Oncoprotein Encoded by Human Papillomavirus Types 16 and 18 Promotes the Degradation of p53. Cell, 63(6). doi: 10.1016/0092-8674(90)90409-8

Schober, M., Schaefer, M., & Knoblich, J. A. (1999). Bazooka recruits Inscuteable to orient asymmetric cell divisions in *Drosophila* neuroblasts. Nature, 402(6761), 548–551. doi: 10.1038/990135

Schuldt, A. J., Adams, J. H. J., Davidson, C. M., Micklem, D. R., Haseloff, J., St Johnston, D., & Brand, A. H. (1998). Miranda mediates asymmetric protein and RNA localization in the developing nervous system. Genes Dev, 12(12), 1847–1857. doi: 10.1101/gad.12.12.1847

Schumacher, B., Hofmann, K., Boulton, S., & Gartner, A. (2001). The C. elegans homolog of the p53 tumor suppressor is required for DNA damage-induced apoptosis. Curr Biol, 11(21), 1722–1727. doi: 10.1016/s0960-9822(01)00534-6

Schwamborn, J. C., Berezikov, E., & Knoblich, J. A. (2009). The TRIM-NHL Protein TRIM32 Activates MicroRNAs and Prevents Self-Renewal in Mouse Neural Progenitors. Cell, 136(5), 913–925. doi: 10.1016/j.cell.2008.12.024

Schwartz, D., & Rotter, V. (1998). p53-dependent cell cycle control: response to genotoxic stress. Semin Cancer Biol, 8(5), 325–336. doi: 10.1006/scbi.1998.0095

Senitzki, A., Safieh, J., Sharma, V., Golovenko, D., Danin-Poleg, Y., Inga, A., & Haran, T. E. (2021). The complex architecture of p53 binding sites. Nucleic Acids Res, 49(3), 1364–1382. doi: 10.1093/nar/gkaa1283

Shan, Z., Tu, Y., Yang, Y., Liu, Z., Zeng, M., Xu, H., Long, J., Zhang, M., Cai, Y., & Wen, W. (2018). Basal condensation of Numb and Pon complex via phase transition during *Drosophila* neuroblast asymmetric division. Nat Comm, 9(1). doi: 10.1038/s41467-018-03077-3

Shen, C.-P., Knoblich, J. A., Chan, Y.-M., Jiang, M.-M., Jan, L. Y., & Jan, Y. N. (1998). Miranda as a multidomain adapter linking apically localized Inscuteable and basally localized Staufen and Prospero during asymmetric cell division in *Drosophila*. Genes Dev, 1*2*(12), 1837–1846. doi:10.1101/gad.12.12.1837

Siegrist, S. E., & Doe, C. Q. (2005). Microtubule-induced pins/Gαi cortical polarity in *Drosophila* neuroblasts. Cell, 123(7), 1323–1335. doi: 10.1016/j.cell.2005.09.043

Siller, K. H., Cabernard, C., & Doe, C. Q. (2006). The NuMA-related Mud protein binds Pins and regulates spindle orientation in *Drosophila* neuroblasts. Nat Cell Biol, 8(6), 594–600. doi: 10.1038/ncb1412

Skeath, J. B., & Carroll, S. B. (1992). Regulation of proneural gene expression and cell fate during neuroblast segregation in the *Drosophila* embryo. Development, 114(4), 939-946. doi: 10.1242/dev.114.4.939

Skeath, J. B., & Thor, S. (2003). Genetic control of Drosophila nerve cord development. Curr Opin Neurobiol, 13(1), 8–15). doi: 10.1016/S0959-4388(03)00007-2

Slack, F. J., & Ruvkun, G. (1998). A novel repeat domain that is often associated with RING finger and B-box motifs. Trends Biochem. Sci, 23(12), 474–475. doi: 10.1016/s0968-0004(98)01299-7

Slováková, J., Speicher, S., Sánchez-Soriano, N., Prokop, A., & Carmena, A. (2012). The actin-binding protein Canoe/AF-6 forms a complex with Robo and is required for Slit-Robo signaling during axon pathfinding at the CNS midline. J Neurosci, 32(29), 10035–10044. doi: 10.1523/JNEUROSCI.6342-11.2012

Smith, C. A., Lau, K. M., Rahmani, Z., Dho, S. E., Brothers, G., She, Y. M., Berry, D. M., Bonneil, E., Thibault, P., Schweisguth, F., Le Borgne, R., & McGlade, C. J. (2007). aPKC-mediated phosphorylation regulates asymmetric membrane localization of the cell fate determinant Numb. EMBO J, 26(2), 468–480. doi: 10.1038/sj.emboj.7601495

Sonoda, J., & Wharton, R. P. (2001). *Drosophila* brain tumor is a translational repressor. Genes Dev, 15(6), 762–773. doi: 10.1101/gad.870801

Sousa-Nunes, R., & Somers, W. G. (2010). Phosphorylation and dephosphorilation events allow for rapid segregation of fate determinants during *Drosophila* neuroblast asymmetric divisions. Comm Integr Biol, 3(1), 46–49. doi: 10.4161/cib.3.1.9635

Sousa-Nunes, R., Yee, L. L., & Gould, A. P. (2011). Fat cells reactivate quiescent neuroblasts via TOR and glial insulin relays in *Drosophila*. Nature, 471(7339), 508–513. doi:10.1038/nature09867

Sousa-Nunes, R., & Somers, W. G. (2013). Mechanisms of Asymmetric Progenitor Divisions in the *Drosophila* Central Nervous System. Adv Exp Med Biol, 786, 79–102. doi: 10.1007/978-94-007-6621-1_6

Spana, E. P., & Doe, C. Q. (1995). The prospero transcription factor is asymmetrically localized to the cortex during neuroblast mitosis in *Drosophila*. Development, 121(10), 3187–3195. doi: 10.1242/dev.121.10.3187

Spana, E. P., & Doe, C. Q. (1996). Numb Antagonizes Notch Signaling to Specify Sibling Neuron Cell Fates. Neuron, 17(1), 21–26. doi: 10.1016/s0896-6273(00)80277-9

Speicher, S., Fischer, A., Knoblich, J., & Carmena, A. (2008). The PDZ Protein Canoe Regulates the Asymmetric Division of *Drosophila* Neuroblasts and Muscle Progenitors. Curr Biol, 18(11), 831–837. doi: 10.1016/j.cub.2008.04.072

Spike, B. T., & Wahl, G. M. (2011). P53, stem cells, and reprogramming: Tumor suppression beyond guarding the genome. Genes Cancer, 2(4), 404–419. doi: 10.1177/1947601911410224

Stagg, S. B., Guardiola, A. R., & Crews, S. T. (2011). Dual role for *Drosophila* lethal of scute in CNS midline precursor formation and dopaminergic neuron and motoneuron cell fate. Development, 138(11), 2171–2183. doi: 10.1242/dev.056507

Stiewe, T. (2007). The p53 family in differentiation and tumorigenesis. Nat Rev Cancer, 7(3), 165–167. doi: 10.1038/nrc2072

Su, D., Wang, X., Campbell, M. R., Song, L., Safi, A., Crawford, G. E., & Bell, D. A. (2015). Interactions of Chromatin Context, Binding Site Sequence Content, and Sequence Evolution in Stress-Induced p53 Occupancy and Transactivation. PLoS Gen, 11(1). doi: 10.1371/journal.pgen.1004885

Sunchu, B., & Cabernard, C. (2020). Principles and mechanisms of asymmetric cell division. Development, 147(13), doi: 10.1242/dev.167650

Tamori, Y., & Deng, W. M. (2011). Cell competition and its implications for development and cancer. J Genet Genomics, 38(10), 483–495. doi: 10.1016/j.jgg.2011.09.006

Tasdemir, E., Maiuri, M. C., Galluzzi, L., Vitale, I., Djavaheri-Mergny, M., D'Amelio, M., Criollo, A., Morselli, E., Zhu, C., Harper, F., Nannmark, U., Samara, C., Pinton, P., Vicencio, J. M., Carnuccio, R., Moll, U. M., Madeo, F., Paterlini-Brechot, P., Rizzuto, R., … Kroemer, G. (2008). Regulation of autophagy by cytoplasmic p53. Nature Cell Biol, 10(6), 676–687. doi: 10.1038/ncb1730

Terzian, T., Suh, Y. A., Iwakuma, T., Post, S. M., Neumann, M., Lang, G. A., Van Pelt, C. S., & Lozano, G. (2008). The inherent instability of mutant p53 is alleviated by Mdm2 or p16 INK4a loss. Genes Dev, 22(10), 1337–1344. doi: 10.1101/gad.1662908

Theodosiou, N. A., & Xu, T. (1998). Use of FLP/FRT System to Study *Drosophila* Development. Methods, 14(4), 355-365. doi: 10.1006/meth.1998.0591

Thompson, S., Pearson, A. N., Ashley, M. D., Jessick, V., Murphy, B. M., Gafken, P., Henshall, D. C., Morris, K. T., Simon, R. P., & Meller, R. (2011). Identification of a novel Bcl-2-interacting mediator of cell death (Bim) E3 ligase, tripartite motif-containing protein 2 (TRIM2), and its role in rapid ischemic tolerance-induced

neuroprotection. J Biol Chem, 286(22), 19331–19339. doi: 10.1074/jbc.M110.197707

Tosoni, D., Zecchini, S., Coazzoli, M., Colaluca, I., Mazzarol, G., Rubio, A., Caccia, M., Villa, E., Zilian, O., Di Fiore, P. P., & Pece, S. (2015). The Numb/p53 circuitry couples replicative self-renewal and tumor suppression in mammary epithelial cells. J Cell Biol, 211(4), 845–862. doi: 10.1083/jcb.201505037

Tsuji, T., Hasegawa, E., & Isshiki, T. (2008). Neuroblast entry into quiescence is regulated intrinsically by the combined action of spatial Hox proteins and temporal identity factors. Development, 135(23), 3859–3869. doi: 10.1242/dev.025189

Uemura, T., Shepherd, S., Ackerman, L., Yeh Jan, L., & Nung Jan, Y. (1989). Numb, a Gene Required in Determination of Cell Fate during Sense-y Organ in *Drosophila* Embryos Formation. Cell, 58(2), 349-360. doi: 10.1016/0092-8467(89)90849-0

Urbach, R., & Technau, G. M. (2004). Neuroblast formation and patterning during early brain development in *Drosophila*. Bioessays, 26(7), 739–751. doi: 10.1002/bies.20062

Vaessin, H., Grell, E., Wolff, E., Bier, E., Yeh Jan, L., & Nung Jan, Y. (1991). Prospero is Expressed in Neuronal Precursors and Encodes a Nuclear Protein That Is Involved in the Control of Axonal Outgrowth in *Drosophila*. Cell, 67(5), 941-953. doi: 10.1016/0092-8674(91)90367-8

Ventura, A., Kirsch, D. G., McLaughlin, M. E., Tuveson, D. A., Grimm, J., Lintault, L., Newman, J., Reczek, E. E., Weissleder, R., & Jacks, T. (2007). Restoration of p53 function leads to tumour regression in vivo. Nature, 445(7128), 661–665. doi: 10.1038/nature05541

Verdi, J. M., Schmandt, R., Bashirullah, A., Jacob, S., Salvino, R., Craig, C. G., Program, A. E., Lipshitz, H. D., & Mcglade, C. J. (1996). Mammalian NUMB is an

evolutionarily conserved signaling adapter protein that specifies cell fate. Curr Biol, 6(9), 1134–1145. doi: 10.1016/s0960-9822(02)70680-5

Vessey, J. P., Amadei, G., Burns, S. E., Kiebler, M. A., Kaplan, D. R., & Miller, F. D. (2012). An asymmetrically localized Staufen2-dependent RNA complex regulates maintenance of mammalian neural stem cells. Cell Stem Cell, 11(4), 517–528. doi: 10.1016/j.stem.2012.06.010

Vogelstein, B., Lane, D., & Levine, A. J. (2000). Surfing the p53 network. Nature, 408(6810), 307–310. doi: 10.1038/35042675

Vousden, K. H., & Prives, C. (2005). P53 and prognosis: New insights and further complexity. Cell, 120(1), 7–10. doi: 10.1016/j.cell.2004.12.027

Vousden, K. H., & Prives, C. (2009). Blinded by the Light: The Growing Complexity of p53. Cell, 137(3), 413–431. doi: 10.1016/j.cell.2009.04.037

Walsh, K. T., & Doe, C. Q. (2017). *Drosophila* embryonic type II neuroblasts: Origin, temporal patterning, and contribution to the adult central complex. Development, 144(24), 4552–4562. doi: 10.1242/dev.157826

Wang, B., Xiao, Z., & Ren, E. C. (2009). Redefining the p53 response element. PNAS , 106(34), 14373–14378. doi: 10.1073/pnas.0903284106

Wang, B., Xiao, Z., Ko, H. L., & Ren, E. C. (2010). The p53 response element and transcriptional repression. Cell Cycle, 9(5), 870–879. doi: 10.4161/cc.9.5.10825

Wang, H., Cai, Y., Chia, W., & Yang, X. (2006). *Drosophila* homologs of mammalian TNF/TNFR-related molecules regulate segregation of Miranda/Prospero in neuroblasts. EMBO J, 25(24), 5783–5793. doi: 10.1038/sj.emboj.7601461

Wang, H., Ouyang, Y., Somers, W. G., Chia, W., & Lu, B. (2007). Polo inhibits progenitor self-renewal and regulates Numb asymmetry by phosphorylating Pon. Nature, 449(7158), 96–100. doi: 10.1038/nature06056

Wei, C. L., Wu, Q., Vega, V. B., Chiu, K. P., Ng, P., Zhang, T., Shahab, A., Yong, H. C., Fu, Y. T., Weng, Z., Liu, J., Zhao, X. D., Chew, J. L., Lee, Y. L., Kuznetsov, V. A., Sung, W. K., Miller, L. D., Lim, B., Liu, E. T., … Ruan, Y. (2006). A global map of p53 transcription-factor binding sites in the human genome. Cell, 124(1), 207–219. doi: 10.1016/j.cell.2005.10.043

Wirtz-Peitz, F., Nishimura, T., & Knoblich, J. A. (2008). Linking Cell Cycle to Asymmetric Division: Aurora-A Phosphorylates the Par Complex to Regulate Numb Localization. Cell, 135(1), 161–173. doi: 10.1016/j.cell.2008.07.049

Wodarz, A., Ramrath, A., Kuchinke, U., & Knust, E. (1999). Bazooka provides an apical cue for Inscuteable localization in *Drosophila* neuroblasts. Nature, 402(6761), 544–547. doi: 10.1038/990128

Wodarz, A., Ramrath, A., Grimm, A., & Knust, E. (2000a). *Drosophila* Atypical Protein Kinase C Associates with Bazooka and Controls Polarity of Epithelia and Neuroblasts. J Cell Biol, 150(6), 1361–1374. doi: 10.1083/jcb.150.6.1361

Wodarz, A. (2000b). Tumor suppressors: Linking cell polarity and growth control. Curr Biol, 10(17), 624–626. doi: 10.1016/s0960-9822(00)00658-8

Wodarz, A., & Huttner, W. B. (2003). Asymmetric cell division during neurogenesis in *Drosophila* and vertebrates. Mech Dev, 120(11), 1297–1309. doi: 10.1016/j.mod.2003.06.003

Wodarz, A. (2005). Molecular control of cell polarity and asymmetric cell division in *Drosophila* neuroblasts. Curr Opin Cell Biol, 17(5), 475–481). doi: 10.1016/j.ceb.2005.08.005

Woods, D. F., & Bryant, P. J. (1991). The Discs-Large Tumor Suppressor Gene of Drosophila Encodes a Guanylate Kinase Homolog Localized at Septate Junctions. Cell, 66(3), 451-464. doi: 10.1016/0092-8674(81)90009-x

Wu, M., Pastor-Pareja, J. C., & Xu, T. (2010). Interaction between RasV12 and scribbled clones induces tumour growth and invasion. Nature, 463(7280), 545–548. doi: 10.1038/nature08702

Xiong, Y., Hannon, G. J., Zhang, H., Casso, D., Kobayashi, R., & Beach, D. (1993). p21 is a universal inhibitor of cyclin kinases. Nature, 366(6456), 701–704. doi: 10.1038/366701a0

Xu, T., & Rubin, G. M. (1993). Analysis of genetic mosaics in developing and adult *Drosophila* tissues. Development, 117(4), 1223–1237. doi: 0.1242/dev.117.4.1223

Xue, W., Zender, L., Miething, C., Dickins, R. A., Hernando, E., Krizhanovsky, V., Cordon-Cardo, C., & Lowe, S. W. (2007). Senescence and tumour clearance is triggered by p53 restoration in murine liver carcinomas. Nature, 445(7128), 656–660. doi: 10.1038/nature05529

Yamashita, Y. M., Yuan, H., Cheng, J., & Hunt, A. J. (2010). Polarity in stem cell division: asymmetric stem cell division in tissue homeostasis. Cold Spring Harb Perspect Biol, 2(1). doi: 10.1101/cshperspect.a001313

Yasugi, T., Umetsu, D., Murakami, S., Sato, M., & Tabata, T. (2008). *Drosophila* optic lobe neuroblasts triggered by a wave of proneural gene expression that is negatively regulated by JAK/STAT. Development, 135(8), 1471–1480. doi:10.1242/dev.019117

Yu, F., Morin, X., Cai, Y., Yang, X., & Chia, W. (2000). Analysis of partner of inscuteable, a Novel Player of *Drosophila* Asymmetric Divisions, Reveals Two Distinct Steps in Inscuteable Apical Localization. Cell, 100(4), 399–409. doi: 10.1016/s0092-8674(00)80676-5

Yu, F., Wang, H., Qian, H., Kaushik, R., Bownes, M., Yang, X., & Chia, W. (2005). Locomotion defects, together with Pins, regulates heterotrimeric G-protein signaling during *Drosophila* neuroblast asymmetric divisions. Genes Dev, 19(11), 1341–1353. doi: 10.1101/gad.1295505

Zhong, W., Feder, J. N., Jiang, M.-M., Yeh Jan, L., & Nung Jan, Y. (1996). Asymmetric Localization of a Mammalian Numb Homolog during Mouse Cortical Neurogenesis. Neuron, 17(1), 43–53. doi:10.1016/s0896-6273(00)80279-2

Zhong, W., Jiang, M.-M., Weinmaster, G., Yeh Jan, L., & Nung Jan, Y. (1997). Differential expression of mammalian Numb, Numblike and Notch1 suggests distinct roles during mouse cortical neurogenesis. Development, 124(10), 1887-1897. Doi: 10.1242/dev.124.10.1887

Zhong, W., & Chia, W. (2008). Neurogenesis and asymmetric cell division. Curr Opin Neurobiol, 18(1), 4-11. doi: 10.1016/j.conb.2008.05.002

ANNEX

Quality indicators

International Journal of
Molecular Sciences

MDPI

Article

Pilot RNAi Screen in *Drosophila* Neural Stem Cell Lineages to Identify Novel Tumor Suppressor Genes Involved in Asymmetric Cell Division

Sandra Manzanero-Ortiz, Ana de Torres-Jurado, Rubí Hernández-Rojas and Ana Carmena *

Developmental Neurobiology Department, Instituto de Neurociencias, Consejo Superior de Investigaciones Científicas/Universidad Miguel Hernández, 03550 Sant Joan d'Alacant, Alicante, Spain; smanzanero@umh.es (S.M.-O.); ana.torrese@umh.es (A.d.T.-J.); rubi.hernandezr@umh.es (R.H.-R.)
* Correspondence: acarmena@umh.es

Abstract: A connection between compromised asymmetric cell division (ACD) and tumorigenesis was proven some years ago using *Drosophila* larval brain neural stem cells, called neuroblasts (NBs), as a model system. Since then, we have learned that compromised ACD does not always promote tumorigenesis, as ACD is an extremely well-regulated process in which redundancy substantially overcomes potential ACD failures. Considering this, we have performed a pilot RNAi screen in *Drosophila* larval brain NB lineages using Ras^{V12} *scribble (scrib)* mutant clones as a sensitized genetic background, in which ACD is affected but does not cause tumoral growth. First, as a proof of concept, we have tested known ACD regulators in this sensitized background, such as *lethal (2) giant larvae* and *warts*. Although the downregulation of these ACD modulators in NB clones does not induce tumorigenesis, their downregulation along with Ras^{V12} *scrib* does cause tumor-like overgrowth. Based on these results, we have randomly screened 79 RNAi lines detecting 15 potential novel ACD regulators/tumor suppressor genes. We conclude that Ras^{V12} *scrib* is a good sensitized genetic background in which to identify tumor suppressor genes involved in NB ACD, whose function could otherwise be masked by the high redundancy of the ACD process.

Keywords: asymmetric cell division; tumorigenesis; neural stem cell; Ras^{V12} *scribble*; *RNAi* screen; tumor suppressor genes; *Drosophila*

Citation: Manzanero-Ortiz, S.; de Torres-Jurado, A.; Hernández-Rojas, R.; Carmena, A. Pilot RNAi Screen in *Drosophila* Neural Stem Cell Lineages to Identify Novel Tumor Suppressor Genes Involved in Asymmetric Cell Division. *Int. J. Mol. Sci.* **2021**, *22*, 11332. https://doi.org/10.3390/ijms222111332

Academic Editor: Dimitrios J. Stravopodis

Received: 16 September 2021
Accepted: 14 October 2021
Published: 20 October 2021

1. Introduction

Asymmetric cell division (ACD) is an effective and conserved strategy to generate cell diversity, an issue especially relevant during the development of the nervous system [1–4]. The neural stem cells of the *Drosophila* central nervous system, called neuroblasts (NBs), divide asymmetrically and have been used as a paradigm for analyzing this process for a long time [5–7]. In ACD, one daughter cell keeps on proliferating while its sibling is committed to initiating a process of differentiation. NB asymmetric division renders another self-renewal NB and a daughter cell called a ganglion mother cell (GMC), which will divide once more asymmetrically to give rise to two neurons or glial cells. A group of proteins called cell-fate determinants, such as the cytoplasmic protein Numb, the transcription factor Prospero (Pros)/Prox 1 in vertebrates, and the translational regulator brain tumor (Brat)/TRIM3, accumulate asymmetrically at the basal pole of the NB; then, when the NB divides only the most basal cell, the GMC receives those determinants, which inhibit proliferation and induce differentiation in this cell [8–16]. The asymmetric localization of cell-fate determinants, as well as the correct orientation of the mitotic spindle along the apical–basal axis of cell polarity, is, in turn, tightly regulated by multiple proteins, sometimes acting redundantly, to finally ensure the correct asymmetry of the division. For example, a group of proteins enriched at the apical pole of the NB at metaphase ("the apical complex") that include the plasma-membrane-located GTPase Cdc42, the

conserved Par proteins Par6 and Par3 (Bazooka, Baz, in *Drosophila*) and aPKC contribute to excluding the determinants from the apical pole [17–22]. These proteins bind the adaptor protein Inscuteable (Insc), which in turn binds Pins/LGN promoting the interaction of Pins/LGN with the Gαi subunit anchored to the membrane [23–30]. Then, the actin-binding protein Canoe (Cno)/Afadin displaces Insc to bind Pins/LGN, fostering the recruitment of Dlg1-Khc73 and the microtubule binding protein Mushroom body defect Mud/NuMA to Pins/LGN and, consequently, the orchestration of the mitotic spindle orientation along the apical–basal axis [31–36].

Intriguingly, a connection between failures in the process of ACD and tumorigenesis was demonstrated about 15 years ago using as a model system the NBs of the *Drosophila* larval brain [37]. In this work, pieces of GFP-labeled mutant brains for genes that regulate ACD were able to induce tumor-like overgrowth after being transplanted into the abdomen of wild-type (wt) adult fly hosts [37]. Remarkably, *Drosophila* genes originally identified as tumor suppressor genes, such as *discs large1* (*dlg1*)/*DLG1*, *lethal (2) giant larvae* (*l(2)gl*)/*LLGL1*, and *brain tumor* (*brat*)/*TRIM3* were shown a posteriori to be key regulators of ACD [38–40], further supporting the link between failures in ACD and tumorigenesis. Nevertheless, not all ACD regulators lead to tumor-like overgrowth when they are compromised [41]. In a recent work, we observed that NB mutant clones in the larval brain for the ACD regulators Cno/Afadin, Scribble (Scrib), L(2)gl/Llgl1 or Dlg1 do not cause tumor-like overgrowth, although all mutant clones show ectopic NBs [42]. In this study, we used the type II NB lineages (NBII) as a model system, in which the NB divides to give rise to another NB and, instead of a GMC, a progenitor cell called an intermediate neural progenitor (INP) that undertakes an additional round of division to generate another INP and a GMC (Figure 1a) [10,43,44]. Thus, given this extra phase of proliferation, these NBII lineages are more prone to induce tumor-like overgrowth when the process of ACD fails. Given that ACD is a highly redundant process, we reasoned that it would be necessary to downregulate more than one ACD regulator to observe more drastic effects. In fact, we showed that *cno scrib* double-mutant NB clones do display tumor-like overgrowth. Intriguingly, this phenotype is the consequence of losing two ACD regulators, but also of Ras upregulation after evading Cno-mediated repression [43]. In fact, the downregulation of Ras in *cno scrib* NBII clones is enough to suppress the tumor-like overgrowth observed in the double-mutant clones [42]. In addition, overexpressing an activated form of Ras (Ras^{V12}) in *scrib* NBII clones is not sufficient to induce those tumoral overgrowths observed in *cno scrib* double mutant clones, even though Ras^{V12} is able to rescue the JNK-mediated apoptosis induced in *scrib* NB mutant clones [42]. With all these results, we hypothesized that Ras^{V12} *scrib* mutant clones could be an excellent sensitized genetic background in which to screen for novel tumor suppressor genes and potential ACD regulators. Here, we show results that validate that hypothesis and a pilot screen to determine the suitability and the efficiency of the process in this search.

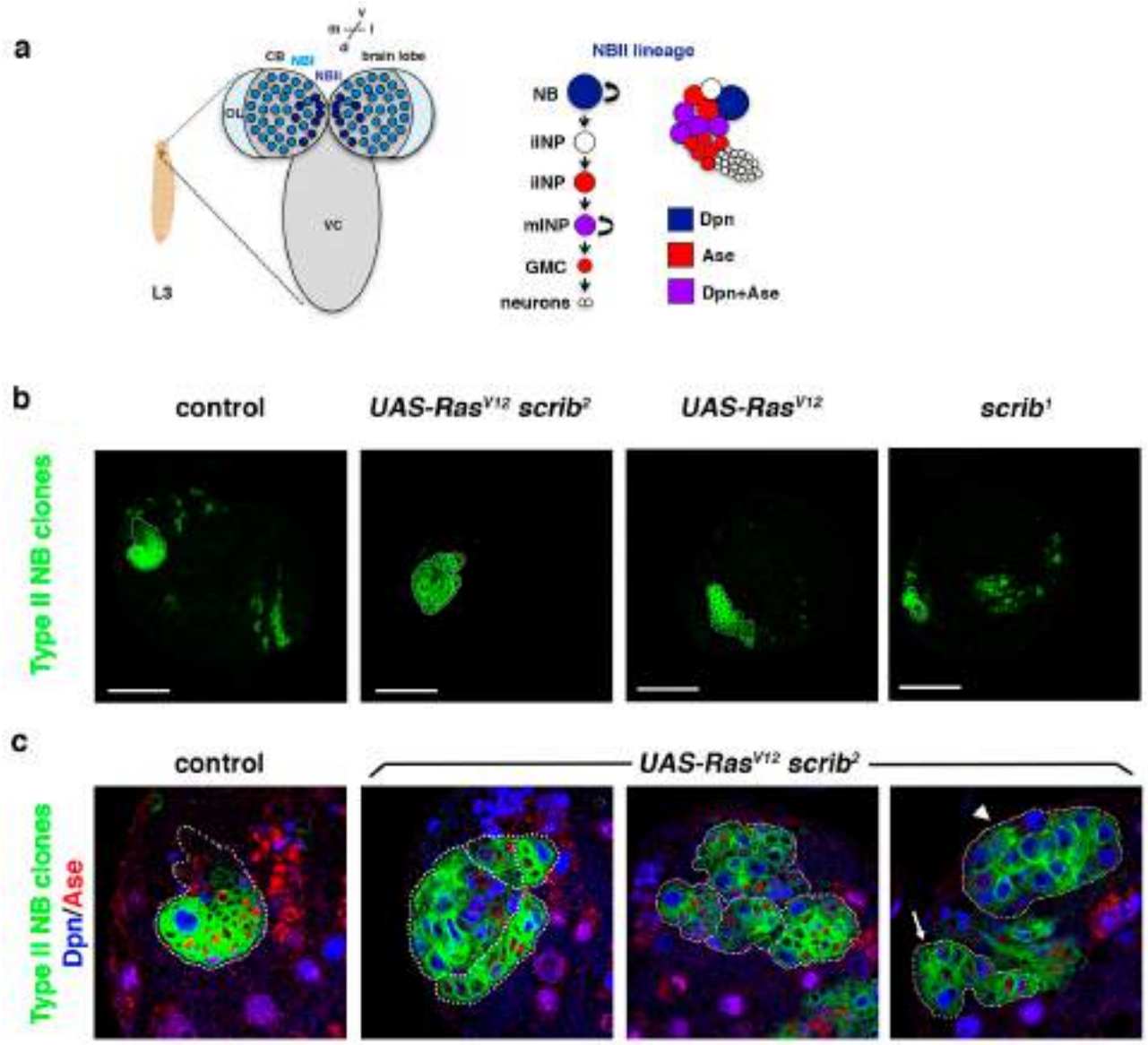

Figure 1. *Ras*^{V12} *scrib* NBII mutant clones do not show tumor-like overgrowth. (**a**) Type II neuroblast (NBII) lineages (8 per brain hemisphere) are found at particular locations at the dorsomedial part of each larval brain hemisphere, whereas type I NB (NBI) lineages are spread over the central brain (CB); L3: third instar larva; OL: optic lobe; VC: ventral cord; d: dorsal; v: ventral; m: medial; l: lateral. In NBII lineages, the NB divides to give rise to an intermediate neural progenitor (INP) that, after a maturation process, divides to generate another INP and a ganglion mother cell (GMC) that will terminally divide to give rise to two different neurons (or glial cells). The NB in NBII lineages expresses the transcription factor Dpn, whereas mature INPs (mINPs) express both transcription factors Dpn and Ase; iINP (immature INP). (**b**) Confocal micrographs showing a brain hemisphere with NBII lineages of the indicated genotypes. *scrib*^{1} NBII null mutant clones are smaller than control clones, whereas *Ras*^{V12} *scrib*^{2} NBII mutant clones show variable sizes as represented in (**c**); *Ras*^{V12} NBII mutant clones are similar to control clones. (**c**) Confocal micrographs showing NBII lineages of the indicated genotypes stained with Dpn (blue) and Ase (red), all at the same magnification; most *Ras*^{V12} *scrib*^{2} NBII mutant clones are smaller than control clones, with ectopic NBs (in blue; Dpn^{+} Ase^{-}), and they appear frequently in groups (dotted lines delimitate each NBII clone); some *Ras*^{V12} *scrib*^{2} NBII mutant clones are similar to control clones (arrow) and a few of them were composed mainly of NBs (arrowhead), but none of them showed tumor-like overgrowth. In both (**b**,**c**), the *Dll-Gal4 UAS-CD8::GFP; FRT82B tub-Gal80* line was used to perform MARCM clones [44] in type II NBs; scale bar: 50 μm.

2. Results and Discussion

2.1. Ras^{V12} scrib NBII Mutant Clones Do Not Show Tumor-like Overgrowth

In *Drosophila* epithelial tissues, oncogenic Ras (Ras^{V12}) induces neoplastic overgrowth in combination with cell polarity genes, including *scrib* [45,46]. However, our previous results showed that Ras^{V12} *scrib* NBII clones survive and show ectopic NBs, but they do not display massive overgrowth [42]. Thus, we reasoned that we could use this sensitized genetic mutant background to screen for novel tumor suppressor genes required in ACD. With this aim, we wanted first to analyze the Ras^{V12} *scrib* double-mutant phenotype in detail. Following our previous work, we focused this analysis on NBII lineages (Figure 1a). In these NBII clones, the transcription factor Deadpan (Dpn) labels all progenitor cells (the stem-like NB and the mature INPs), whereas the transcription factor Asense (Ase) is only expressed in the INPs (Figure 1a). We observed that *scrib* null mutant clones appeared with low frequency (in 5 brains out of 19) and were of small size compared with control clones (Figure 1b). However, Ras^{V12} *scrib* NBII clones were detected at the same frequency (in 17 brains out of 30) as control clones and their size was variable. Most of the Ras^{V12} *scrib* NBII clones were smaller than control clones, with some ectopic NBs and appearing frequently in groups; some were similar to control clones and few of them were composed mainly of NBs, but none of them show tumor-like overgrowth (Figure 1c).

2.2. Downregulation of Known ACD Regulators in Ras^{V12} scrib NBII Clones Induces Tumor-like Overgrowth

Based on the Ras^{V12} *scrib* NBII mutant clone phenotype, we inferred that the tumor-like overgrowth observed in *cno scrib* null mutant NBII clones [42] was induced not just by the upregulation of Ras, caused by the absence of its inhibitor Cno, but also by the simultaneous loss of two ACD regulators, Cno and Scrib. This would imply that we could search for novel ACD regulators, whose loss along with the Ras^{V12} *scrib* condition could induce tumor-like overgrowth. To prove this hypothesis, we first performed a qualitative inquiry approach testing known ACD regulators. We started looking at *dlg1* and *l(2)gl*, as we had observed that the downregulation of each of them in NBII clones does not cause tumoral growth [42]. Intriguingly, we observed some brains with $dlg1^{RNAi}$; Ras^{V12} *scrib* NBII clones bigger than Ras^{V12} *scrib* clones and filled mainly by NBs (Dpn^{+} Ase^{-}) (Figure 2a), a phenotype that also appeared and was much more exacerbated in brains with $l(2)gl^{RNAi}$; Ras^{V12} *scrib* NBII clones, which expanded in some cases throughout the brain hemisphere (Figure 2b). Previously, we described a novel function of Warts (Wts), a core component of the Hippo tumor suppressor signaling pathway, in ACD, phosphorylating and stabilizing Cno/Afadin at the apical pole of mitotic NBs. However, as in the case of *l(2)gl* and *dlg1*, wts^{x1} NBII single-mutant clones do not show tumor-like overgrowth [32]. Hence, we looked at the effect of downregulating *wts* along with Ras^{V12} *scrib* observing big wts^{RNAi}; Ras^{V12} *scrib* NBII clones showing tumor-like overgrowth. (Figure 2c). In conclusion, the above results strongly supported the reasoning of our hypothesis to find novel ACD regulators/tumor suppressor genes and, based on that, we decided to design and carry out a pilot screen to further prove it.

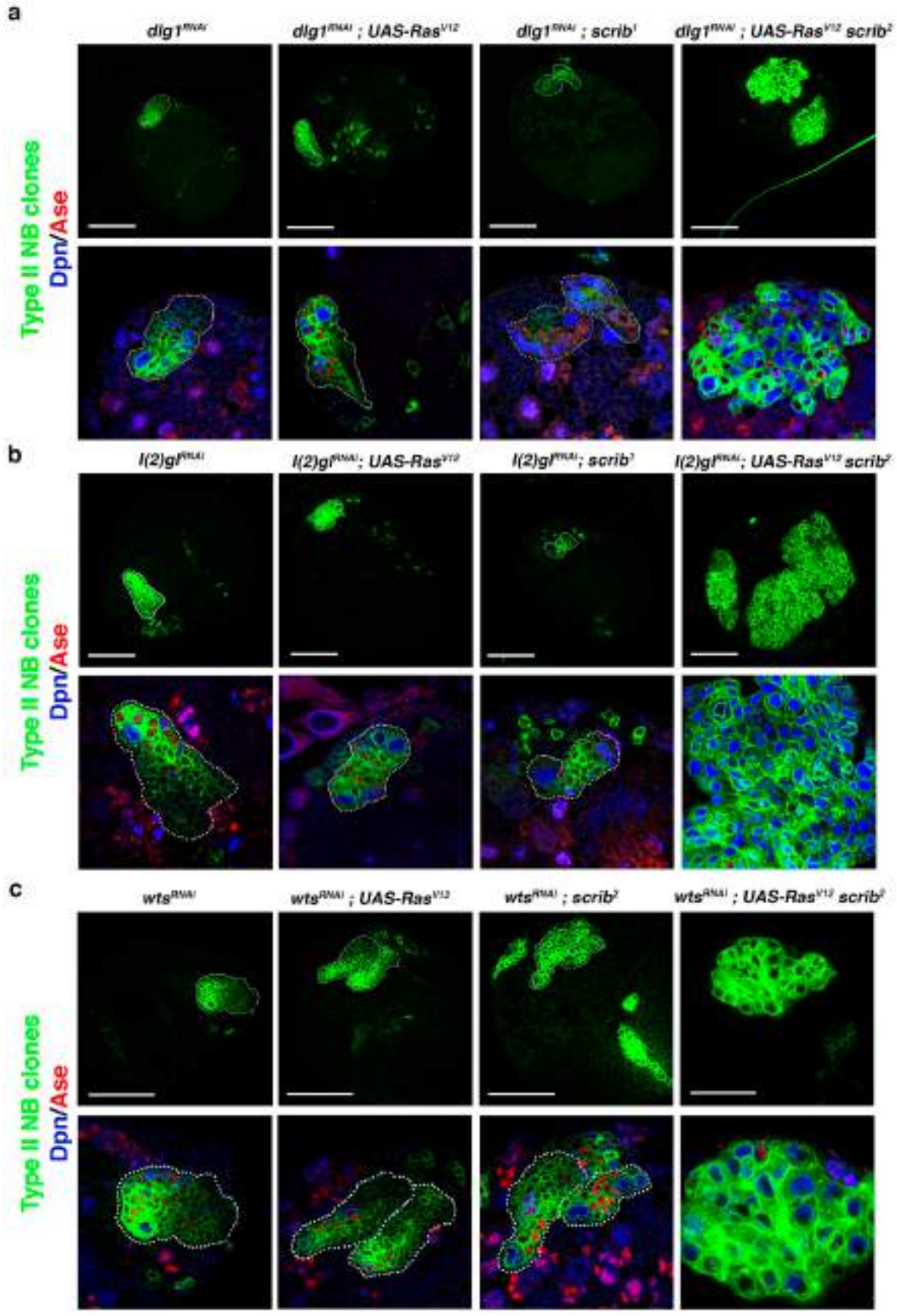

Figure 2. Downregulation of known ACD regulators in Ras^{V12} *scrib* NBII mutant clones induces tumor-like overgrowth.

(**a**) Confocal micrographs showing brain hemispheres with NBII lineages of the indicated genotypes. Below each hemisphere, detailed views of the corresponding NBII lineage stained with Dpn (blue) and Ase (red) are displayed at the same magnification. Some *dlg1*^{RNAi}; *Ras*^{V12} *scrib*^{2} NBII clones, as the clone shown, present tumor-like overgrowth, with the clone filled mainly by NBs (in blue; Dpn^{+}Ase^{-}), whereas the other genetic combinations never show tumor-like overgrowth. (**b**) Confocal micrographs showing brain hemispheres with NBII lineages of the indicated genotypes. Below each hemisphere, detailed views of the corresponding NBII lineage stained with Dpn and Ase are displayed at the same magnification. Only *l(2)gl*^{RNAi}; *Ras*^{V12} *scrib*^{2} NBII clones show tumor-like overgrowth, tumoral masses filled mainly by ectopic NBs (in blue; Dpn^{+}Ase^{-}). (**c**) Confocal micrographs showing brain hemispheres with NBII lineages of the indicated genotypes. Below each hemisphere, detailed views of the corresponding NBII lineage stained with Dpn and Ase are displayed at the same magnification. Only *wts*^{RNAi}; *Ras*^{V12} *scrib*^{2} NBII clones show tumor-like overgrowth, tumoral masses filled mainly by ectopic NBs (in blue; Dpn^{+}Ase^{-}); scale bar: 50 µm.

2.3. Screen Outline and Controls

A total of 79 second chromosome *UAS-RNAi* lines from Vienna *Drosophila* Resource Center (VDRC) GD or KK collections were randomly screened. Those *UAS-RNAi* lines were combined with *UAS-Ras*^{V12} *FRT82B scrib (Ras*^{V12} *scrib)* on the third chromosome to perform MARCM clones [44] and to search under the fluorescence microscope for NBII clones with tumor-like overgrowth (TLO from hereon) (Figure 3). To facilitate the analysis and identification of potential "positive" *UAS-RNAi* lines among the screened lines, different controls were first run. For example, to clearly identify larval brains with GFP clones, instead of any leaky GFP expression, we carried out a "background" control, in which recombination of the Gal4 repressor Gal80 is not taking place; thus, Gal4 cannot drive the expression of *UAS-CD8::GFP* and any GFP detected would correspond to leaky GFP or autofluorescence (Figure 4a and Table 1). In addition, a negative control consisting of *Ras*^{V12} *scrib* mutant clones, without any *UAS-RNAi* line on the second chromosome, was also taken into account. A total of 35 larvae with *Ras*^{V12} *scrib* clones were analyzed to define the biggest *Ras*^{V12} *scrib* clones we were able to detect (Figure 4b and Table 1). Thus, any experimental line showing mutant clones similar to those would be considered negative, whereas those mutant clones clearly above that size would be classified as lines with TLO and potential "positive" lines. Finally, as positive controls, we included the *UAS-RNAi* lines of *l(2)gl*, *dlg1*, and *wts*, which were analyzed following the scheme of the screening (Figure 3 and Table 1). We could unambiguously detect a significant percentage of *l(2)gl*^{RNAi}; *Ras*^{V12} *scrib* and *wts*^{RNAi}; *Ras*^{V12} *scrib* larvae showing brains with TLO (Figure 4c and Table 1). However, under the conditions of the screen, we were not able to detect clear cases of TLO in *dlg1*^{RNAi}; *Ras*^{V12} *scrib* larval brains (Figure 4c and Table 1). We already noticed in the "proof of concept" experiment, the staining with Dpn/Ase (see above), that the expressivity and penetrance of the *dlg1*^{RNAi}; *Ras*^{V12} *scrib* phenotype was lower than in *l(2)gl*^{RNAi}; *Ras*^{V12} *scrib* or than in *wts*^{RNAi}; *Ras*^{V12} *scrib* mutant combinations. In addition, under the screen conditions, Dpn/Ase markers, which helped to identify tumoral masses in the brain filled with NBs, stem-like cells, are not present. The fact that we were not able to detect clear cases of TLO in *dlg1*^{RNAi}; *Ras*^{V12} *scrib* larval brains indicated that we were probably going to miss some potential candidates (ACD regulators) that behave similarly to *dlg1*. Nevertheless, the evident cases of TLO found in the other positive controls, *l(2)gl* and *wts*, ensured the identification of those potential ACD regulators that display such strong interactions with *Ras*^{V12} *scrib* as *l(2)gl* and *wts* do.

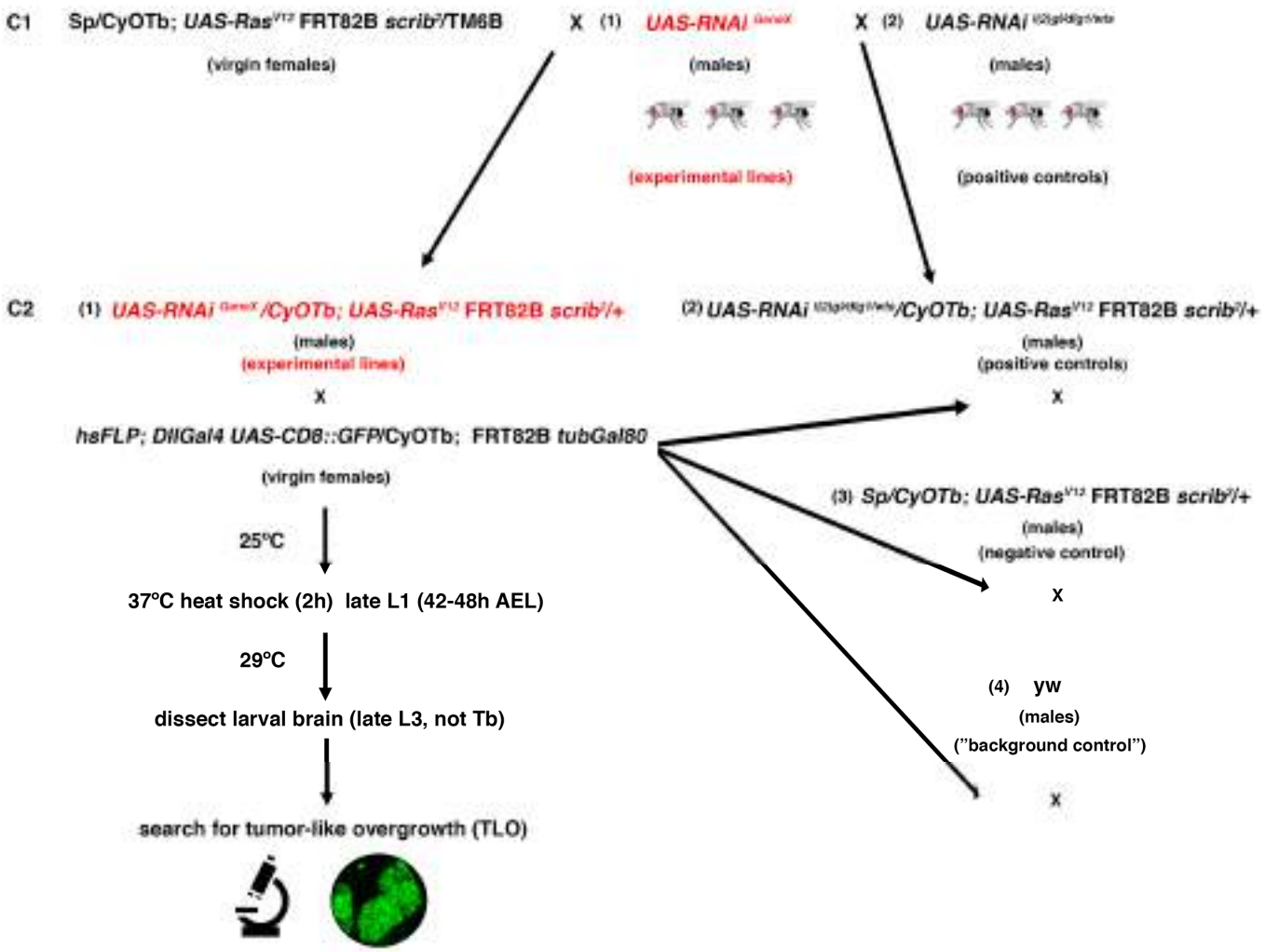

Figure 3. Outline of the crossing scheme and workflow for the RNAi screen. C1: Crosses 1; C2: Crosses 2; L1: first instar larvae; L3: third instar larvae; AEL: after egg laying; TLO: tumor-like overgrowth.

2.4. Positive UAS-RNAi Lines

Once we established all the controls, we started to randomly screen the "experimental" *UAS-RNAi* lines. Seventy-nine *UAS-RNAi* lines on the second chromosome were analyzed in combination with Ras^{V12} *scrib*. At least 12 larvae with clones from each line were observed under the microscope. We decided that those lines in which TLO clones were not detected after analyzing 12 larvae would be directly classified as "negative". In addition, we considered that at least 2 larvae with evident cases of TLO clones should be detected to establish the line as a "positive". Thus, those lines in which only 1 TLO was observed after analyzing 12 larvae were further screened (until a maximum of 30 larvae) looking for at least another case of clear TLO to confirm the line as positive (Table 1). After finishing the screen, we had identified 15 potential positive lines (Figure 5 and Table 1).

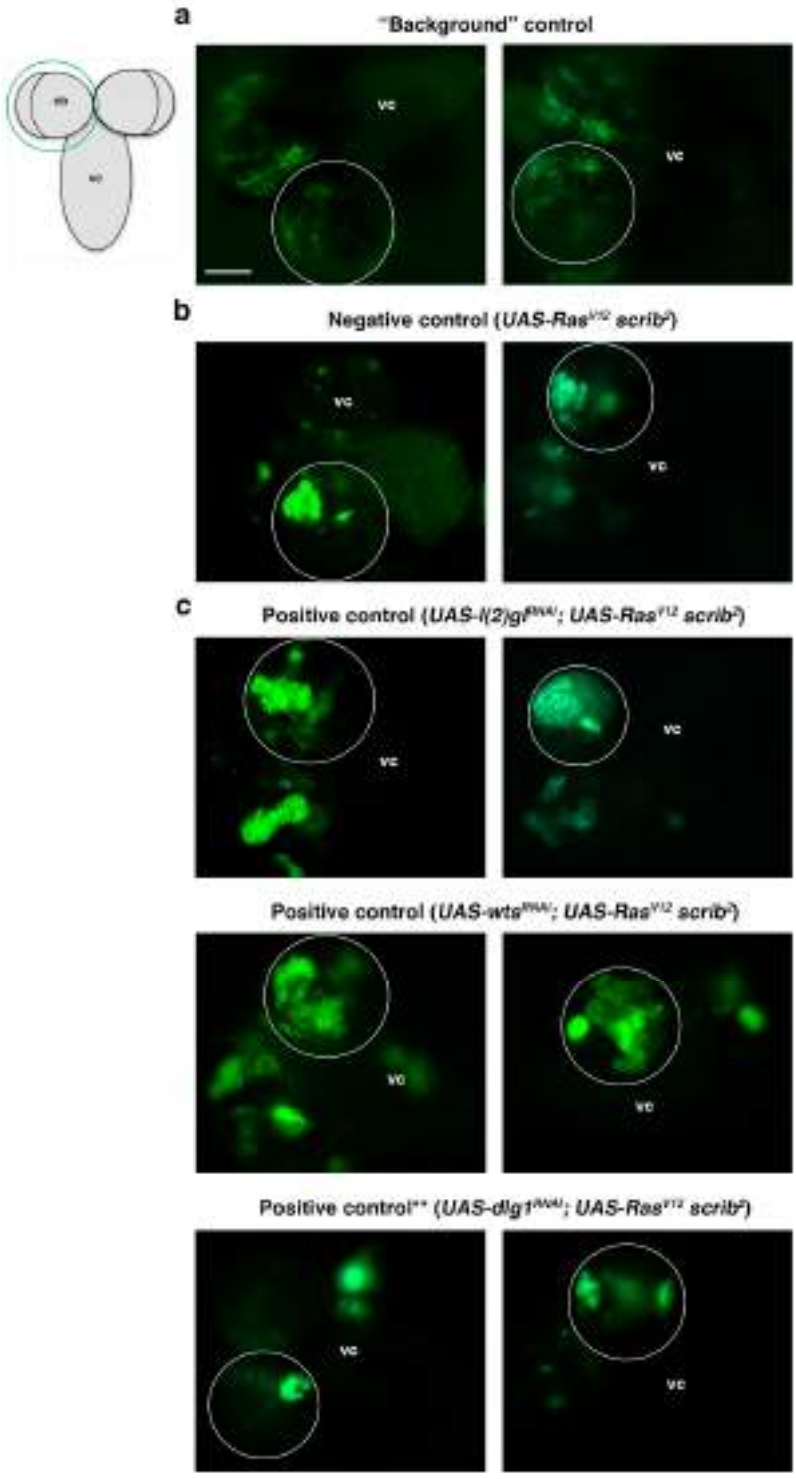

Figure 4. Screen controls. All panels show a dorsal view of a larval CNS that includes the ventral cord (vc) and the two brain hemispheres, one of which is encircled, as represented in the schematic larval CNS; cb (central brain). (**a**) A background control in which the GFP detected is leaky GFP or autofluorescence, as the Gal80 repressor is present to inhibit the CD8::GFP expression driven by the Gal4 line (see also Figure 3). (**b**) Two examples of the biggest Ras^{V12} $scrib^{2}$ NBII clones found, which is our established "negative control" (i.e., not considered TLO). Clones in the experimental lines above that size are considered TLO and potential "positive lines." (**c**) Positive controls, which are known ACD regulators, including *l(2)gl* and *wts*, whose downregulation in Ras^{V12} $scrib^{2}$ NBII clones induce TLO; (**) The downregulation of *dlg1*, another potential positive control, in Ras^{V12} $scrib^{2}$ NBII clones does not show clear TLO when tested under the conditions of the screen workflow (see also text and Table 1). Scale bar: 100 µm for all panels.

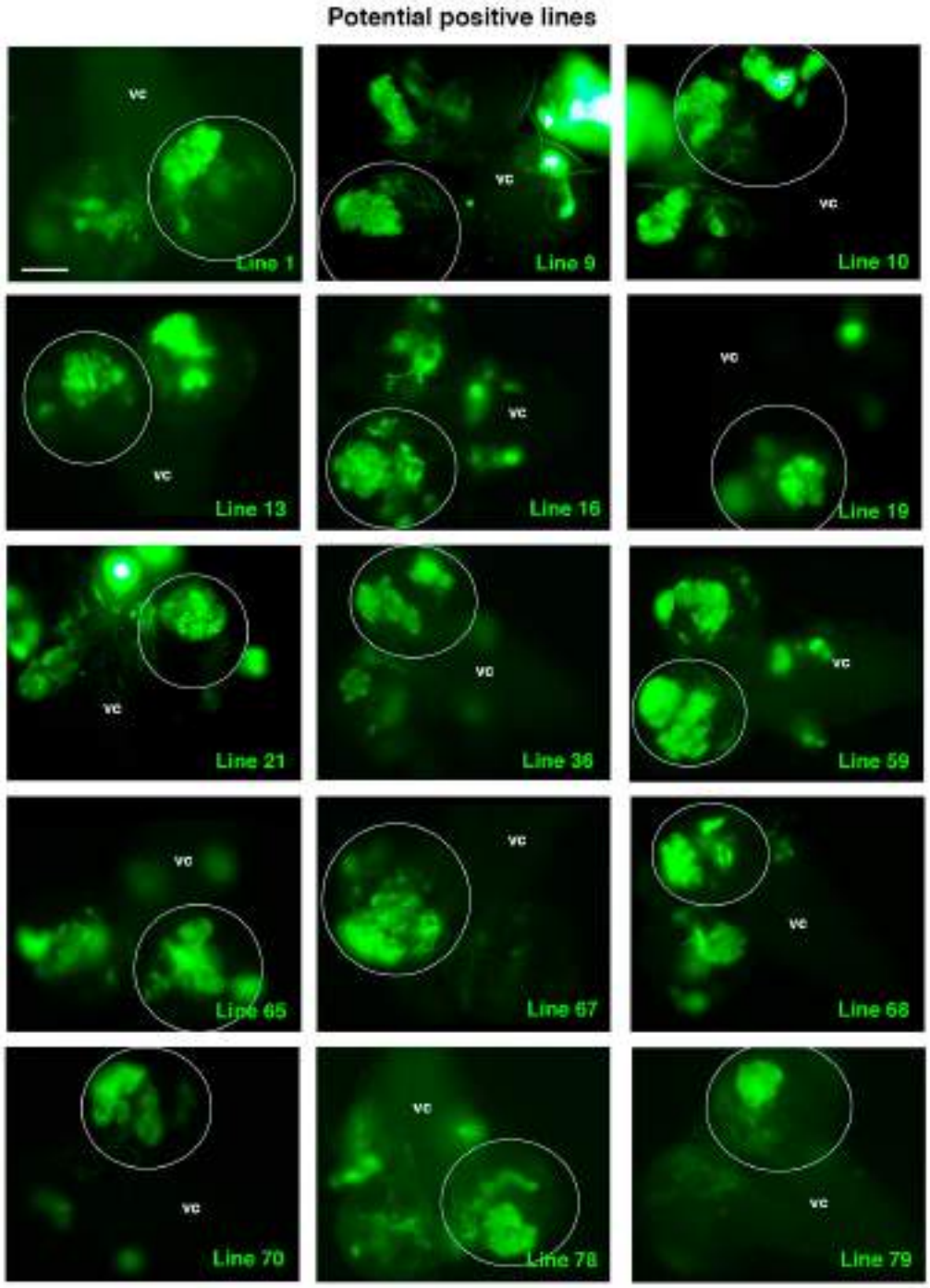

Figure 5. Potential positive lines selected. All panels show a dorsal view of a larval CNS that includes the ventral cord (vc) and the two-central brain (cb) hemispheres, one of which is encircled. All the selected experimental *UAS-RNAi* lines shown present clones with TLO and were considered potential positive lines following the established criteria (see text and Table 1). Scale bar: 100 µm for all panels.

Table 1. Control and *UAS-RNAi* lines were analyzed on the screen. Background, negative and positive controls were run (see Figure 3 for detailed genotypes). *dlg1*^{RNAi}; *Ras*^{V12} *scrib*^{2} larval brains did not show clear cases of TLO in the larvae analyzed (see also text). An additional control for the KK library landing site (LS) at 40D, without any RNAi line, was carried out, as the *UAS-wts*^{RNAi} line was inserted at that location. Fifteen potential positive lines (highlighted in green), i.e., those that showed TLO following the established criteria (see text for details), were selected out of 79 *UAS-RNAi* lines screened, which finally corresponded with 77 different genes (as lines 47 and 48 represent the same gene, as well as lines 61 and 75). Lines 28, 37, 38, 49, and 50 are currently discarded in VDRC.

Controls	Genotype	# Larvae Dissected	# Larvaewith Clones	# Larvae with TLO Clones	% Larvae with TLO Clones	VDRC ID	OFF Targets	CG Number	Gene Symbol
Background	*yw*	30	0	0	0.0%				
Negative	*Ras*^{V12} *scrib*^{2}	93	35	0	0.0%				
Positives:	*l(2)gl*^{RNAi}; *Ras*^{V12} *scrib*^{2}	58	21	8	**38.0%**				
	wts^{RNAi}; *Ras*^{V12} *scrib*^{2}	70	40	6	**15.0%**				
	dlg1^{RNAi}; *Ras*^{V12} *scrib*^{2}	42	16	0	0.0%				
Control LS	*40D-UAS*; *Ras*^{V12} *scrib*^{2}	34	13	0	0.0%				
RNAi LINES:	**1**	77	27	2	**7.4%**	105852/KK	0	CG8815	*Sin3A*
	2	27	13	0	0.0%	104803/KK	0	CG4336	*rux*
	3	47	21	0	0.0%	104829/KK	0	CG10756	*Taf13*
	4	44	16	0	0.0%	105478/KK	0	CG44247	*CG44247*
	5	49	17	0	0.0%	105384/KK	0	CG6093	*abo*
	6	47	16	0	0.0%	105462/KK	0	CG8428	*spin*
	7	60	27	0	0.0%	104335/KK	0	CG2917	*Orc4*
	8	45	12	0	0.0%	105502/KK	1	CG5216	*Sirt1*
	9	63	23	**2**	**8.7%**	104496/KK	0	CG17870	*14.3.3ζ*
	10	51	20	**2**	**10.0 %**	105409/KK	0	CG5343	*Bug22*
	11	22	12	0	0.0%	105367/KK	0	CG1616	*dpa*
	12	37	16	0	0,0%	105501/KK	2	CG5271	*RpS27A*

Table 1. *Cont.*

Controls	Genotype	# Larvae Dissected	# Larvaewith Clones	# Larvae with TLO Clones	% Larvae with TLO Clones	VDRC ID	OFF Targets	CG Number	Gene Symbol
	13	18	15	**2**	**13.3%**	103716/KK	0	CG4088	*Orc3*
	14	34	15	0	0.0%	106526/KK	0	CG13403	*CG13403*
	15	32	16	0	0.0%	106688/KK	1	CG5193	*TfIIB*
	16	46	19	**3**	**15.8%**	109108/KK	0	CG12559	*rl*
	17	30	12	0	0.0%	106185/KK	0	CG10052	*Rx*
	18	24	15	0	0.0%	106153/KK	0	CG2914	*Ets21C*
	19	50	19	**3**	**15.8%**	108828/KK	2	CG18497	*spen*
	20	32	12	0	0.0%	107026/KK	0	CG31739	*AspRS-m*
	21	30	18	**2**	**11.1%**	105739/KK	0	CG3291	*pcm*
	22	33	14	0	0.0%	106142/KK	0	CG8817	*lilli*
	23	23	13	0	0.0%	106196/KK	0	CG9576	*Phf7*
	24	59	13	0	0.0%	34113/GD	1	CG4494	*smt3*
	25	36	19	0	0.0%	32889/GD	0	CG1736	*Prosα3T*
	26	45	14	0	0.0%	1603/GD	2	CG3066	*Sp7*
	27	34	13	0	0.0%	35061/GD	0	CG6061	*mip120*
	28	28	12	0	0.0%	27424/GD	104	CG43398	*scrib*
	29	25	13	0	0.0%	34210/GD	1	CG8023	*eIF4E3*
	30	17	16	0	0.0%	30587/GD	0	CG3886	*Psc*
	31	28	12	0	0.0%	27467/GD	1	CG5604	*Ufd4*
	32	25	12	0	0.0%	9396/GD	0	CG3352	*ft*
	33	29	14	0	0.0%	105948/KK	0	CG40486	*CG40486*

Table 1. *Cont.*

Controls	Genotype	# Larvae Dissected	# Larvaewith Clones	# Larvae with TLO Clones	% Larvae with TLO Clones	VDRC ID	OFF Targets	CG Number	Gene Symbol
	34	25	16	0	0.0%	2919/GD	0	CG9653	*brk*
	35	34	13	0	0.0%	25387/GD	0	CG1977	*α-Spec*
	36	38	16	4	**25.0%**	105471/KK	2	CG2577	*CG2577*
	37	33	12	0	0.0%	16331/GD	1	CG42616	*Cul3*
	38	21	12	0	0.0%	32652/GD	2	CG15835	*Kdm4A*
	39	25	12	0	0.0%	35709/GD	0	CG16799	*CG16799*
	40	34	12	0	0.0%	3122/GD	0	CG17610	*grk*
	41	49	15	0	0.0%	38233/GD	1	CG43758	*sli*
	42	36	13	0	0.0%	12965/GD	1	CG17280	*levy*
	43	23	12	0	0.0%	25344/GD	0	CG1848	*LIMK1*
	44	20	12	0	0.0%	25549/GD	0	CG7762	*Rpn1*
	45	28	12	0	0.0%	30586/GD	0	CG3886	*Psc*
	46	28	13	0	0.0%	26888/GD	0	CG7771	*sim*
	47	44	16	0	0.0%	2947/GD	0	CG10798	*Myc*
	48	59	16	0	0.0%	2948/GD	0	CG10798	*Myc*
	49	30	12	0	0.0%	36086/GD	0	CG9124	*eIF3h*
	50	21	12	0	0.0%	16381/GD	0	CG12000	*Prosβ7*
	51	23	16	0	0.0%	106071/KK	0	CG14226	*dome*
	52	33	13	0	0.0%	106155/KK	3	CG10325	*abd-A*
	53	45	29	0	0.0%	103619/KK	2	CG7538	*Mcm2*
	54	29	18	0	0.0%	106459/KK	1	CG1716	*Set2*

Table 1. *Cont.*

Controls	Genotype	# Larvae Dissected	# Larvaewith Clones	# Larvae with TLO Clones	% Larvae with TLO Clones	VDRC ID	OFF Targets	CG Number	Gene Symbol
	55	28	13	0	0.0%	105865/KK	0	CG11158	*CG11158*
	56	21	12	0	0.0%	104415/KK	0	CG1354	*CG1354*
	57	29	13	0	0.0%	105494/KK	0	CG4400	*Brms1*
	58	25	13	0	0.0%	102054/KK	1	CG8367	*cg*
	59	25	17	**2**	**11.8%**	104775/KK	0	CG9907	*para*
	60	17	13	0	0.0%	106542/KK	0	CG14817	*CG14817*
	61	41	16	0	0.0%	2915/GD	4	CG5055	*baz*
	62	26	15	0	0.0%	106449/KK	0	CG2272	*slpr*
	63	34	13	0	0.0%	105371/KK	0	CG17437	*wds*
	64	43	22	0	0.0%	104753/KK	1	CG10445	*CG10445*
	65	43	23	**2**	8.7%	105946/KK	1	CG12238	*e(y)3*
	66	53	33	0	0.0%	106505/KK	0	CG12728	*CG12728*
	67	47	21	**3**	**14.3%**	106503/KK	0	CG1561	*pkm*
	68	30	14	**3**	**21.4%**	104425/KK	0	CG7846	*Arp8*
	69	23	14	0	0.0%	104770/KK	0	CG15865	*CG15865*
	70	32	13	2	**15.4%**	105374/KK	1	CG11734	*HERC2*
	71	53	30	1	3.3%	104792/KK	0	CG33980	*Vsx2*
	72	31	13	0	0.0%	21867/GD	0	CG4547	*Atx-1*
	73	38	14	0	0.0%	104427/KK	2	CG32697	*Ptpmeg2*
	74	30	15	0	0.0%	106491/KK	1	CG4320	*raptor*
	75	32	13	0	0.0%	2914/GD	4	CG5055	*baz*

Table 1. *Cont.*

Controls	Genotype	# Larvae Dissected	# Larvaewith Clones	# Larvae with TLO Clones	% Larvae with TLO Clones	VDRC ID	OFF Targets	CG Number	Gene Symbol
	76	26	13	0	0.0%	104963/KK	1	CG33323	*Fer1*
	77	27	15	0	0.0%	104600/KK	0	CG42267	*RunxB*
	78	35	13	2	**15.4%**	105942/KK	0	CG7280	*shop*
	79	31	17	2	**11.8%**	105509/KK	0	CG1803	*regucalcin*

Intriguingly, among those potential positive lines, we detected known ACD regulators, such as line 9, RNAi corresponding to the gene *14-3-3-ζ*, which encodes a protein that participates in the proper orientation of the mitotic spindle in dividing NBs [47]. Another positive line, line 65, was identified as an *enhancer of yellow 3*, *e(y)3*, which encodes a nuclear protein that physically and functionally interacts with both the transcription initiation factor TFIID and the SWI/SNF chromatin remodeling complex [48,49]. This complex is key to preventing tumorigenesis within *Drosophila* larval brain neural lineages by avoiding the de-differentiation of intermediate neural progenitors to an NB, stem-like cell fate [50]. Hence, the identification of these lines supports the suitability of the screen to identify novel ACD regulators.

2.5. Analysis of the UAS-RNAi Line 68

To further validate the screen, we decided to select the line that showed the highest percent of TLO cases without showing any off-target effects, the line 68, to perform additional analyses. This line was identified as *Actin-related protein 8 (Arp8)*, which encodes a proposed core component of the chromatin remodeling INO80 complex (Flybase). First, we determined the size of the selected *UAS-RNAi* line single-mutant clone; this was to discard the possibility that the TLO phenotype observed in the *UAS-RNAi; Ras*^{V12} *scrib* combination was just due to the downregulation of the gene associated with the line (that, otherwise, would also be interesting). The downregulation of the gene associated with that line in NBII lineages did not show TLO by itself in any of the larvae examined (n = 15; Figure 6a). Then, we analyzed the phenotype of the selected *UAS-RNAi line* in NBII clones, looking for defects in the ACD process. Specifically, we searched for potential failures in the localization of two ACD regulators, the apical protein aPKC and the cell fate determinant Numb, in dividing progenitors within the clone. Although no significant defects in the localization of Numb were observed, we detected significant failures in the localization of the apical protein aPKC in metaphase progenitors (Figure 6b). Thus, although it will be required to perform further and detailed analyses in the future, these results already suggest that Arp8 somehow contributes to the regulation of ACD, and that other "positive lines" might also represent known or novel ACD modulators.

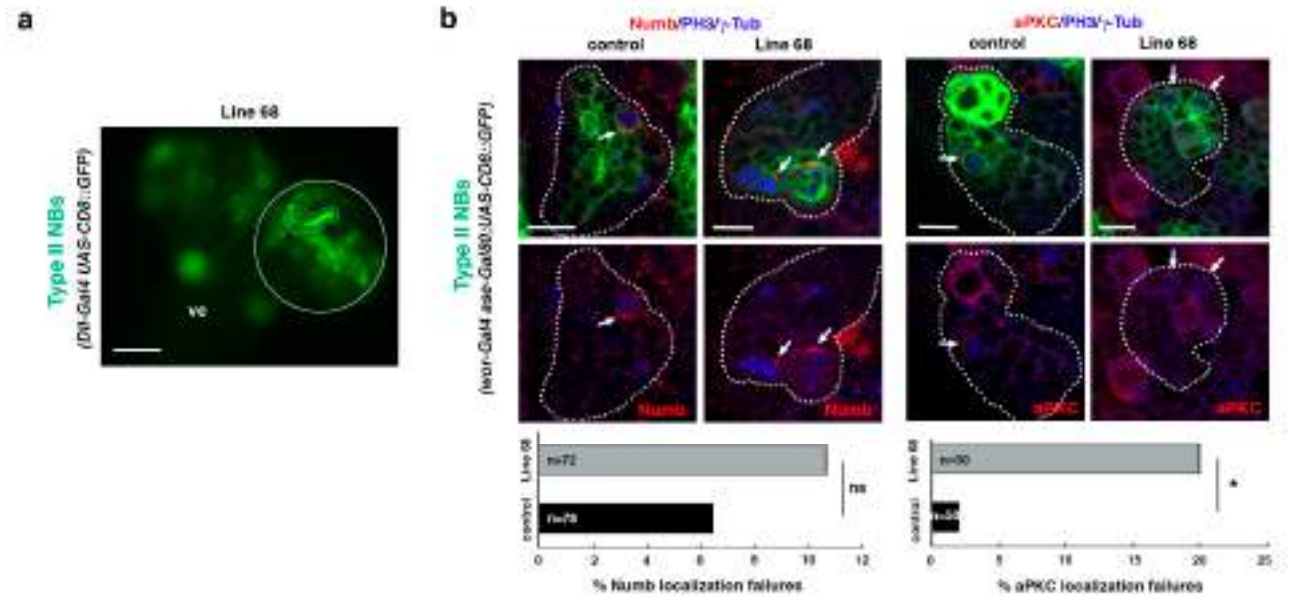

Figure 6. Line 68 is a potential ACD regulator. (**a**) Dorsal view of line 68 larval CNS, which includes the ventral cord (vc) and the two-central brain (cb) hemispheres, one of which is encircled. One NBII MARCM clone is shown surrounded by a dotted line. Scale bar: 100 µm. "Line 68" represents the genotype: *hsFLP; Dll-Gal4 UAS-CD8::GFP/UAS-RNAi*^{68}*; FRT82B/*

FRT82B (mutant clone) with *hsFLP; Dll-Gal4 UAS-CD8::GFP/UAS-RNAi^{68}; FRT82B tubGal80/FRT82B tubGal80* (twin wild-type clone, not labeled), all in an *hsFLP; Dll-Gal4 UAS-CD8::GFP/UAS-RNAi^{68}; FRT82B tubGal80/FRT82B* background. (**b**) Confocal micrographs of control and line 68 NBII lineages. The downregulation of the gene associated with line 68 induces significant failures in the localization of aPKC, whereas no significant defects in the localization of Numb are detected. In all panels, PH3 labels mitotic cells and γ-Tub the centrosomes. White arrows indicate the crescent correctly formed in metaphase progenitors in control clones and the absence of the aPKC crescent in the mutant condition. Data were analyzed with a chi-squared test (Yates correction), * $p < 0.05$ ($p = 0.011$) and ns: not significant ($p > 0.05$); n depicts the number of dividing cells analyzed; scale bars: 10 μm. "Control" corresponds to the genotype: *wor-Gal4 aseGal80/wor-Gal4 aseGal80*; *UAS-CD8::GFP/UAS-CD8::GFP*, and "Line 68" represents the genotype: *wor-Gal4 aseGal80/UAS-RNAi^{68}; UAS-CD8::GFP/+*.

3. Conclusions

The pilot screen presented here was performed at a low scale and, therefore, the number of positive lines identified are not yet enough to establish further relationships among them in the context of gene ontology (GO) terms and other similar parameters, an enrichment analysis that could be made in a more robust way on the results of a screen carried out at a higher scale. Nevertheless, this pilot screen strongly supports the hypothesis on which it was based. Likewise, the identification of known ACD regulators, as well as the validation of some of the positive lines, already show that we can isolate novel tumor suppressor genes involved in regulating ACD. Similarly, as we had predicted, we can miss some ACD regulators in this type of screen, as has been the case, for example, of the apical protein Par-3/Bazooka, which was found among the "negative" lines. Finally, the high percentage of positive lines identified was unexpected. Hence, additional analyses will be carried out in all those lines; this will further validate and confirm the capability of this screen to uncover novel regulators and mechanisms involved in ACD modulation.

4. Materials and Methods

4.1. Drosophila Strains and Genetics

The fly stocks used were from the Bloomington *Drosophila* Stock Center (BDSC) and the Vienna *Drosophila* Resource Center (VDRC), unless otherwise stated: *hs-FLP* (X chromosome); *UAS-Ras^{V12} FRT82B; UAS-Ras^{V12} FRT82B scrib^{2}; FRT82B scrib^{2}* (all from H. Richardson); *FRT82B scrib^{1}* (both *scrib^{1}* and *scrib^{2}* are null alleles [45,51,52] *FRT82B; Dll-Gal4 UAS-CD8::GFP*; *FRT82B tub-Gal80*; *UAS-CD8::GFP*; *wor-Gal4 ase-Gal80* [53]; *UAS-l(2)gl^{RNAi}* (VDRC: 109604); *UAS-dlg1^{RNAi}* (VDRC: 41134); *UAS-wts^{RNAi}* (VDRC: 106174); *40D-UAS* (control for KK library landing site at 40D; VDRC: 60101); all the 79 *UAS-RNAi* lines screened were lines on the second chromosome from the GD or the KK VDRC collection. These lines were randomly selected from a big UAS-RNAi collection belonging to M. Domínguez, who kindly let us pick the 79 lines used in this screen. We knew nothing a priori about the identity of the genes; the only requisite we followed was that the lines were on the second chromosome because of the design of the screen (Figure 3).

4.2. Histology, Immunofluorescence, and Microscopy

To analyze the *UAS-RNAi* lines of the screen, late L3 larval brains were dissected, mounted without fixation, and analyzed under a Carl Zeiss microscope (Axio Imager.A1), EC Plan-Neofluar 20× objective (Figures 4, 5 and 6a) and an AxioCam Hrc Carl Zeiss camera. Images were assembled using Adobe Photoshop CS6.

To perform the immunofluorescence, L3 larval brains were dissected in PBS and fixed with 4% PFA in PBT (PBS and Triton X-100 0.1%) for 20 min at room temperature with gentle rocking. Fixed brains were washed 3 times for 15 min with PBT (PBS and Triton X-100 0.3%) and then incubated in PBT-BSA for at least 1h before incubation with the corresponding primary antibody/antibodies. The following primary antibodies were used in this study: guinea pig anti-Dpn (1:2,000; [42]), rabbit anti-Ase (1:100; [42]), goat anti-Numb (1:200; Santa Cruz Biotechnology, sc-23579), and rabbit anti-PKCζ (1:100; Santa Cruz Biotechnology, sc-216). Fluorescence images corresponding to Figures 1 and 2a,b were recorded using an Inverted Leica laser-scanning spectral confocal microscope TCS

SP2. Fluorescence images in Figures 2c and 6b were recorded using a Super-resolution Inverted Confocal Microscope Zeiss LSM 880-Airyscan Elyra PS.1 (Figure 2c) or an Inverted Confocal Microscope Olympus FV1200 (Figure 6b), respectively.

4.3. Statistics

Data related to the ACD regulator localization failures were analyzed with a chi-squared test (with a Yates correction). The sample size (n) and the *p*-value are indicated in the figure or figure legend; * $p < 0.05$, ns: not significant ($p > 0.05$).

Author Contributions: Conceptualization, analysis and supervision, A.C.; analysis, and validation, S.M.-O., A.d.T.-J. and R.H.-R.; writing—original draft preparation, writing—review and editing, A.C. All authors have read and agreed to the published version of the manuscript.

Funding: Our lab was supported by Spanish grants from the Ministry of Economy and Competitiveness BFU2015-64251, from the Ministry of Science and Innovation PGC2018-097093-B-100, and by FEDER (European Regional Development Fund). S.M. was supported by a predoctoral FPI fellowship associated with the BFU2015-64251 grant, A.T.-J. was supported by a predoctoral FPI fellowship associated with the Severo Ochoa (SO) Project (2014–2018) and R.H. was supported by a Master fellowship associated with the SO project (2019–2222). The "Instituto de Neurociencias" in Alicante is a "Severo Ochoa Center of Excellence".

Acknowledgments: We are grateful to H. Richardson and M. Domínguez, as well as the Bloomington *Drosophila* Stock Center at the University of Indiana and the Vienna *Drosophila* Resource Center for kindly providing fly strains.

Conflicts of Interest: The authors declare no conflict of interest.

References

1. Zhong, W.; Chia, W. Neurogenesis and asymmetric cell division. *Curr. Opin. Neurobiol.* **2008**, *18*, 4–11. [CrossRef] [PubMed]
2. Huttner, W.B.; Kosodo, Y. Symmetric versus asymmetric cell division during neurogenesis in the developing vertebrate central nervous system. *Curr. Opin. Cell Biol.* **2005**, *17*, 648–657. [CrossRef]
3. Wodarz, A.; Huttner, W.B. Asymmetric cell division during neurogenesis in Drosophila and vertebrates. *Mech. Dev.* **2003**, *120*, 1297–1309. [CrossRef]
4. Venkei, Z.G.; Yamashita, Y.M. Emerging mechanisms of asymmetric stem cell division. *J. Cell Biol.* **2018**, *217*, 3785–3795. [CrossRef]
5. Doe, C.Q. Neural stem cells: Balancing self-renewal with differentiation. *Development* **2008**, *135*, 1575–1587. [CrossRef]
6. Gallaud, E.; Pham, T.; Cabernard, C. Drosophila melanogaster Neuroblasts: A Model for Asymmetric Stem Cell Divisions. In *Asymmetric Cell Division in Development, Differentiation and Cancer*; Tassan, J.-P., Kubiak, J.Z., Eds.; Springer International Publishing: Cham, Switzerland, 2017; pp. 183–210.
7. Knoblich, J.A. Mechanisms of asymmetric stem cell division. *Cell* **2008**, *132*, 583–597. [CrossRef] [PubMed]
8. Bello, B.; Reichert, H.; Hirth, F. The brain tumor gene negatively regulates neural progenitor cell proliferation in the larval central brain of Drosophila. *Development* **2006**, *133*, 2639–2648. [CrossRef] [PubMed]
9. Betschinger, J.; Mechtler, K.; Knoblich, J.A. Asymmetric segregation of the tumor suppressor brat regulates self-renewal in Drosophila neural stem cells. *Cell* **2006**, *124*, 1241–1253. [CrossRef] [PubMed]
10. Bowman, S.K.; Rolland, V.; Betschinger, J.; Kinsey, K.A.; Emery, G.; Knoblich, J.A. The tumor suppressors Brat and Numb regulate transit-amplifying neuroblast lineages in Drosophila. *Dev. Cell* **2008**, *14*, 535–546. [CrossRef]
11. Hirata, J.; Nakagoshi, H.; Nabeshima, Y.; Matsuzaki, F. Asymmetric segregation of the homeodomain protein Prospero during Drosophila development. *Nature* **1995**, *377*, 627–630. [CrossRef] [PubMed]
12. Knoblich, J.A.; Jan, L.Y.; Jan, Y.N. Asymmetric segregation of Numb and Prospero during cell division. *Nature* **1995**, *377*, 624–627. [CrossRef] [PubMed]
13. Lee, C.Y.; Wilkinson, B.D.; Siegrist, S.E.; Wharton, R.P.; Doe, C.Q. Brat is a Miranda cargo protein that promotes neuronal differentiation and inhibits neuroblast self-renewal. *Dev. Cell* **2006**, *10*, 441–449. [CrossRef]
14. Rhyu, M.S.; Jan, L.Y.; Jan, Y.N. Asymmetric distribution of numb protein during division of the sensory organ precursor cell confers distinct fates to daughter cells. *Cell* **1994**, *76*, 477–491. [CrossRef]
15. Spana, E.P.; Doe, C.Q. The prospero transcription factor is asymmetrically localized to the cell cortex during neuroblast mitosis in Drosophila. *Development* **1995**, *121*, 3187–3195. [CrossRef] [PubMed]
16. Uemura, T.; Shepherd, S.; Ackerman, L.; Jan, L.Y.; Jan, Y.N. Numb, a gene required in determination of cell fate during sensory organ formation in Drosophila embryos. *Cell* **1989**, *58*, 349–360. [CrossRef]
17. Atwood, S.X.; Chabu, C.; Penkert, R.R.; Doe, C.Q.; Prehoda, K.E. Cdc42 acts downstream of Bazooka to regulate neuroblast polarity through Par-6 aPKC. *J. Cell Sci.* **2007**, *120*, 3200–3206. [CrossRef] [PubMed]

18. Kuchinke, U.; Grawe, F.; Knust, E. Control of spindle orientation in Drosophila by the Par-3-related PDZ-domain protein Bazooka. *Curr. Biol.* **1998**, *8*, 1357–1365. [CrossRef]
19. Petronczki, M.; Knoblich, J.A. DmPAR-6 directs epithelial polarity and asymmetric cell division of neuroblasts in Drosophila. *Nat. Cell Biol.* **2001**, *3*, 43–49. [CrossRef]
20. Schober, M.; Schaefer, M.; Knoblich, J.A. Bazooka recruits Inscuteable to orient asymmetric cell divisions in Drosophila neuroblasts. *Nature* **1999**, *402*, 548–551. [CrossRef] [PubMed]
21. Wodarz, A.; Ramrath, A.; Grimm, A.; Knust, E. Drosophila atypical protein kinase C associates with Bazooka and controls polarity of epithelia and neuroblasts. *J. Cell Biol.* **2000**, *150*, 1361–1374. [CrossRef]
22. Wodarz, A.; Ramrath, A.; Kuchinke, U.; Knust, E. Bazooka provides an apical cue for Inscuteable localization in Drosophila neuroblasts. *Nature* **1999**, *402*, 544–547. [CrossRef] [PubMed]
23. Culurgioni, S.; Alfieri, A.; Pendolino, V.; Laddomada, F.; Mapelli, M. Inscuteable and NuMA proteins bind competitively to Leu-Gly-Asn repeat-enriched protein (LGN) during asymmetric cell divisions. *Proc. Natl. Acad. Sci. USA* **2011**, *108*, 20998–21003. [CrossRef] [PubMed]
24. Kraut, R.; Campos-Ortega, J.A. Inscuteable, a neural precursor gene of Drosophila, encodes a candidate for a cytoskeleton adaptor protein. *Dev. Biol.* **1996**, *174*, 65–81. [CrossRef] [PubMed]
25. Kraut, R.; Chia, W.; Jan, L.Y.; Jan, Y.N.; Knoblich, J.A. Role of inscuteable in orienting asymmetric cell divisions in Drosophila. *Nature* **1996**, *383*, 50–55. [CrossRef] [PubMed]
26. Parmentier, M.L.; Woods, D.; Greig, S.; Phan, P.G.; Radovic, A.; Bryant, P.; O'Kane, C.J. Rapsynoid/partner of inscuteable controls asymmetric division of larval neuroblasts in Drosophila. *J. Neurosci.* **2000**, *20*, RC84. [CrossRef]
27. Schaefer, M.; Petronczki, M.; Dorner, D.; Forte, M.; Knoblich, J.A. Heterotrimeric G proteins direct two modes of asymmetric cell division in the Drosophila nervous system. *Cell* **2001**, *107*, 183–194. [CrossRef]
28. Schaefer, M.; Shevchenko, A.; Shevchenko, A.; Knoblich, J.A. A protein complex containing Inscuteable and the Galpha-binding protein Pins orients asymmetric cell divisions in Drosophila. *Curr. Biol.* **2000**, *10*, 353–362. [CrossRef]
29. Yu, F.; Cai, Y.; Kaushik, R.; Yang, X.; Chia, W. Distinct roles of Galphai and Gbeta13F subunits of the heterotrimeric G protein complex in the mediation of Drosophila neuroblast asymmetric divisions. *J. Cell Biol.* **2003**, *162*, 623–633. [CrossRef]
30. Yu, F.; Morin, X.; Cai, Y.; Yang, X.; Chia, W. Analysis of partner of inscuteable, a novel player of Drosophila asymmetric divisions, reveals two distinct steps in inscuteable apical localization. *Cell* **2000**, *100*, 399–409. [CrossRef]
31. Johnston, C.A.; Hirono, K.; Prehoda, K.E.; Doe, C.Q. Identification of an Aurora-A/PinsLINKER/Dlg spindle orientation pathway using induced cell polarity in S2 cells. *Cell* **2009**, *138*, 1150–1163. [CrossRef]
32. Keder, A.; Rives-Quinto, N.; Aerne, B.L.; Franco, M.; Tapon, N.; Carmena, A. The hippo pathway core cassette regulates asymmetric cell division. *Curr. Biol.* **2015**, *25*, 2739–2750. [CrossRef]
33. Siegrist, S.E.; Doe, C.Q. Microtubule-induced Pins/Galphai cortical polarity in Drosophila neuroblasts. *Cell* **2005**, *123*, 1323–1335. [CrossRef] [PubMed]
34. Speicher, S.; Fischer, A.; Knoblich, J.; Carmena, A. The PDZ protein Canoe regulates the asymmetric division of Drosophila neuroblasts and muscle progenitors. *Curr. Biol.* **2008**, *18*, 831–837. [CrossRef] [PubMed]
35. Wee, B.; Johnston, C.A.; Prehoda, K.E.; Doe, C.Q. Canoe binds RanGTP to promote Pins(TPR)/Mud-mediated spindle orientation. *J. Cell Biol.* **2011**, *195*, 369–376. [CrossRef] [PubMed]
36. Yamada, K.H.; Hanada, T.; Chishti, A.H. The effector domain of human Dlg tumor suppressor acts as a switch that relieves autoinhibition of kinesin-3 motor GAKIN/KIF13B. *Biochemistry* **2007**, *46*, 10039–10045. [CrossRef] [PubMed]
37. Caussinus, E.; Gonzalez, C. Induction of tumor growth by altered stem-cell asymmetric division in Drosophila melanogaster. *Nat. Genet.* **2005**, *37*, 1125–1129. [CrossRef]
38. Albertson, R.; Doe, C.Q. Dlg, Scrib and Lgl regulate neuroblast cell size and mitotic spindle asymmetry. *Nat. Cell. Biol.* **2003**, *5*, 166–170. [CrossRef]
39. Ohshiro, T.; Yagami, T.; Zhang, C.; Matsuzaki, F. Role of cortical tumour-suppressor proteins in asymmetric division of Drosophila neuroblast. *Nature* **2000**, *408*, 593–596. [CrossRef]
40. Peng, C.Y.; Manning, L.; Albertson, R.; Doe, C.Q. The tumour-suppressor genes lgl and dlg regulate basal protein targeting in Drosophila neuroblasts. *Nature* **2000**, *408*, 596–600. [CrossRef]
41. Carmena, A. Compromising asymmetric stem cell division in Drosophila central brain: Revisiting the connections with tumorigenesis. *Fly (Austin)* **2018**, *12*, 71–80. [CrossRef]
42. Rives-Quinto, N.; Franco, M.; de Torres-Jurado, A.; Carmena, A. Synergism between canoe and scribble mutations causes tumor-like overgrowth via Ras activation in neural stem cells and epithelia. *Development* **2017**, *144*, 2570–2583. [CrossRef] [PubMed]
43. Carmena, A.; Speicher, S.; Baylies, M. The PDZ protein Canoe/AF-6 links Ras-MAPK, Notch and Wingless/Wnt signaling pathways by directly interacting with Ras, Notch and Dishevelled. *PLoS ONE* **2006**, *1*, e66. [CrossRef] [PubMed]
44. Lee, T.; Luo, L. Mosaic analysis with a repressible cell marker for studies of gene function in neuronal morphogenesis. *Neuron* **1999**, *22*, 451–461. [CrossRef]
45. Brumby, A.M.; Richardson, H.E. Scribble mutants cooperate with oncogenic Ras or Notch to cause neoplastic overgrowth in Drosophila. *EMBO J.* **2003**, *22*, 5769–5779. [CrossRef] [PubMed]
46. Pagliarini, R.A.; Xu, T. A genetic screen in Drosophila for metastatic behavior. *Science* **2003**, *302*, 1227–1231. [CrossRef]

47. Lu, M.S.; Prehoda, K.E. A NudE/14-3-3 pathway coordinates dynein and the kinesin Khc73 to position the mitotic spindle. *Dev. Cell* **2013**, *26*, 369–380. [CrossRef]
48. Vorobyeva, N.E.; Soshnikova, N.V.; Nikolenko, J.V.; Kuzmina, J.L.; Nabirochkina, E.N.; Georgieva, S.G.; Shidlovskii, Y.V. Transcription coactivator SAYP combines chromatin remodeler Brahma and transcription initiation factor TFIID into a single supercomplex. *Proc. Natl. Acad. Sci. USA* **2009**, *106*, 11049–11054. [CrossRef]
49. Chalkley, G.E.; Moshkin, Y.M.; Langenberg, K.; Bezstarosti, K.; Blastyak, A.; Gyurkovics, H.; Demmers, J.A.; Verrijzer, C.P. The transcriptional coactivator SAYP is a trithorax group signature subunit of the PBAP chromatin remodeling complex. *Mol. Cell. Biol.* **2008**, *28*, 2920–2929. [CrossRef]
50. Eroglu, E.; Burkard, T.R.; Jiang, Y.; Saini, N.; Homem, C.C.F.; Reichert, H.; Knoblich, J.A. SWI/SNF complex prevents lineage reversion and induces temporal patterning in neural stem cells. *Cell* **2014**, *156*, 1259–1273. [CrossRef]
51. Ganguly, I.; Mackay, T.F.; Anholt, R.R. Scribble is essential for olfactory behavior in Drosophila melanogaster. *Genetics* **2003**, *164*, 1447–1457. [CrossRef]
52. Courbard, J.R.; Djiane, A.; Wu, J.; Mlodzik, M. The apical/basal-polarity determinant Scribble cooperates with the PCP core factor Stbm/Vang and functions as one of its effectors. *Dev. Biol.* **2009**, *333*, 67–77. [CrossRef] [PubMed]
53. Neumuller, R.A.; Richter, C.; Fischer, A.; Novatchkova, M.; Neumuller, K.G.; Knoblich, J.A. Genome-wide analysis of self-renewal in Drosophila neural stem cells by transgenic RNAi. *Cell Stem Cell* **2011**, *8*, 580–593. [CrossRef] [PubMed]